

# **Computer Aided Drug Designing for Combinatorial Immunotherapeutics**

*A Major Project dissertation submitted in partial fulfillment of the requirement for the degree of*

**Master of Technology**

**In**

**Bioinformatics**

*Submitted by*

**Jaspreet Kaur Dhanjal**  
**(Roll No.: 2K11/BIO/09)**

**Delhi Technological University, Delhi, India**

*Under the supervision of*

**Dr. Asmita Das**



Department of Biotechnology  
Delhi Technological University  
(Formerly Delhi College of Engineering)  
Shahbad Daultpur, Main Bawana Road, Delhi-110042, India



## CERTIFICATE

This is to certify that the M. Tech dissertation entitled “**Computer Aided Drug Designing for Combinatorial Immunotherapeutics**”, submitted by **Jaspreet Kaur Dhanjal (Roll No.: 2K11/BIO/09)** in partial fulfillment of the requirement for the award of the degree of Master of Technology, Delhi Technological University (formerly Delhi College of Engineering), is an authentic record of the candidate’s own work carried out by her under my guidance.

The information and data enclosed in this dissertation is original and has not been submitted elsewhere for honouring of any other degree.

**Date:** July 8, 2013

**Dr. Asmita Das**

Assistant professor

Department of Bio-Technology

Delhi Technological University

(Formerly Delhi College of Engineering, University of Delhi)

## DECLARATION

I, **Jaspreet Kaur Dhanjal**, hereby declare that the work entitled “**Computer Aided Drug Designing for Combinatorial Immunotherapeutics**” has been carried out by me under the guidance of Dr. Asmita Das, in Delhi Technological University, Delhi.

This dissertation is part of partial fulfillment of requirement for the degree of M.Tech in Bioinformatics. This is the original work and has not been submitted for any other degree in any other university.

Jaspreet Kaur Dhanjal

Roll No.: 2K11/BIO/09

## **ACKNOWLEDGEMENT**

*I would like to acknowledge my deep sense of gratitude to **Prof. S. Maji, (Head of Department) Department of Biotechnology, Delhi Technological University, Delhi-110042** for giving me an opportunity to study and work in this prestigious Institute.*

*I am extremely thankful to my mentor, **Dr. Asmita Das, Assistant professor, Department of Biotechnology, Delhi Technological University, Delhi-110042** for her exemplary guidance, monitoring and constant encouragement throughout the M. Tech course. I would also like to thank her for sparing the efforts in compiling the work presented here.*

*I wish to express my sincere gratitude to **Dr. Abhinav Grover, Assistant Professor, School of Life Sciences, Jawaharlal Nehru University, Delhi-110067** for providing me continuous support throughout this project.*

*At last, I am extremely thankful to my parents, family members and friends whose blessings and support were always with me.*

**JASPREET KAUR DHANJAL**

**Roll No.: 2K11/BIO/09**

## CONTENTS

<b>TOPIC</b>	<b>PAGE NO.</b>
<i>List of figures</i>	<i>i-iii</i>
<i>List of tables</i>	<i>iv</i>
<i>List of abbreviations</i>	<i>v-vi</i>
<b>ABSTRACT</b>	<i>1</i>
<b>BACKGROUND</b>	<i>2-4</i>
<b>CHAPTER 1</b>	
<b>Introduction</b>	<i>6-7</i>
<b>Review of Literature</b>	<i>7-10</i>
• <i>PI3K signaling pathway</i>	<i>7-8</i>
• <i>PI3K activation in cancer</i>	<i>8</i>
• <i>p110<math>\alpha</math> as a target for isoform specific inhibitors</i>	<i>9</i>
• <i>QSAR, a powerful in silico approach for lead optimization</i>	<i>9-10</i>
<b>Materials and Methods</b>	<i>10-12</i>
• <i>Preparation of data set</i>	<i>10</i>
• <i>Molecular modeling study</i>	<i>10</i>
• <i>Computation of values for descriptors and data selection for training and test set</i>	<i>11</i>
• <i>3D QSAR model building</i>	<i>11</i>
• <i>Validation of the 3D QSAR Model</i>	<i>11</i>
• <i>Prediction of Biological activity of 1,69,109 natural compounds using the generated 3D QSAR model</i>	<i>12</i>
• <i>Protein and ligand preparation for docking studies</i>	<i>12</i>
<b>Results and Discussion</b>	<i>12-25</i>
• <i>QSAR molecular modeling</i>	<i>12-19</i>
• <i>Interpretation of the built 3D QSAR model</i>	<i>20</i>
• <i>Prediction of biological activity for a large dataset comprising of 1,69,109 natural compounds</i>	<i>20</i>
• <i>Interaction analysis of the predicted natural compounds using in silico docking studies</i>	<i>20-25</i>
<b>Conclusion</b>	<i>25</i>

<b>CHAPTER 2</b>	
<b>Introduction</b>	27-28
<b>Review of Literature</b>	28-37
• <i>Use of multiple target drug design strategy</i>	28-29
• <i>FASN, a potential cancer target</i>	29-32
• <i>Targeting PI3K signaling in cancer</i>	32-34
• <i>SCF E3 ubiquitin ligases as anticancer targets</i>	34-37
<b>Materials and Methods</b>	37-38
• <i>Protein preparation and dataset</i>	37
• <i>High throughput virtual screening and docking studies</i>	37
• <i>Molecular dynamics simulations of ligand-bound complexes</i>	38
<b>Results and Discussion</b>	38-51
• <i>High Throughput virtual screening and docking studies</i>	38-39
• <i>Interaction analysis of MTD with TE domain of FASN</i>	39-43
• <i>MTD with potential to hamper interaction between Skp2 and Cks1</i>	44-47
• <i>MTD, a natural molecule with potential to inhibit PI3K<math>\alpha</math></i>	48-51
<b>Conclusion</b>	52
<b>CHAPTER 3</b>	
<b>Introduction</b>	54-55
<b>Review of Literature</b>	55-58
• <i>T cell based therapy and its limitations</i>	55-57
• <i>Role of NK cells in defense against tumors</i>	57-59
<b>Materials and Methods</b>	59-60
• <i>Protein preparation and dataset</i>	59
• <i>High throughput virtual screening and docking studies</i>	60
• <i>Molecular Dynamics Simulations of ligand-bound complex</i>	60
<b>Results and Discussion</b>	60-64
• <i>Virtual screening of 1,69,109 natural compounds representing a diverse subset of ZINC database</i>	60-61
• <i>Interaction analysis of DHM at C-terminal of TLR3 dimer</i>	61-62
• <i>IEH interacting with functionally important residues at N terminal of TLR3</i>	62-64
<b>Conclusion</b>	65
<b>FUTURE PROSPECTS</b>	66
<b>REFERENCES</b>	67-86

## LIST OF FIGURES

<b>CHAPTER 1</b>		
<b>S.No.</b>	<b>Figure</b>	<b>Page No.</b>
1.	(A) Structure of template used for template based alignment of optimized molecules (B) 3D alignment of optimized PI3K inhibitors	10
2.	Data fitness plot for the 3D QSAR model generated	18
3.	(A) Graph of actual and predicted biological activity for training set (B) Graph of actual and predicted biological activity for test set	18
4.	(A) 3D-alignment of molecules with the important steric and hydrophobic points contributing to the biological activity of the ligands (B) Graph showing the contribution of molecular descriptors in controlling the activity of the inhibitors	19
5.	(A) Chemical structures of first natural compound, HPM (B) Chemical structures of second natural compound, MNT	21
6.	(A) Hydrogen bond interactions between comp19 and PI3K $\alpha$ (B) Ligplot showing hydrogen bond interactions and hydrophobic interactions between comp19 and PI3K $\alpha$	22
7.	(A) Residues of PI3K $\alpha$ involved in hydrogen bond interactions with HPM (B) Ligplot showing hydrogen bond interactions and hydrophobic interactions between HPM and PI3K $\alpha$	23
8.	(A) Residues of PI3K $\alpha$ involved in hydrogen bond interactions with MNT (B) Ligplot showing hydrogen bond interactions and hydrophobic interactions between MNT and PI3K $\alpha$	24
9.	Relative position of all the three ligands in the cavity of PI3K $\alpha$	25

## CHAPTER 2

S.No.	Figure	Page No.
1.	Chemical structure of MTD	39
2.	(A) Hydrogen bond interaction between MTD and TE domain of FASN (B) Ligplot showing the interactive phase between MTD and TE domain of FASN	41
3.	(A) RMSD trajectory of MTD bound FASN complex during the 10 ns MD simulation run (B) Superimposition of Pre-MD (green) and Post-MD (Brown) MTD-FASN complexes	42
4.	(A) Hydrogen bonding pattern in dynamically stable MTD-FASN complex. (B) Ligplot of post MD MTD-FASN complex illustrating hydrogen and hydrophobic interactions.	43
5.	(A) Residues of Skp2 involved in hydrogen bond interaction with MTD (B) Ligplot showing $\pi$ -bonds and hydrophobic interactions between Skp2 and MTD	45
6.	(A) RMSD trajectory of MTD-Skp2 complex during 10 ns long simulation run (B) Change in the position of MTD docked into Skp2 before (green) and after (purple) MD simulation	46
7.	(A) Skp2 residues involved in hydrogen bonding with MTD after MD simulation (B) Ligplot showing dynamically stabilized molecular interactions between MTD and Skp2	47
8.	(A) Hydrogen bond interaction between MTD and residues lining the active cleft of PI3K $\alpha$ (B) Ligplot showing the hydrogen bonds and hydrophobic interactions between MTD and PI3K $\alpha$	49
9.	(A) RMSD trajectory of MTD-PI3K $\alpha$ complex during 10 ns long simulation run (B) Change in the position of MTD docked into PI3K $\alpha$ before (green) and after (pink) MD simulation.	50
10.	(A) PI3K $\alpha$ residues involved in hydrogen bonding with MTD after MD simulation (B) Ligplot showing dynamically stabilized molecular interactions between MTD and PI3K $\alpha$	51



## CHAPTER 3

S.No.	Figure	Page No.
1.	(A) Chemical structure of DHM (B) Chemical structure of IEH	61
2.	(A) Interaction between TLR3 and the dsRNA at C terminal thereby stabilizing the functional receptor dimer (B) DHM, natural compound interacting at the C terminal site of TLR3 molecules (C) Hydrogen and hydrophobic interactions of DHM with chain A of dimerized TLR3 receptor (D) Molecular interaction pattern shown by DHM with chain B of functionally active TLR3 dimer	63
3.	(A) Binding of dsRNA at the N terminal of TLR3 (B) IEH, the screened natural compound bound at the N terminal region of TLR3 (C) IEH mimicking the interactions between dsRNA and TLR3 N terminal	64

## LIST OF TABLES

<b>CHAPTER 1</b>		
<b>S. No.</b>	<b>Table legends</b>	<b>Page No.</b>
1.	The list of PI3K inhibitors along with their chemical structures, $K_i$ and $pK_i$ values.	13-17
2.	Statistics of the significant model generated using SW-MR	17
3.	Statistical measures with their minimum recommended values	17
4.	List of natural chemical compounds with their $pK_i$ value predicted on the basis of the generated 3D QSAR model	21

## LIST OF ABBREVIATIONS

ACP	Acyl carrier protein
ADCC	Antibody-dependent cell-mediated cytotoxicity
AICD	<i>Activation-induced cell death</i>
ATP	Adenosine triphosphate
bp	Base pair
CoA	Coenzyme A
CTL	Cytotoxic T lymphocyte
DNA	Deoxyribonucleic acid
ds	Double stranded
ECD	Ectodomain
FASN	<i>Fatty acid synthase</i>
FDA	<i>Food and Drug Administration</i>
fs	Femtosecond
GHz	Giga Hertz
HLA	<i>Human leukocyte antigen</i>
HTS	High throughput screening
HTVS	High throughput virtual screening
IFN $\gamma$	<i>Interferon gamma</i>
IL	<i>Interleukin</i>
K	Kelvin
K <sub>i</sub>	Inhibitor constant
LAK	<i>Lymphokine activated killer</i>
mAb	Monoclonal antibody
MD	Molecular dynamics
MDS	Molecular design suite
MHC	<i>Major histocompatibility complex</i>
MMFF	<i>Merck molecular force field</i>
MPP	4-Methylpyridopyrimidinone

NK	Natural killer
nM	Nanomolar
ns	Nanosecond
OPLS	Optimized potentials for liquid simulations
PDB	Protein Data Bank
PI3K	Phosphoinositide 3-kinase
PIP2	Phosphatidylinositol-4,5-bisphosphate
PIP3	Phosphatidylinositol-3,4,5-trisphosphate
QSAR	Quantitative structure activity relationship
RBC	Red blood cell
RMSD	Root mean square deviation
RNA	Ribonucleic acid
RTK	Receptor tyrosine kinases
SCF	Skp1, Cullins, F-box proteins
siRNA	Small interfering RNA
SPC	<i>Simple point charge</i>
SW-MR	Stepwise-Multiple regression
TE	Thioesterase
TGF- $\beta$	Transforming growth factor beta
TIR	Toll IL-1 receptor
TLR	<i>Toll-like receptor</i>
TRAIL	Tumor Necrosis Factor-related apoptosis-inducing ligand
UPS	Ubiquitin-Proteasome System
WBC	White blood cell
XP	Extra precision

## ABSTRACT

*Cancer is one of the leading causes of adult deaths worldwide. Chemotherapy, radiation therapy, immunotherapy, hormonal therapy and surgical removal of tumors are the most common clinical approaches being used for the treatment of cancer. Today, there are more than 100 FDA approved drugs in the markets for cancer therapy. Unfortunately, the chemotherapy treatment is almost always accompanied by a varied range of short and long term adverse effects. Also the cancerous cells evolve and develop resistance against these drugs during the course of treatment to escape the process of cell death and sustain their survival. Hence, the need arises to explicate the various molecular mechanisms which get altered and support the survival of transformed cells. This would help us find novel targets highly specific to tumor or cancer cells and design drugs against them. Since natural compounds offer a potentially infinite source of chemical diversity which cannot be matched by any synthetic chemical collection or combinatorial chemistry approach, in this study we have used in silico methods to identify small molecule natural compounds with inhibitory activity against cancer specific molecular targets. Firstly, we have used a series of 4-methylpyridopyrimidinone derived PI3K inhibitors to develop a 3D-QSAR model which was then used to screen a dataset of natural compounds to predict more potent PI3K inhibitors. In complex diseases like cancer, single target approach sometimes do not result in desired outcome as the transformed cells find for an alternate pathway to compensate for the loss. In such cases, multi target approach is more efficient for a significant modification in the environment of cancer cells. With this perspective in mind, secondly we have proposed another natural compound with potential to simultaneously inhibit three cancer specific targets- Fatty acid synthase, Phosphatidylinositol 3-kinase (p110 $\alpha$ ) and Skp2 component of SCF E3 Ubiquitin Ligase. Lastly, we have reported a molecule of natural origin that shows the ability to stimulate body's own immune system to fight against cancerous cells by activating NK cells through TLR3 receptor.*

## BACKGROUND

Cancer is an umbrella term used to describe a variety of diseases in which cells start dividing abnormally. These cells then spread through blood and lymph system to invade other tissues of the body. There exists more than 100 different types of cancer. Depending upon the site of origin, cancer can be grouped as carcinoma (starting in the skin or tissue lining of internal organs), sarcoma (cancer of connective and supportive tissue), leukemia (starting in the blood forming tissue), lymphoma or myeloma (beginning in the immune cells) and central nervous system cancer (originating in brain or spinal cord) (National Cancer Institute).

Cancer is one of the leading causes of adult deaths worldwide. One in every four deaths in United States is due to cancer. American Cancer Society projected an estimate of about 1,638,910 new cancer cases and 577,190 deaths from cancer in US for the year 2012. Prostate cancer is the most prevalent one among the males whereas in females breast cancer tops the chart (Siegel *et al.*, 2012). In India the most common fatal cancers include oral, stomach and lung cancer in males and cervical, stomach and breast cancer in females (Dikshit *et al.*, 2012).

The effective therapies for completely removing the cause of cancer are not yet available but efficient measures can be taken to control the growth of cancer. The traditional treatment options available for controlling cancer include chemotherapy, radiation therapy, childhood hematopoietic cell transplantation, bone marrow transplantation, surgical procedures and biological therapies for cancer. The newer technologies include hyperthermia, photodynamic therapy, gene therapy and targeted cancer therapies (National Cancer Institute).

Chemotherapy (also described by the terms antineoplastic or cytotoxic therapy) is a treatment that involves the use of drugs for destroying the transformed cells or slowing the growth of rapidly dividing cancerous cells. Unlike radiation and surgery, which are considered to be local treatments, chemotherapy has a systemic effect as the drug enters the circulation to encounter the cancer cells wherever they are present. More than 100 FDA approved drugs are available today to be used for the treatment of cancer. If possible, cure otherwise control or palliation in the advanced stages of cancer, are the three possible goals of chemotherapy. Along with the drug specific side effect, the chemotherapy treatment is almost always accompanied by a varied range of adverse effects. Normal cells of the body which divide more rapidly like bone marrow/blood cells, cells comprising the hair follicles and the ones lining the reproductive tract and digestive tract are most likely to get damaged. The other common side effects include low RBC, WBC and platelet count, nausea and vomiting, appetite loss, constipation, diarrhea, mouth or throat sores, fatigue, heart damage, reproductive and sexual problems, damage to liver, kidney, urinary system, and much more. Permanent damage to organs, delay in development of children, nervous damage, elevated risk of secondary cancer are some of the long term adverse effects associated with the administration of these drugs (American\_Cancer\_Society, 2011).

Owing to the severe side effects associated with the use of these chemotherapeutic agents, the focus of the ongoing research is shifting from the drugs which have an systemic effect on the body to the therapies targeting molecules which either over express or differentially express in specific tumor or cancer cells and hence use the therapies which differentiate cancerous cells from normal cells of healthy tissues. Since these are more target specific, they often have lesser side effects as compared to the conventional chemotherapy drugs. Some of the biomolecules used for targeted therapies include aromatases, tyrosine kinases, serine/threonine kinases, growth factor receptors and many more enzymes which are specific for cancer cells or tissues (American\_Cancer\_Society, 2011).

Hormonal and immunotherapy are two more options available for cancer treatment. Hormonal therapy is generally used for the treatment of breast, prostate, and endometrial (uterine) cancers, which show growth in response to hormones found in the body. It makes use of sex hormones or hormones like drugs to alter the production of male or female sex hormones. It either prevents the body from producing the hormone or prevents the cancer cells from using the synthesized hormone. Immunotherapy uses the drugs which stimulate the natural immune system of a patient to recognize and attack the transformed cells. It uses two approaches: preparing body's own immune system for fighting (Active Immunotherapy) or using *ex vivo* created immune system components to be inserted into the patient's body to strengthen its defense mechanism (Passive Immunotherapy) (American\_Cancer\_Society, 2011).

Cancer is a very active area of research. Despite of having hundreds of drugs, many potential drug candidates are being proposed each day for combating the limitations of the previously known drugs. Here the need arises for a fast and reliable technique to screen a huge number of chemical products available to explore their potential therapeutic activities to cut down on time and cost involved in *in-vivo* identification of drugs. Virtual Screening is a computational approach to drug discovery that successfully complements High Throughput Screening (HTS) for hit detection (Sun, 2008). But since most of the proposed synthetic inhibitors fail to clear preclinical or clinical trial because of the drug related or drug induced toxicities, the need arises for finding natural products or their derivatives having the potential to act as inhibitors against the cancer molecular targets. Most of the natural products follow the lipinski's rule of five. Even the exceptions with high molecular weight, rotatable bonds and more stereogenic centers retain relatively low logP values. Thus, these have a high tendency to get absorbed more easily as compared to the conventional synthetic drugs. With the availability of more number of chiral centers (Feher and Schmidt, 2003) along with a wider distribution of molecular attributes like octanol-water partition coefficient, molecular mass and diversity of ring system, make natural products more suitable to be used as drugs (Lee and Schneider, 2001).

In this study we have used *in silico* approach to identify small molecule natural compounds with inhibitory activity against cancer specific molecular targets. Firstly, we have used a series of 4-methylpyridopyrimidinone derived PI3K inhibitors to develop a 3D-QSAR model and derive a relationship between the physiochemical properties and biological

activity ( $pK_i$  value) of the inhibitors. The generated model was then used to screen a dataset of natural compounds and their biological activity was predicted. The compounds with high predicted activity were then analyzed for their molecular mode of interaction with human PI3K $\alpha$ . In complex diseases like cancer, single target approach sometimes do not result in desired outcome as the transformed cells find for an alternate pathway to compensate for the loss. In such cases, multi target approach is more efficient for a significant modification in the environment of cancer cells. With this perspective in mind, secondly we have proposed another natural compound with potential to simultaneously inhibit three cancer specific targets- Fatty acid synthase, Phosphatidylinositol 3-kinase (p110 $\alpha$ ) and Skp2 component of SCF E3 Ubiquitin Ligase. Lastly, we have reported a molecule of natural origin that shows the ability to stimulate body's own immune system to fight against cancerous cells by activating NK cells through TLR3 receptor.



# Chapter 1

QSAR study on a series of 4-methylpyridopyrimidinone derived PI3K inhibitors for finding more potent drug candidates against PI3K

## INTRODUCTION

PI3K signaling plays an important role in several cellular processes critical for cancer progression, including metabolism, growth, survival, and motility. There are three classes of PI3Ks according to their structure and function. Class IA of PI3Ks has been most clearly implicated in human cancer (Yuan and Cantley, 2008). Class IA PI3Ks consist of a regulatory subunit and a catalytic subunit. Three mammalian genes, *PIK3R1*, *PIK3R2*, and *PIK3R3* encode p85 $\alpha$  (p85 $\alpha$ , p55 $\alpha$ , and p50 $\alpha$  isoforms), p85 $\beta$ , and p55 $\gamma$  regulatory subunits respectively, which are collectively referred to as p85 (Engelman *et al.*, 2006; Katso *et al.*, 2001; Yuan and Cantley, 2008). The catalytic isoforms- p110 $\alpha$ , p110 $\beta$ , and p110 $\gamma$ , are the products of three genes, *PIK3CA*, *PIK3CB*, and *PIK3CD*. Many studies have shown that *PIK3CA* and *PIK3R1* are somatically mutated in cancers, promoting activation of the PI3K pathway (Ikenoue *et al.*, 2005; Mizoguchi *et al.*, 2004; Philp *et al.*, 2001; Samuels and Velculescu, 2004).

Class IA PI3Ks are activated by growth factor stimulation through receptor tyrosine kinases (RTKs) (Kang *et al.*, 2006; Skolnik *et al.*, 1991; Zhao and Vogt, 2008). The regulatory subunit, p85, directly binds to phosphotyrosine residues on RTKs and/or adaptors (Carpenter *et al.*, 1993). This binding relieves the intermolecular inhibition of the p110 catalytic subunit by p85 and localizes PI3K to the plasma membrane where its substrate, Phosphatidylinositol-4,5-bisphosphate (PIP2), resides (Carpenter *et al.*, 1993; Zhao and Vogt, 2008). More recently, somatic mutations in *PIK3CA* have been identified in a variety of human tumors, including breast, colon, and endometrial cancers and glioblastomas. Expression of these *PIK3CA* mutants leads to increased oncogenic potential in vitro and in vivo (Isakoff *et al.*, 2005). They cause constitutive signaling along the PI3K pathway in the absence of growth factors and therefore seem to obviate the usual obligate interactions with tyrosine phosphorylated RTKs and/or adaptors. Expression of mutated *PIK3CA* in fibroblasts and mammary epithelial cells has been shown to result in transformation, growth factor-independent proliferation, and resistance to apoptosis (Isakoff *et al.*, 2005; Zhao *et al.*, 2005). In another experiment it was shown that lung-specific induction of the kinase-domain mutant p110 $\alpha$  H1047R lead to the development of lung adenocarcinomas in transgenic mice (Engelman *et al.*, 2008).

Inhibition of PI3K signaling can diminish cell proliferation, and in some circumstances, promote cell death. A number of PI3K pathway inhibitors have been developed and are being evaluated in preclinical studies and in early clinical trials (Courtney *et al.*, 2010). Many *in silico* approaches have come up with the ability to improve upon the existing drug candidates and modify them to make them more potent with better affinity for the target. Quantitative structure activity relationship (QSAR) is one such powerful approach being used to establish a correlation between the physicochemical properties of the chemical compounds and their biological activity to obtain a reliable statistical model. This model serves as a valuable tool for the design of new chemical entities and to predict their activity. The QSAR model so developed facilitates identification of promising lead candidates, thus

decreasing the number of compounds required to be synthesized and tested *in vitro* (Verma *et al.*, 2010).

PF-04691502 has been reported to be a highly potent and selective ATP competitive kinase inhibitor of class 1 PI3Ks, and has progressed to phase I/II clinical trials for the treatment of solid tumors (Cheng *et al.*, 2010; Yuan *et al.*, 2011). PF-04691502, derived from 4-methylpyridopyrimidinone (MPP) series was shown to exhibit potent *in vitro* activity against class I PI3K isoforms with mPI3K $\alpha$  K<sub>i</sub> of 0.57 nM (Cheng *et al.*, 2013). A series of MPP derivatives was synthesized with different heteroaryl groups, cis or trans-cyclohexyl and terminal alcohol or terminal amide. Table 1 mentions MPP derived compound series so developed along with their K<sub>i</sub> values. We have used this congeneric series containing 23 compounds for building the 3D-QSAR model to identify the molecular features essential for effective interaction between the inhibitors and the active cleft of the PI3K $\alpha$ . The model thus generated using the same series of representative inhibitors was then used to predict the activity of a large dataset of natural compounds. The compounds whose predicted biological activity was greater than the most potent inhibitor of the congeneric series were then analyzed using *in silico* docking studies to elucidate their molecular mode of interaction with the target protein molecule, PI3K $\alpha$ .

## REVIEW OF LITERATURE

### *PI3K signaling pathway*

The PI3K family of lipid kinases phosphorylates the 3'OH group of phosphatidylinositols. There are three classes of PI3K, each with its own substrate specificity and distinct lipid products (Engelman *et al.*, 2006; Katso *et al.*, 2001; Zhao and Vogt, 2008). The Class IA of PI3Ks is the most widely implicated class in cancer. Class I<sub>A</sub> PI3Ks primarily phosphorylate phosphatidylinositol-4,5-bisphosphate (PIP<sub>2</sub>) on the plasma membrane to generate the second messenger, phosphatidylinositol-3,4,5-trisphosphate (PIP<sub>3</sub>). Class I<sub>A</sub> PI3Ks are heterodimers that consist of a p85 regulatory and a p110 catalytic subunit. There are several isoforms of both the catalytic (p110 $\alpha$ , p110 $\beta$  and p110 $\delta$ ) and regulatory (p50 $\alpha$ , p55 $\alpha$ , p85 $\alpha$ , p85 $\beta$  and p55 $\gamma$ ) subunits. Class I<sub>A</sub> PI3Ks are most often activated by receptor tyrosine kinase (RTK) signaling, although the p110 $\beta$ -containing enzymes might also be activated by G protein-coupled receptors (Kurosu *et al.*, 1997; Roche *et al.*, 1998). The p85 regulatory subunit is crucial in mediating class IA PI3K activation by RTKs. The Src-homology 2 (SH2) domains of p85 bind to phosphotyrosine residues in the sequence context pYxxM (in which a 'pY' indicates a phosphorylated tyrosine) on activated RTKs, as in the case of platelet-derived growth factor receptors, or on adaptor molecules, such as ERBB3 or GRB2-associated binding protein 1. This binding of SH2 domains serves both to recruit the p85–p110 heterodimer to the plasma membrane, where its substrate PIP<sub>2</sub> resides, and to relieve basal inhibition of p110 by p85 (Yu *et al.*, 1998). The 3'-phosphatase PTEN dephosphorylates PIP<sub>3</sub> and therefore terminates PI3K signaling. Accumulation of PIP<sub>3</sub> on the cell membrane leads to the colocalization of signaling proteins with pleckstrin

homology (PH) domains. This leads to the activation of these proteins and propagation of downstream PI3K signaling. Akt and phosphoinositide-dependent protein kinase 1 (PDK1) directly bind to PIP<sub>3</sub> and are thereby recruited to the plasma membrane. The phosphorylation of Akt at T308 (which is in the activation loop of Akt) by PDK1 and at S473 (which is in a hydrophobic motif of Akt) by mTOR complex 2 (mTORC2) results in full activation of this protein kinase (Sarbasov *et al.*, 2005). In turn, Akt phosphorylates several cellular proteins, including glycogen synthase kinase 3 $\alpha$  (GSK3 $\alpha$ ), GSK3 $\beta$ , forkhead box transcription factors (FoxO), MDM2, BCL2-interacting mediator of cell death (BIM) and BCL2-associated agonist of cell death (BAD) to facilitate cell survival and cell cycle entry (Bader *et al.*, 2005; Cantley, 2002; Shaw and Cantley, 2006). Although Akt is the PI3K effector that is most widely implicated in cancer, there are Akt-independent pathways activated by PI3K, which include the Bruton tyrosine kinase (BTK); the Tec families of non-receptor tyrosine kinases; serum- and glucocorticoid-regulated kinases (SGKs) (Qiu and Kung, 2000); and regulators of small GTPases that are implicated in cell polarity and migration (Cain and Ridley, 2009). However, the roles of these Akt-independent pathways in human cancer are currently less well defined.

#### *PI3K activation in cancer*

The PI3K signaling pathway is inappropriately activated in many cancers. To date, the two most widely observed mechanisms of PI3K activation in human cancers are activation by receptor tyrosine kinases (RTKs) and somatic mutations in specific components of the signaling pathway. More recently, somatic activating mutations were identified in the class IA PI3K catalytic subunit, p110 $\alpha$  (encoded by *PIK3CA*) (Samuels *et al.*, 2004). Somatic mutations in *PIK3CA* occur in around 30% of some types of common epithelial cancers, which includes breast, colon, prostate and endometrial cancers. It is not yet clear whether *PIK3CA* mutations are early or late genetic events in cancer progression. However, a recent study of *in situ* and invasive breast cancers suggests that *PIK3CA* mutations arise before the development of an invasive phenotype (Dunlap *et al.*, 2010). Most mutations (~80%) reside in one of two hotspot regions in the kinase domain and the helical domain. These mutant p110 $\alpha$  subunits increase *in vitro* lipid kinase activity, maintain PI3K signaling under conditions of growth factor deprivation and can transform cells. Recently, it was found that the expression of the kinase domain mutant H1047R of p110 $\alpha$  in mouse lungs induced adenocarcinomas *in vivo* (Engelman *et al.*, 2008). The two classes of *PIK3CA* mutations promote constitutive PI3K signaling through distinct mechanisms. In the wild-type PI3K holoenzyme, p85 inhibits p110 $\alpha$  through an intermolecular interaction, and this inhibition is relieved by a conformational change that is induced by the engagement of the p85 amino-terminal SH2 domain with phosphotyrosines (Yu *et al.*, 1998). X-ray crystal data and molecular modeling studies suggest that the helical domain mutants E545K and E542K abrogate this inhibitory intermolecular interaction between p85 and p110 (Huang *et al.*, 2007; Miled *et al.*, 2007). Accordingly, the activity of the helical domain p110 $\alpha$  mutant was not increased by the presence of tyrosine phosphorylated peptides *in vitro* (Carson *et al.*, 2008). The kinase domain mutant H1047R is located near the activation loop and seems to promote constitutive PI3K signaling through a different mechanism.

### *p110 $\alpha$ as a target for isoform specific inhibitors*

The PI3K inhibitors can be divided into isoform-specific inhibitors or pan-PI3K inhibitors. The pan-PI3K inhibitors target all class IA PI3Ks in the tumor. However, a theoretical advantage of isoform-specific inhibitors is that they might be tolerated at doses that result in complete target inhibition without producing untoward side effects, such as immunosuppression and glucose intolerance. Indeed, isoform-specific inhibitors might be particularly effective in certain cancers; for example, p110 $\alpha$ -specific inhibitors might effectively shut off PI3K signaling in cancers with *PIK3CA* mutations. In addition, recent data suggest that p110 $\alpha$  might be the predominant catalytic isoform in vasculogenesis, and that specific p110 $\alpha$  inhibitors might block angiogenesis (Graupera *et al.*, 2008). Furthermore, a preliminary study that compared isoform-selective PI3K inhibitors suggests that p110 $\alpha$  might be the crucial PI3K isoform in breast cancers with *ERBB2* amplifications (Torbett *et al.*, 2008). Using RNA interference, one group found that silencing p110 $\alpha$ , but not p110 $\beta$  or p110 $\delta$ , led to decreased growth and increased apoptosis of medulloblastoma cells (Guerreiro *et al.*, 2008).

### *QSAR, a powerful in silico approach for lead optimization*

The most popular approaches for ligand-based drug design are the QSAR method and pharmacophore modeling. QSAR is a computational method to quantify the correlation between the chemical structures of a series of compounds and a particular chemical or biological process. The underlying hypothesis behind QSAR method is that similar structural or physicochemical properties yield similar activity (Akamatsu, 2002; Verma and Hansch, 2008). Initially a group of chemical entities or lead molecules are identified which show the desired biological activity of interest. A quantitative relationship is established between the physicochemical features of the active molecules and the biological activity. The developed QSAR model is then used to optimize the active compounds to maximize the relevant biological activity. The predicted compounds are then tested experimentally for the desired activity. The QSAR method thus can be used as a guiding tool for identification of compound modifications with improved activity. Depending on the goal of the study, the appropriate biological activity is experimentally measured for a series of compounds and this data serves as the dependent variable in QSAR modeling. Once the molecules are selected for the study they are modeled *in silico* and energy is minimized using molecular mechanics or quantum mechanical method (Bohl *et al.*, 2004; Holloway, 1998; Wade *et al.*, 2004). Next, relevant molecular descriptors are generated for the set of molecules to describe the chemical features of the molecules that are required for their biological activity. Molecular descriptors can be structural as well as physicochemical. The goal here is to create a molecular “fingerprint” for each molecule that relates to its activity. Depending on the QSAR method, knowledge-based, molecular mechanical or quantum chemical tools can be used to generate the molecular descriptors. Molecular descriptors are then used to develop a mathematical relation that can explain the variability of the biological activity of the molecules. In the final step, the developed models are subjected to various internal and external validation procedures to test their statistical significance, robustness and predictive power. Over the years the strategies to

execute these steps have evolved to make the QSAR technique an essential part of the drug optimization process (Acharya *et al.*, 2011).

## MATERIALS AND METHODS

### *Preparation of data set*

A data set consisting of 23 inhibitors of PI3K derived from 4-methylpyridopyrimidinone scaffold was taken from a previously reported study (Cheng *et al.*, 2013). The reported biological activity data ( $K_i$  values in nM) for these inhibitors was converted into logarithmic scale ( $pK_i$ ) to be used for QSAR study.

### *Molecular modeling study*

The 2D structures were sketched using VlifeEngine of VLife MDS and then converted to 3D form. The 3D structures so obtained were optimized to attain a stable conformation with minimum energy using force field batch minimization platform of VlifeEngine (VlifeMDS, 2004). Merck Molecular Force Field (MMFF) and Gasteiger charges were used with maximum number of cycles as 10000, convergence criteria (root mean square gradient) as 0.01 and dielectric constant (for vacuum) as 1.0. A structure common to all 23 inhibitors was deduced and used as template (Figure 1(A)) to align all the geometry optimized PI3K inhibitors. Alignment of all the inhibitors to the template molecule, taking compound 1 (comp1) as the reference molecule, is shown in Figure 1(B). The whole study was performed on Intel® Xeon (R) CPU E31230 @ 3.20 GHz with 8.00 GB RAM using Vlife MDS, Molecular Design Suite, version 4.3, supplied by Vlife Sciences, Pune, India.

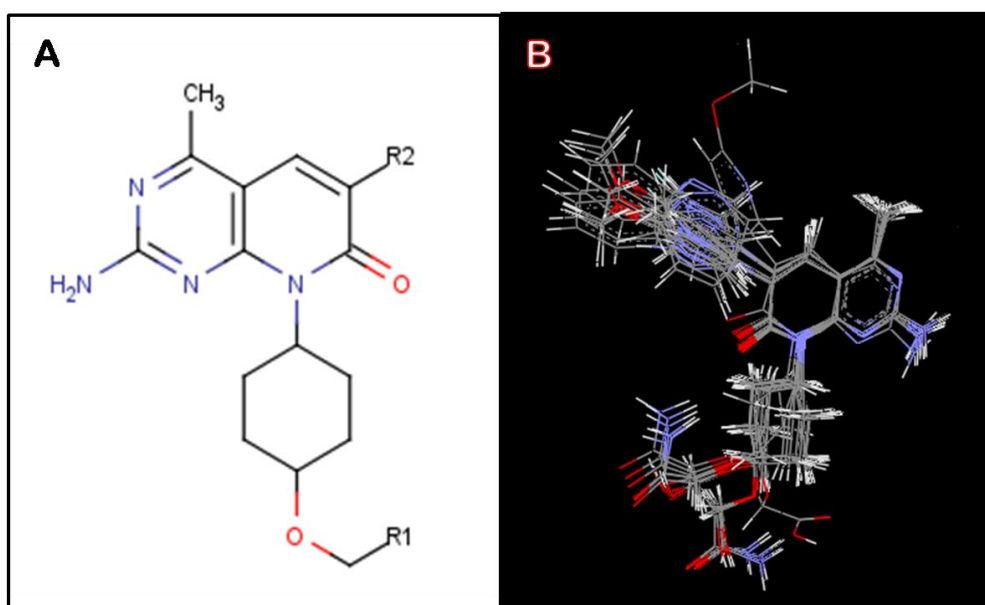


**Figure 1:** (A) Structure of template used for template based alignment of optimized molecules (B) 3D alignment of optimized PI3K inhibitors

### *Computation of values for descriptors and data selection for training and test set*

A molecular field was computed for a grid of points in space around the aligned molecules using Merck Molecular Force Field. Descriptors representing hydrophobic, electrostatic and steric energies between the atoms of the aligned molecules and a methyl probe with +1 charge placed at each lattice point of the grid were computed. These molecular descriptors describe how each of the inhibitory molecules binds to the target in its active site. For the external validation of the model, the data set was divided into training and test set using the approach of random selection to avoid any kind of bias. The training set (75% of the total molecules in the data set) with known biological activity was used to generate the 3D QSAR model. The test set, compounds of which were not included for building the model, was used to challenge the generated model to assess its predictive effectiveness.

### *3D QSAR model building*

The model was generated using statistical method of multiple regression in conjunction with stepwise forward variable selection algorithm.  $pK_i$  value was used as dependent variable and the descriptors as independent variables. Software generates a large number of molecular descriptors that can be used for the QSAR study. Because of this huge data, the choice of selection of appropriate descriptors having a considerable role in governing the biological activity of interest becomes difficult. The general purpose of multiple regression is to establish relationship between several independent or predictor variables and a dependent or criterion variable. Various parameters were set for the execution of stepwise principle component regression analysis. The cross correlation limit was set as 0.5, maximum number of variable in final equation as 3 ( $n/5$ , where  $n$  is number of compounds in training set), term selection criteria as  $r^2$ , variance cut-off as 0 and scaling as auto scaling.

### *Validation of the 3D QSAR Model*

To establish a QSAR model two types of validations are required - internal and external. For internal validation leave-one-out cross validation method was used. In this method one observation was taken as validation data and the rest of the observations made up the training set. The coefficients of QSAR model were estimated using this new training set which were then used for predicting the activity of the test compound. The procedure was repeated until all the compounds had once served as a test compound. The predictive ability of the model was then assessed using the cross validated  $r^2$  and  $q^2$  (Foldes *et al.*, 1990). External validation was done by predicting the activities of the compounds of the test set which were not used for model generation.

## *Prediction of Biological activity of 1,69,109 natural compounds using the generated 3D QSAR model*

A data set consisting of 1,69,109 natural compounds by 10 different suppliers was obtained from ZINC database (Irwin and Shoichet, 2005) in SMILES format. The pK<sub>i</sub> values were predicted for these natural compounds using the generic prediction platform of VlifeMDS. The prediction was done based on the QSAR model generated using the congeneric series consisting of 23 PI3K inhibitors. The most potent compound in this series had a pK<sub>i</sub> value of 0.506. So the natural compounds with predicted activity above this threshold were selected for further analysis as they could prove to be more potent and selective novel candidates to be used as PI3K inhibitors.

### *Protein and ligand preparation for docking studies*

The crystal structure of PI3K $\alpha$  of human origin was obtained from Protein Data Bank [PDB ID: 3HIZ] (Mandelker *et al.*, 2009). The protein structure was pre-processed by removing water molecules and all non-bonded heteroatoms using Accelrys Viewerlite 5.0 (Viewerlite\_5.0). This processed protein was further prepared using Schrödinger's protein preparation wizard (Schrödinger, 2009). Hydrogen were added and optimized to the structure. In further preparation steps bad contacts were removed, bond lengths were optimized, disulfide bonds were created, protein terminals were capped and selenomethionine residues were converted to methionine. The missing residues were fixed manually. The top two natural compounds with predictive pK<sub>i</sub> values above 0.506 were prepared for docking studies to study their molecular mode of interactions with PI3K $\alpha$ . LigPrep's ligand preparation protocol was used to prepare these natural compounds. It generated different tautomeric, stereochemical and ionization variants of the small molecules along with energy minimization and flexible filtering.

A grid was generated at the active site of the prepared protein structure using the Glide docking module of Schrödinger (Friesner *et al.*, 2004; Halgren *et al.*, 2004). Prepared natural compounds were subjected to docking using Glide's HTVS protocol. The two top scoring compounds were investigated to study their molecular interactions with the protein. The hydrophobic interactions and H-bonds were calculated using the Ligplot program (Wallace *et al.*, 1995). H-bonds were taken into consideration when the distance between acceptor–donor atoms was less than 3.3 Å, with maximum hydrogen-acceptor atom distance of 2.7 Å and acceptor-H-donor angle greater than 90°.

## **RESULTS AND DISCUSSION**

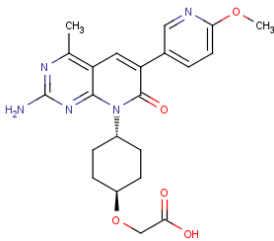
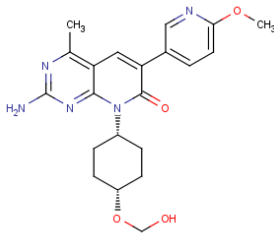
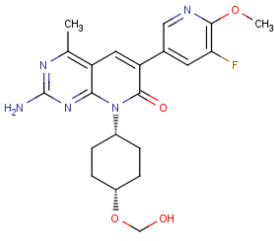
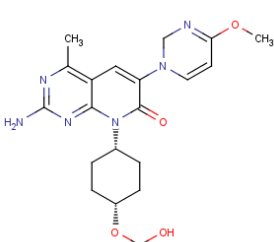
### *QSAR molecular modeling*

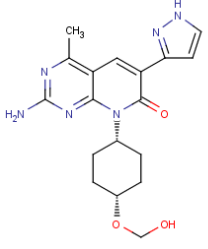
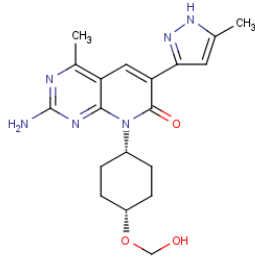
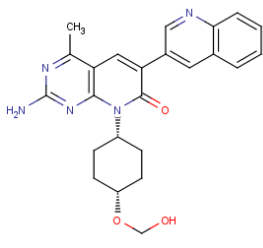
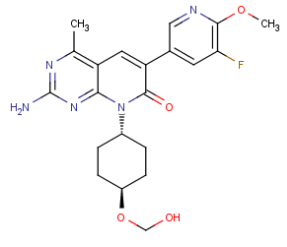
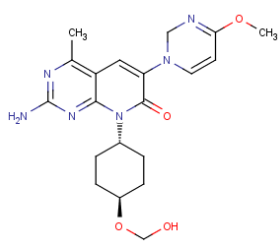
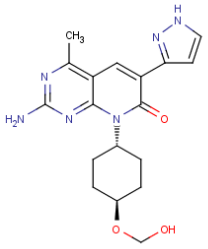
QSAR study requires ligands with experimentally measured values of the desired biological activity. The ligands should ideally be a part of a congeneric series but should also

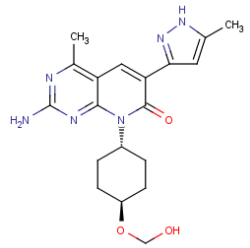
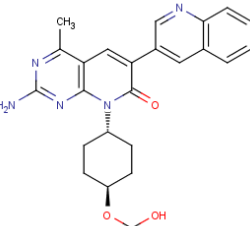
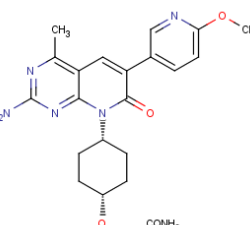
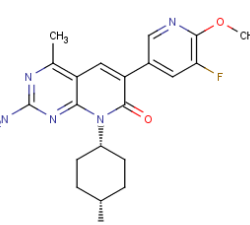
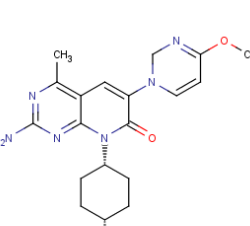
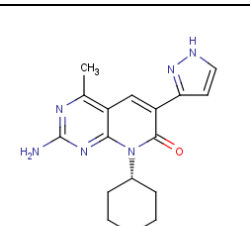


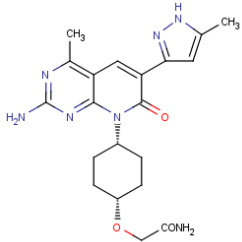
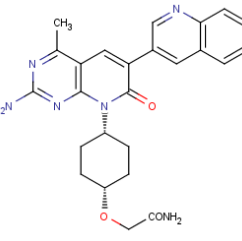
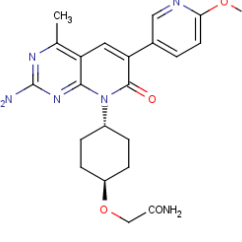
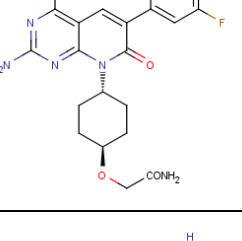
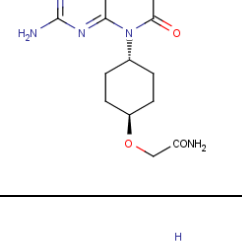
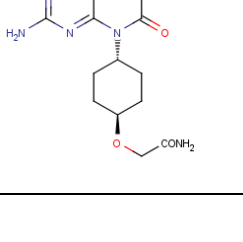
possess adequate chemical variability to have a diverse range of activity. Table 1 shows 2D structures of the 23 PI3K inhibitors of the congeneric series along with their  $K_i$  and values. After optimization and template based alignment of these compounds, descriptors representing steric, electrostatic and hydrophobic energies at all lattice points of the grid around the molecules were computed. Training and test sets were selected for MMP derivatives using random data selection method. 70 % of the total compounds i.e., 16 molecules were selected for the training set and the rest comprised the test set (7 compounds).

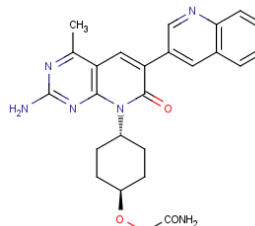
**Table 1:** The list of PI3K inhibitors along with their chemical structures,  $K_i$  and  $pK_i$  values

S. No.	cis/trans *	R <sub>1</sub>	R <sub>2</sub>	Chemical Structure	$K_i$ (nm)	$pK_i$
1.	trans	-COOH	4-MeO-3-pyridine		0.350	0.456
2.	cis	-OH	4-MeO-3-pyridine		4.510	-0.654
3.	cis	-OH	4-MeO-5-F-3-pyridine		1.180	-0.072
4.	cis	-OH	4-MeO-3-pyrimidine		2.410	-0.382

5.	cis	-OH	3-Pyrazole		13.50	-1.130
6.	cis	-OH	3-Me-3-pyrazole		26.40	-1.422
7.	cis	-OH	3-Quinoline		24.10	-1.382
8.	trans	-OH	4-MeO-5-F-3-pyridine		0.654	0.184
9.	trans	-OH	4-MeO-3-pyrimidine		1.000	0
10.	trans	-OH	3-Pyrazole		3.440	-0.537

11.	trans	-OH	3-Me-3-pyrazole		10.10	-1.004
12.	trans	-OH	3-Quinoline		1.670	-0.223
13.	cis	-CONH <sub>2</sub>	4-MeO-3-pyridine		0.7000	0.155
14.	cis	-CONH <sub>2</sub>	4-MeO-5-F-3-pyridine		1.820	-0.260
15.	cis	-CONH <sub>2</sub>	4-MeO-3-pyrimidine		6.890	-0.838
16.	cis	-CONH <sub>2</sub>	3-Pyrazole		24.80	-1.394

17.	cis	-CONH <sub>2</sub>	3-Me-3-pyrazole	 <p>The structure shows a central pyridine ring substituted at the 3-position with a methyl group and a pyrazole ring. The pyrazole ring has a methyl group at its 3-position. The pyridine ring is also substituted at the 4-position with an amino group and a methyl group. A cyclohexane ring is attached to the pyridine ring at the 2-position, and a primary amide group (-CONH<sub>2</sub>) is attached to the cyclohexane ring at the 1-position. The stereochemistry is cis.</p>	7.410	-0.870
18.	cis	-CONH <sub>2</sub>	3-Quinoline	 <p>The structure shows a central pyridine ring substituted at the 3-position with a methyl group and a quinoline ring. The pyridine ring is also substituted at the 4-position with an amino group and a methyl group. A cyclohexane ring is attached to the pyridine ring at the 2-position, and a primary amide group (-CONH<sub>2</sub>) is attached to the cyclohexane ring at the 1-position. The stereochemistry is cis.</p>	1.910	-0.281
19.	trans	-CONH <sub>2</sub>	4-MeO-3-pyridine	 <p>The structure shows a central pyridine ring substituted at the 3-position with a methyl group and a pyridine ring. The pyridine ring has a methoxy group (-OCH<sub>3</sub>) at its 4-position. The pyridine ring is also substituted at the 4-position with an amino group and a methyl group. A cyclohexane ring is attached to the pyridine ring at the 2-position, and a primary amide group (-CONH<sub>2</sub>) is attached to the cyclohexane ring at the 1-position. The stereochemistry is trans.</p>	0.3120	0.506
20.	trans	-CONH <sub>2</sub>	4-MeO-5-F-3-pyridine	 <p>The structure shows a central pyridine ring substituted at the 3-position with a methyl group and a pyridine ring. The pyridine ring has a methoxy group (-OCH<sub>3</sub>) at its 4-position and a fluorine atom (-F) at its 5-position. The pyridine ring is also substituted at the 4-position with an amino group and a methyl group. A cyclohexane ring is attached to the pyridine ring at the 2-position, and a primary amide group (-CONH<sub>2</sub>) is attached to the cyclohexane ring at the 1-position. The stereochemistry is trans.</p>	1.820	-0.260
21.	trans	-CONH <sub>2</sub>	3-Pyrazole	 <p>The structure shows a central pyridine ring substituted at the 3-position with a methyl group and a pyrazole ring. The pyridine ring is also substituted at the 4-position with an amino group and a methyl group. A cyclohexane ring is attached to the pyridine ring at the 2-position, and a primary amide group (-CONH<sub>2</sub>) is attached to the cyclohexane ring at the 1-position. The stereochemistry is trans.</p>	6.160	-0.790
22.	trans	-CONH <sub>2</sub>	3-Me-3-pyrazole	 <p>The structure shows a central pyridine ring substituted at the 3-position with a methyl group and a pyrazole ring. The pyrazole ring has a methyl group at its 3-position. The pyridine ring is also substituted at the 4-position with an amino group and a methyl group. A cyclohexane ring is attached to the pyridine ring at the 2-position, and a primary amide group (-CONH<sub>2</sub>) is attached to the cyclohexane ring at the 1-position. The stereochemistry is trans.</p>	21.80	-1.338

23.	trans	-CONH <sub>2</sub>	3-Quinoline		5.740	-0.760
-----	-------	--------------------	-------------	--	-------	--------

\* Relative stereochemistry of the two substituents on cyclohexyl

Stepwise forward algorithm in combination with multiple regression analysis (SW-MR) was used to generate the model. The model developed by SW-MR using random data selection method is shown in table 2. Table 3 shows the minimum recommended values for various statistical measures used to evaluate the model. Data fitness plot for the generated model is shown in figure 2. The plot reflected its effectiveness as all the points lied close to the regression line. Figure 3(A) and 3(B) illustrates the radar plot of observed versus predicted biological activity values for both training and test sets of the developed model. The model can be used for external predictions as it has a high predictive correlation coefficient value of 0.8520. The contour map (Figure 4(A)) provided further understanding of the relationship between structural features of MMP derivatives and their activities which could be applied to design newer potential inhibitors of PI3K.

**Table 2:** Statistics of the significant model generated using SW-MR

Parameters	Statistical Value
Training Set Size (n)	16
Test Set Size	7
Degree of freedom	12
r <sup>2</sup>	0.9215
q <sup>2</sup>	0.8146
F test	46.9577
r <sup>2</sup> se	0.1710
q <sup>2</sup> se	0.2628
pred_r <sup>2</sup>	0.8520
pred_r <sup>2</sup> se	0.2822

**Table 3:** Statistical measures with their minimum recommended values

Statistical measures	Minimum recommended values
K	number of descriptors in a model (statistically n/5 descriptors in a model)
Df	degree of freedom (n-k-1) (higher is better)
q <sup>2</sup>	cross-validated r <sup>2</sup> (>0.5)
q <sup>2</sup> se	Error term for q <sup>2</sup>
pred_r <sup>2</sup>	r <sup>2</sup> for external test set (>0.5)
pred_r <sup>2</sup> se	Error term for pred_r <sup>2</sup>

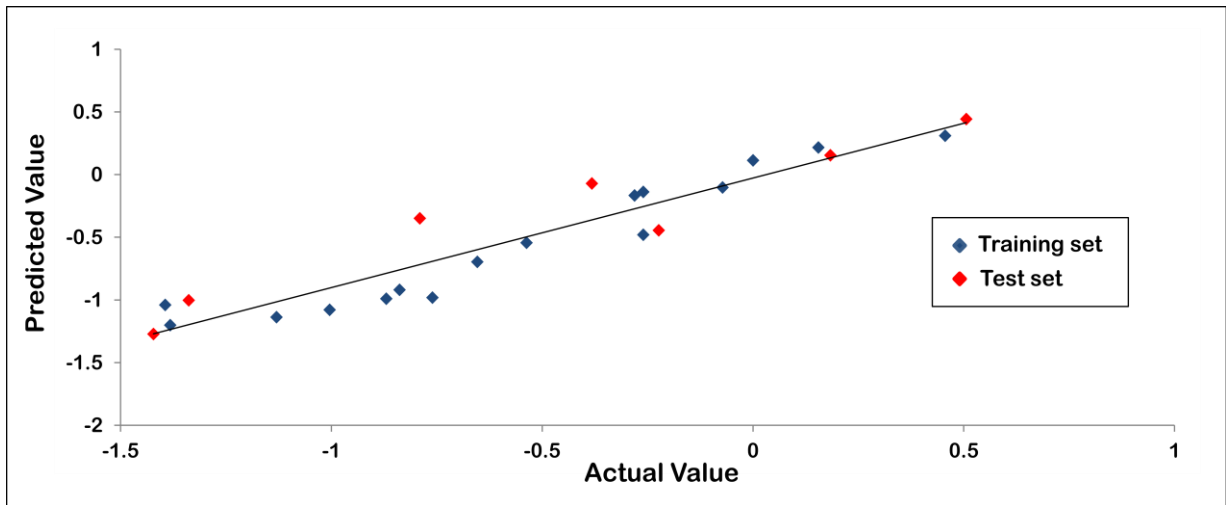


**Figure 2:** Data fitness plot for the 3D QSAR model generated

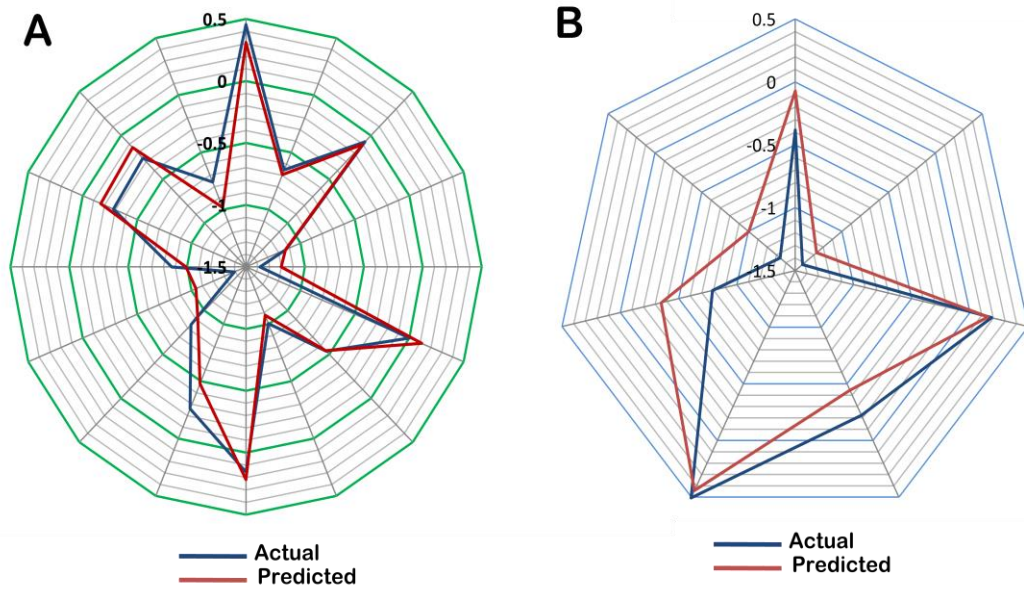


**Figure 3:** Graph of actual and predicted biological activity for (A) training (B) test set

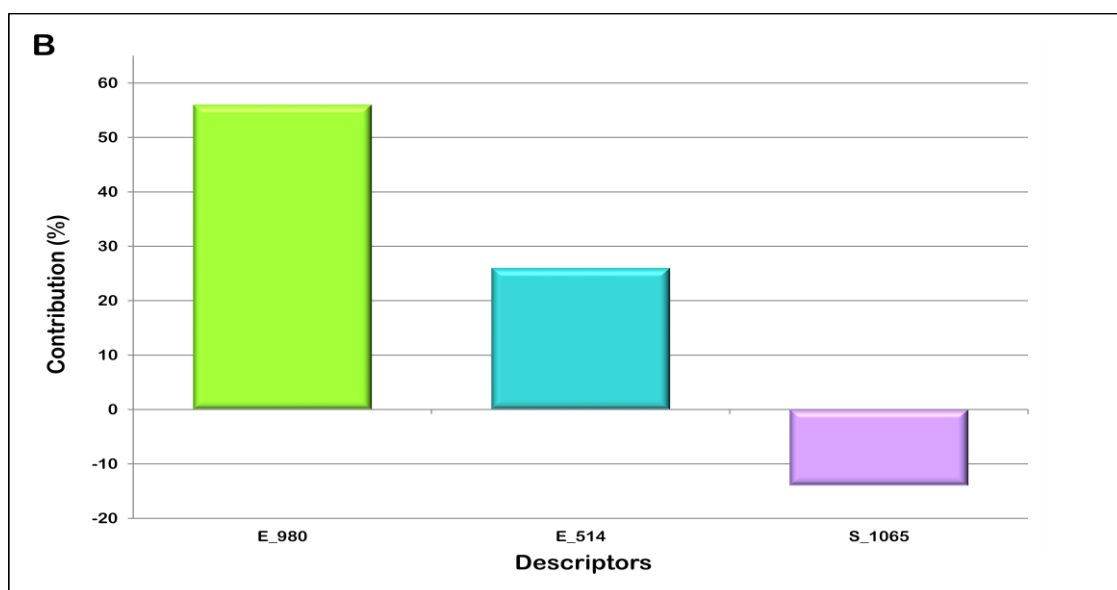
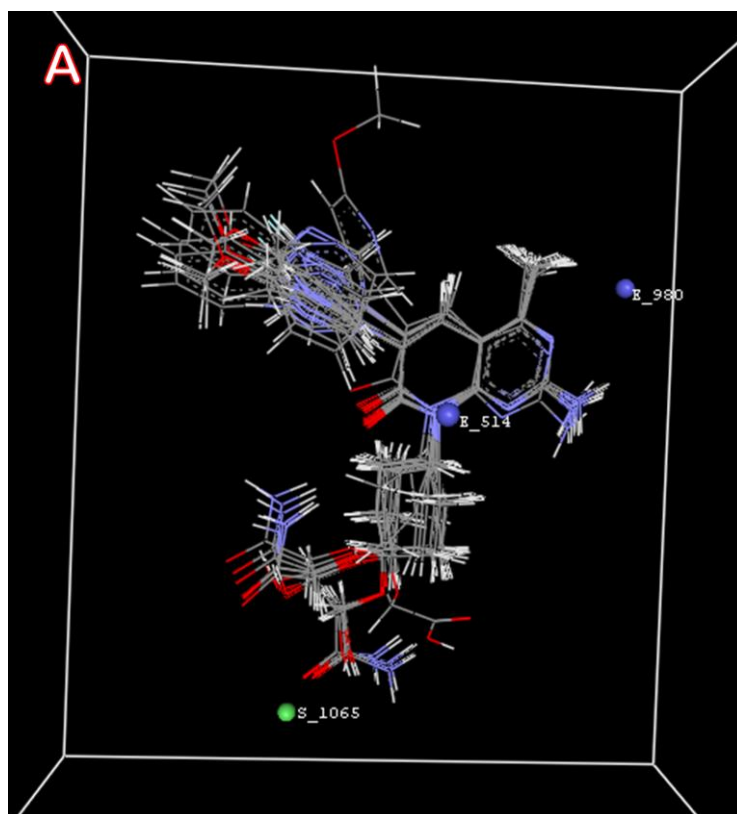


**Figure 4:** (A) 3D-alignment of molecules with the important steric and hydrophobic points contributing to the biological activity of the ligands (B) Graph showing the contribution of molecular descriptors in controlling the activity of the inhibitors

### *Interpretation of the built 3D QSAR model*

The model had a good internal as well as external predictive power as indicated by the  $q^2$  value of 0.9215 and predicted  $r^2$  of 0.8520 respectively. It was observed that steric and hydrophobic descriptors at grid points E\_514, E\_980 and S\_1065 play important role in imparting inhibitory activity against PI3K. Figure 4(B) illustrates the contribution of these descriptors in controlling the activity of the inhibitors. The correlation between the molecular descriptors representing the physiochemical parameters of the ligands and their biological activity is given by the following equation:

$$pKi = 0.0950 E_{514} + 0.5878 E_{980} - 0.1425 S_{1065} - 0.3019$$

The positive coefficient of E\_514 and E\_980 indicated that positive electrostatic potential is preferred in that region and hence substitution of more electrostatic groups will result in increased activity of the compounds. Presence of charged or polar groups around these grid points would be preferred for effective inhibitor design. Steric field descriptor (S\_1065) had a negative coefficient which suggested that the presence of small groups in this region would enhance the activity of the inhibitors. Descriptor at position E\_980 was contributing the most towards the inhibitory activity of the compounds. The model provided a 3D fingerprint of the compounds which helped in developing a relationship of physiochemical parameters with structure and biological activity, making it capable of predicting activities of novel compounds. Thus, the 3D QSAR model generated was used for predicting the biological activity of 1,69,109 naturally occurring chemical compounds.

### *Prediction of biological activity for a large dataset comprising of 1,69,109 natural compounds*

A special subset of ZINC database consisting of 1,69,109 small molecules of natural origin was downloaded. The generated model had the statistical characteristics which proved it to be quite effective for external predictions. The generic prediction platform in 3D QSAR module of VlifeMDS was used to predict the activity values of these natural compounds. Table 4 lists the natural compounds which had the predicted  $pK_i$  value greater than that of the most potent PI3K inhibitor (comp19 with  $pK_i$  of 0.506) of the congeneric series.

### *Interaction analysis of the predicted natural compounds using in silico docking studies*

The two top scoring natural compounds with predicted  $pK_i$  value greater than 0.506, were docked against the crystal structure of PI3K $\alpha$  using XP docking protocol of Glide to find their mode of interactions with the target protein. Interactions between comp19 ( $pK_i=0.506$ ) and PI3K $\alpha$  were taken as reference (Figure 6(A)). Comp19 was forming 4 strong hydrogen bonds with Ser 774, Lys 802, Val 851 and His 855 of PI3K $\alpha$ . It also showed hydrophobic interactions with various surrounding residues of the kinase, namely Trp 780, Glu 849, Val 850, Ser 854, Gln 859, Met 922 and Asp 933 (Figure 6(B)).



**Table 4:** List of natural chemical compounds with their  $pK_i$  value predicted on the basis of the generated 3D QSAR model

S.No.	ZINC IDs of natural compounds	$pK_i$ value
1.	ZINC19371512	5.848
2.	ZINC04073321	5.720
3.	ZINC35442546	5.697
4.	ZINC35442546	5.686
5.	ZINC02412844	5.643
6.	ZINC12898750	5.638
7.	ZINC67903457	5.631
8.	ZINC68606315	5.615
9.	ZINC67912403	5.592
10.	ZINC68574511	5.591

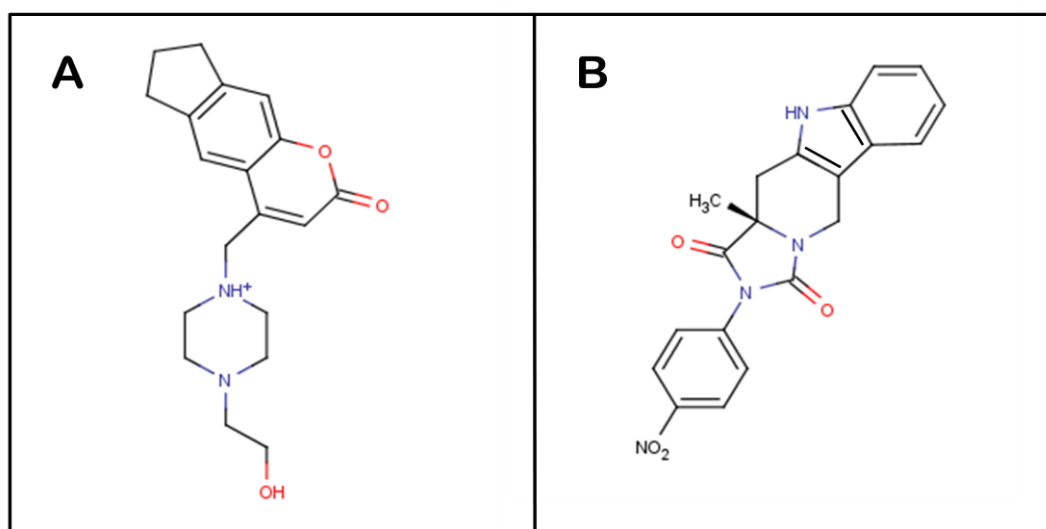


**Figure 5:** Chemical structures of (A) first natural compound, HPM (B) second natural compound, MNT

The chemical structure of two top scoring compounds is shown in Figure 5(A) and 5(B). Since all further studies have been conducted on these two compounds, they have henceforth been referred to as HPM and MNT respectively. The first compound, HPM, 4-((4-(2-hydroxyethyl) piperazin-1-yl) methyl)-7,8-dihydrocyclopenta[*g*] chromen-2(6*H*)-one had an activity value of 5.848 and showed good affinity for PI3K $\alpha$ . Trp 836 and Val 851 were involved in hydrogen bond formation while residues participating in hydrophobic interactions were Trp 780, Ile 848, Val 850, Asn 853, Ser 854, Met 922, Phe 930, Ile 932 and Asp 933 (Figure 7(A) and 7(B)). The second compound, MNT, (S)-11*b*-methyl-2-(4-nitrophenyl)-5,6,11,11*b*-tetrahydro-1*H*-imidazo[1',5':1,2]pyrido[3,4-*b*]indole-1,3(2*H*)-dione also showed good binding affinity for PI3K $\alpha$  and  $pK_i$  of 5.720. It was found forming hydrogen bond with residue Asn 853 and hydrophobic interactions with Pro 778, Trp 780, Ile 800, Lys 802, Ile

848, Val 851, Ser 854, Met 922 and Ile 932 (Figure 8(A) and 8(B)). Both the compounds were showing interaction with most of the residues which were also involved in the interaction with comp19. It was observed that all the three compounds had almost similar orientation or docking conformation, with ligands docked at the same position (Figure 9). They were occupying the same space. Hence we can strongly suggest that these two compounds can potentially inhibit PI3K $\alpha$  enzymatic activity.

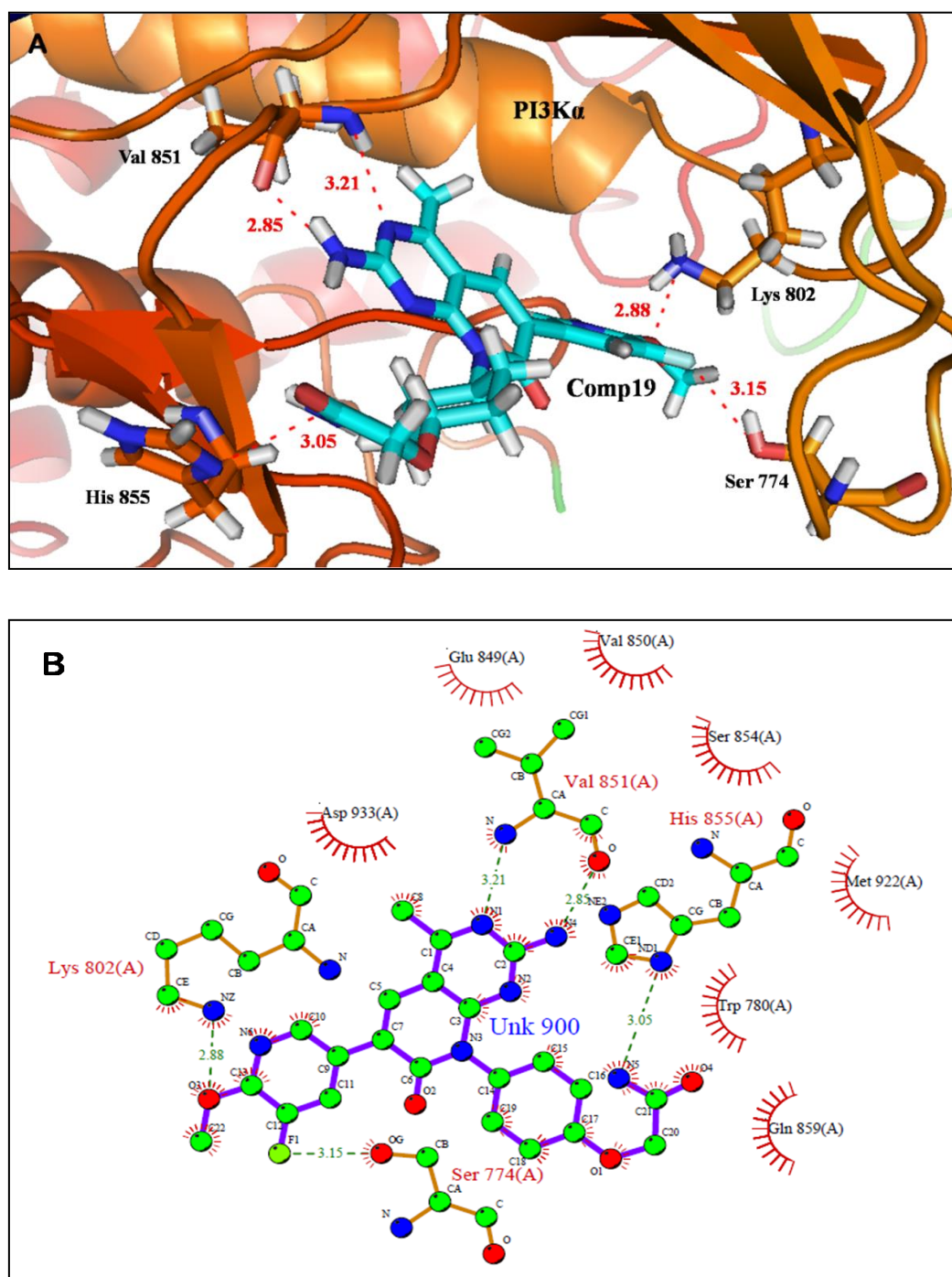


**Figure 6:** (A) Hydrogen bond interactions between comp19 and PI3K $\alpha$  (B) Ligplot showing hydrogen bond interactions and hydrophobic interactions between comp19 and PI3K $\alpha$

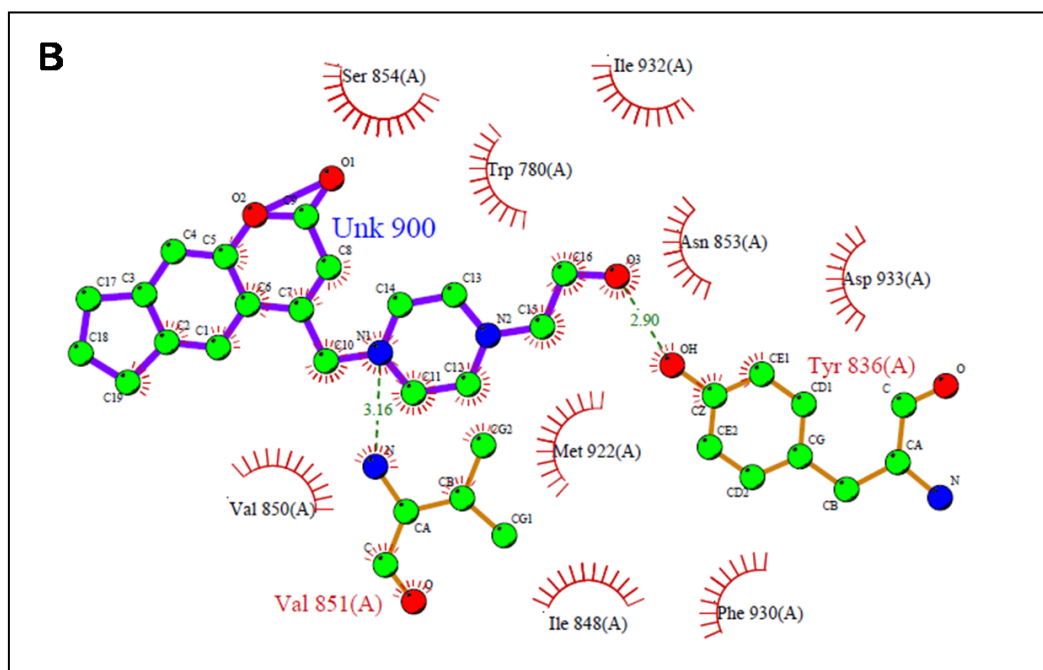
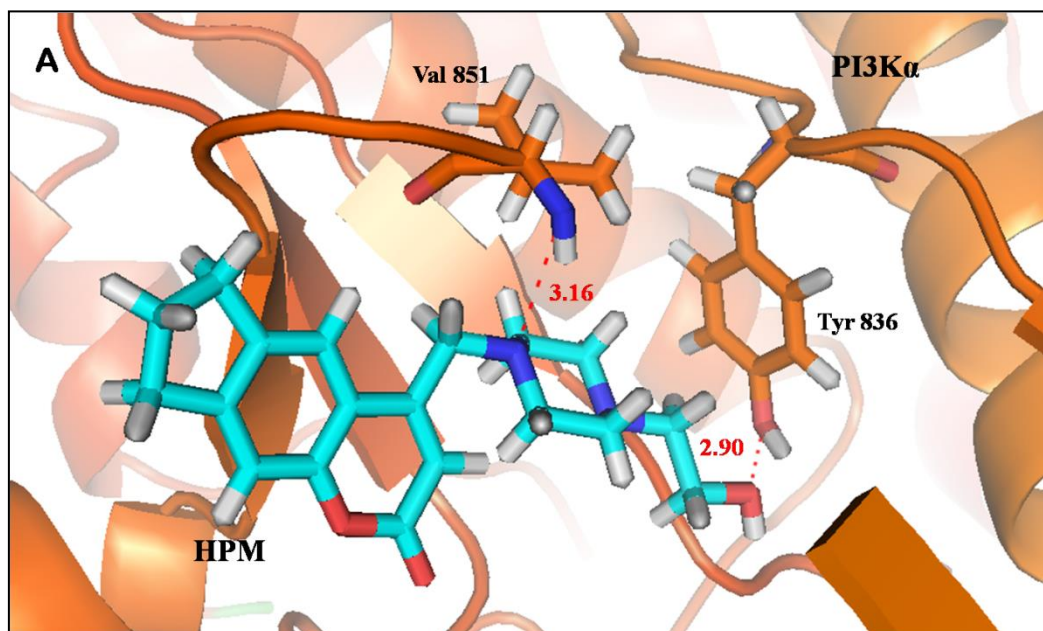


**Figure 7:** (A) Residues of PI3K $\alpha$  involved in hydrogen bond interactions with HPM (B) Ligplot showing hydrogen bond interactions and hydrophobic interactions between HPM and PI3K $\alpha$ .

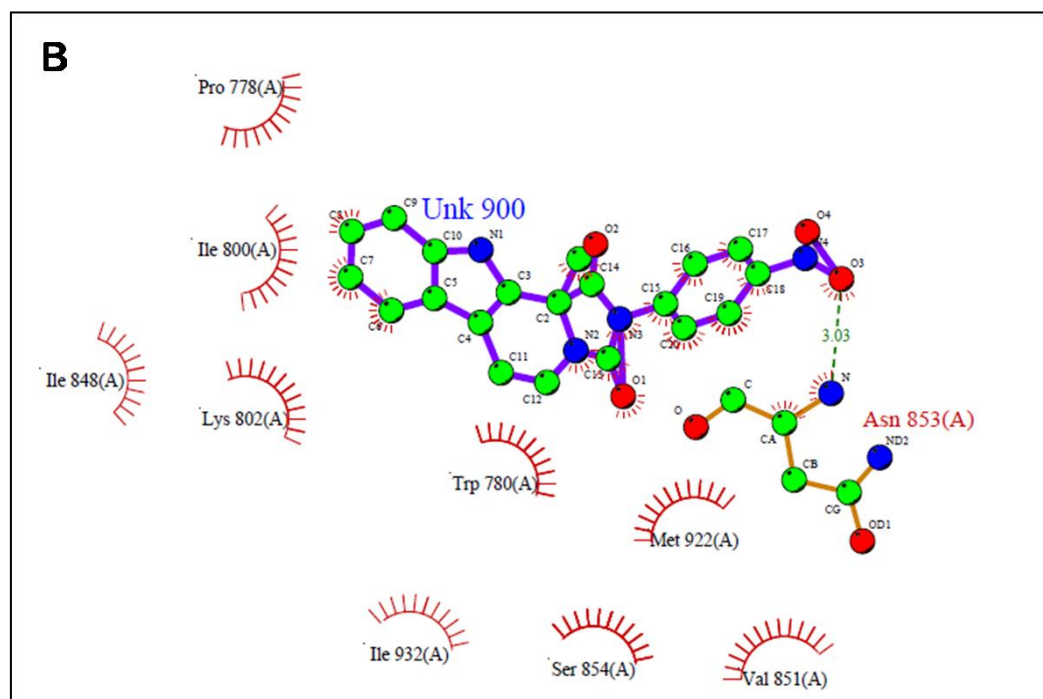
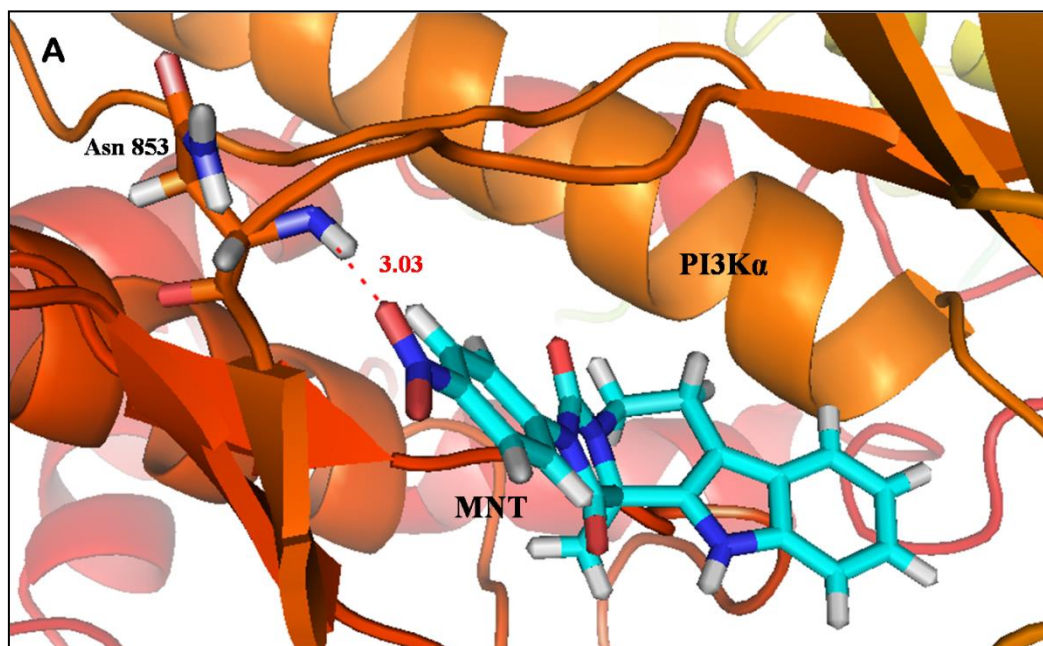


**Figure 8:** (A) Residues of PI3K $\alpha$  involved in hydrogen bond interactions with MNT (B) Ligplot showing hydrogen bond interactions and hydrophobic interactions between MNT and PI3K $\alpha$ .

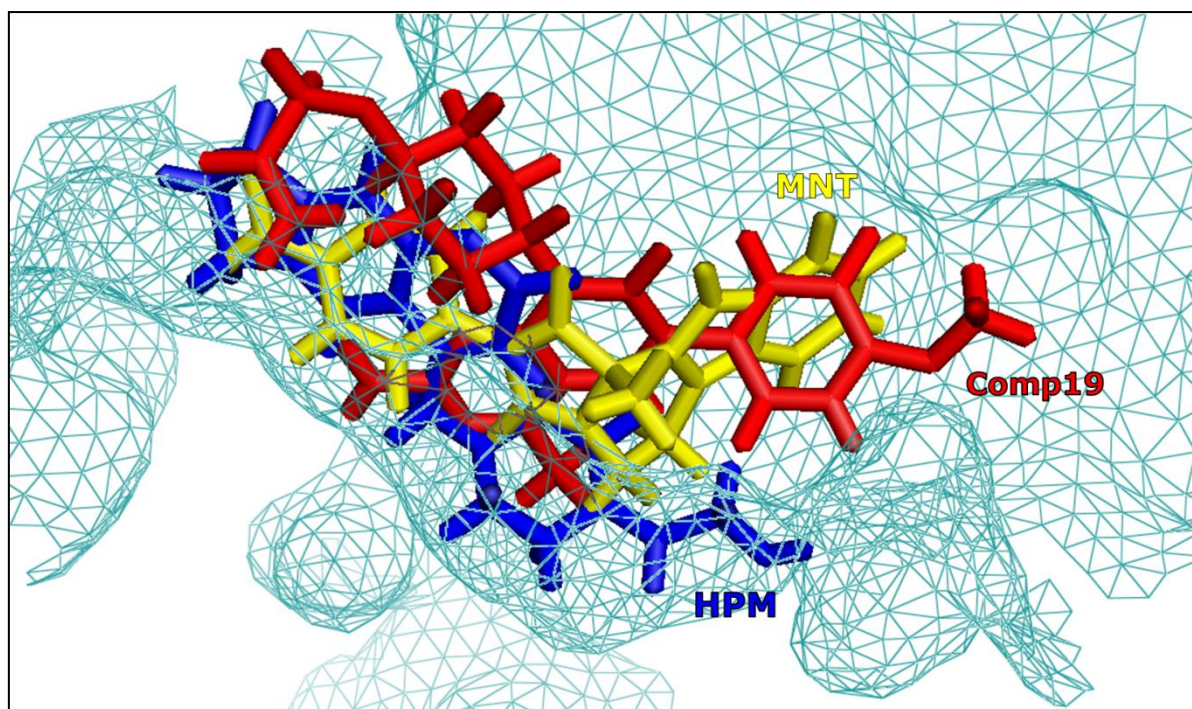


**Figure 9:** Relative position of all the three ligands in the cavity of PI3K $\alpha$

## CONCLUSION

A 3D QSAR model was generated for a congeneric series of 4-methylpyridopyrimidinone derivatives having inhibitory activity against PI3K. The model was generated using statistical method of multiple regression analysis in conjunction with stepwise variable selection method. The statistical measures  $r^2$ ,  $q^2$ , F-test and standard error for the training set and the  $\text{pred}_r^2$  for the test set fulfilled the conditions for the model to be considered robust and predictive. The developed model was used to predict the activity values for a large set of natural compounds. The top scoring compounds were analyzed to find their molecular mode of interactions with PI3K $\alpha$ . We finally reported two natural compounds HPM and MNT which had high activity value ( $\text{pK}_i$ ) of 5.848 and 5.720 respectively. They had a better affinity for PI3K $\alpha$  in comparison to the most potent compound of the congeneric series with  $\text{pK}_i$  of 0.506, as observed from the interaction pattern between these compounds and the targeted kinase. The present study provides substantial evidence for considering these natural compounds as prospective leads for the treatment of cancerous cells. Thus, 3D QSAR is an attractive discipline which not only provides graphical results that are often less attractive for scientific community but also has the ability to forecast the activity or potency of compounds being considered for inhibition of target protein. As QSAR approach already plays an important role in lead structure optimization, it is anticipated that it will soon become essential for handling large amount of data generated using combinatorial chemistry.

# Chapter 2

Computational identification of multi-target drug to treat tumors: Hitting fatty acid synthase, phosphatidylinositol-3-kinase (p110 $\alpha$ ) and SCF E3 ubiquitin ligase.

## INTRODUCTION

The emergence of knowledge about tumor-specific molecular targets has shifted the approach of conventional cancer therapy towards targeted therapy. In contrast to conventional chemotherapy which acts on all dividing cells generating toxic effects and damage of normal tissues, targeted drugs allow to hit, in a more specific manner, subpopulations of cells directly involved in tumor progression. Although the diversity of targets giving rise to this new generation of anticancer drugs has expanded, many challenges still persist in the design of effective treatment regimens. The complex interplay of signal-transduction pathways further complicates the customization of cancer treatments to target single mechanisms. The problem of relapse, as almost invariably cancer patients developed drug resistance, is the major hindrance so far that often occurs due to the activation of alternative pathways (Sebolt-Leopold and English, 2006). Therefore, the number of successful single target drugs did not increase appreciably during the past decade. Some recent studies have suggested that partial inhibition of a small number of targets can be more efficient than the complete inhibition of a single target (Csermely *et al.*, 2005). With the approval by FDA and EMEA of Sorafenib and Sunitinib - targeting VEGFR, PDGFR, FLT-3 and c-Kit - a different scenario is emerging, where a new generation of anti-cancer drugs, able to inhibit more than one pathway, would probably play a major role (Petrelli and Giordano, 2008). In this study we have identified a novel small molecule natural compound that shows inhibitory activity against three important cancer targets- Fatty acid synthase, Phosphatidylinositol 3-kinase (p110 $\alpha$ ) and SCF E3 Ubiquitin Ligase.

Fatty acid synthase (FASN) is an important enzyme that performs lipogenesis in neoplastic tissues. Cancer or tumor cells require more energy for the rapid proliferation of cells. The glucose uptake increases in these transformed cells leading to higher production of pyruvate via glycolytic pathway. This pyruvate is utilized for the generation of more ATP using Krebs cycle. The intermediate product, acetyl-CoA acts as a substrate for FASN enzyme. Lipogenesis leads to the production of long-chain fatty acids from acetyl-CoA and malonyl-CoA. Most of the normal cells have a low expression of FASN, that is tightly regulated by diet, hormones and growth factors. To meet the energy and lipid demands of highly proliferating cells for membrane synthesis,  $\beta$ -oxidation and lipid modification of proteins, they start *de novo* synthesis of fatty acids, thereof showing high expression of FASN. Many studies report an important role of FASN in tumor growth and survival. Knockdown or inhibition of this enzyme results in apoptosis of cancerous cells. It is believed that the selective anti tumor activity of FASN inhibitors might be due to the accumulation of toxic intermediate metabolites leading to cytostatic and cytotoxic effects. It has also been proposed that the over expression of FASN makes cells resistant to many chemotherapeutic agents. Thus, FASN blockage represents an attractive strategy for cancer treatment (Flavin *et al.*, 2010).

The Phosphatidylinositol-3-kinase (PI3K) signaling has an impact on cancer cell growth, survival, motility, and metabolism. This pathway is activated by several different

mechanisms in cancers, including somatic mutation and amplification of genes encoding key components. Class IA PI3Ks are activated by growth factor stimulation through receptor tyrosine kinases (RTKs). The regulatory subunit, p85, directly binds to phosphotyrosine residues on RTKs and/or adaptors. This binding relieves the intermolecular inhibition of the p110 catalytic subunit by p85 and localizes PI3K to the plasma membrane where its substrate, Phosphatidylinositol-4,5-bisphosphate (PIP2), resides. More recently, somatic mutations in *PIK3CA* have been identified in a variety of human tumors, including breast, colon, and endometrial cancers and glioblastomas. Expression of these *PIK3CA* mutants leads to increased oncogenic potential in vitro and in vivo. They cause constitutive signaling along the PI3K pathway in the absence of growth factors. Inhibition of PI3K signaling can diminish cell proliferation, and in some circumstances, promote cell death. A number of PI3K pathway inhibitors have been developed and are being evaluated in preclinical studies and in early clinical trials (Courtney *et al.*, 2010).

The SCF (Skp1, Cullins, F-box proteins) multisubunit E3 ubiquitin ligase, also known as CRL (Cullin-RING ubiquitin Ligase) is the largest E3 ubiquitin ligase family that promotes the ubiquitination of various regulatory proteins for targeted degradation, thus regulating many biological processes. The majority of SCF E3 ligase substrates are involved in regulation of cell cycle progression, gene transcription, signal transduction and DNA replication among others. Through targeted degradation of these substrates, SCF E3 ligases regulate many biological processes. Accumulated evidence strongly suggests that abnormal regulation of SCF E3 ubiquitin ligases contributes to uncontrolled proliferation, genomic instability, and cancer. Among the components of SCF, some are oncogenes (e.g. Skp2) that promote degradation of tumor suppressors and are amplified and/or overexpressed in human cancers, whereas others are tumor-suppressors (e.g. Fbxw7) that target the degradation of oncoproteins and are mutated in human cancers. Therefore, targeting such a specific E3 ligase component, known to be activated in human cancer would provide a high level of specificity and selectivity with less associated toxicity. Hence inhibition of cancer specific E3 ligase components can prove to be an effective approach for cancer treatment (Jia and Sun, 2011).

## **REVIEW OF LITERATURE**

### *Use of multiple target drug design strategy*

Agents that affect one target only ('single hits') might not always affect complex systems in the desired way even if they completely change the behavior of their immediate target. For example, single targets might have 'back-up' systems that are sometimes different enough not to respond to the same drug, and many cellular networks are robust and prevent major changes in their outputs despite dramatic changes in their constituents (Ocampo *et al.*, 2002; Papp *et al.*, 2004). Therefore despite considerable progress in genome- and proteome-based high-throughput screening methods and rational drug design, the number of successful single target drugs did not increase appreciably during the past decade (Szuromi *et al.*, 2004).



Several highly efficient drugs, such as non-steroidal anti-inflammatory drugs (NSAIDs), salicylate, metformin or Gleevece, affect many targets simultaneously. Furthermore, combinatorial therapy, which represents another form of multi-target drugs, is used increasingly to treat many types of diseases, such as AIDS, cancer and atherosclerosis (Borisy *et al.*, 2003; Huang, 2002; Kaelin, 2004). Snake and spider venoms are both multi-component systems and plants also employ batteries of various factors to fence off pathogenic attack; thus, the use of multiple molecules is apparently an evolutionary success story. Finally, traditional medical treatments often use multi-component extracts of natural products. Based on these examples (Agoston *et al.*, 2005) it could be proposed that systematic drug-design strategies should be directed against multiple targets, and that this novel drug-design paradigm might often result in the development of more-efficient molecules than the currently favored single-target drugs. Development of a multi-target drug is likely to produce a drug that interacts with lower affinity than a single-target drug because it is unlikely that a small, drug-like molecule will bind to a variety of different targets with equally high affinity. However, low-affinity drug binding is apparently not a disadvantage. For example, memantine (a drug used to treat Alzheimer's disease) and other multi-target noncompetitive NMDA receptor antagonists show that low affinity, multi-target drugs might have a lower prevalence and a reduced range of side-effects than high-affinity, single-target drugs (Lipton, 2004; Rogawski, 2000). Most components of cellular protein, signaling and transcriptional networks are in 'weak linkage' with each other (Rogawski, 2000). A 'weak linker' is an interacting partner that binds with low affinity or only transiently to the other partner. Thus, most multi-target drugs are weak linkers. Because most links in cellular networks are weak, a low-affinity multi-target drug might be sufficient to achieve a significant modification (Csermely, 2004).

#### *FASN, a potential cancer target*

Fatty acid synthase (FASN) is a key biosynthetic enzyme involved in lipogenesis and the production of long-chain fatty acids from acetyl-coenzyme A (CoA) and malonyl-CoA. Uptake of glucose into cancer cells leads to the production of pyruvate via the glycolytic pathway. Pyruvate is utilized to produce ATP via the Krebs cycle in the mitochondria; in turn, acetyl-CoA, one of the products, acts as a substrate for neoplastic lipogenesis. Normal cells (except liver and adipose tissue) have low levels of expression and activity of FASN, which is tightly regulated by diet, hormones and growth factors (Menendez and Lupu, 2007). However, in rapidly proliferating cancer cells, fatty acids can be synthesized *de novo* in order to provide lipids for membrane formation and energy production via  $\beta$ -oxidation and lipid modification of proteins. As such, FASN is highly expressed in many cancers, including prostate, ovarian, breast, endometrial, thyroid, colorectal, bladder, lung, thyroid, oral, tongue, esophageal, hepatocellular, pancreatic and gastric carcinomas, as well as malignant melanoma, mesothelioma, nephroblastoma and retinoblastoma, soft tissue sarcoma (Kuhajda, 2000, 2006; Menendez and Lupu, 2004, 2006, 2007; Menendez *et al.*, 2005; Swinnen *et al.*, 2006), gastrointestinal stromal tumor (Rossi *et al.*, 2006), Paget's disease of the vulva (Alo *et al.*, 2005) and multiple myeloma (Wang *et al.*, 2008). Interestingly, increased FASN expression has also been observed in some benign and pre-invasive lesions of prostate,

breast, lung, stomach, colon and cutaneous nevi (Innocenzi *et al.*, 2003; Kuhajda, 2000; Kusakabe *et al.*, 2002; Milgraum *et al.*, 1997; Piyathilake *et al.*, 2000). Elevated expression of FASN has been linked to poor prognosis (Ogino *et al.*, 2008; Rossi *et al.*, 2003; Shurbaji *et al.*, 1996; Takahiro *et al.*, 2003; Visca *et al.*, 2004). In addition, several reports have demonstrated that FASN plays an important role in tumor cell development and survival, with siRNA knockdown or pharmacological inhibition of FASN resulting in apoptosis of cancer cells and prolonged survival of xenograft tumors (De Schrijver *et al.*, 2003; Graner *et al.*, 2004; Kridel *et al.*, 2004; Pizer *et al.*, 2000). Overexpression studies in immortalized non-transformed human prostate epithelial cells and in transgenic mice have demonstrated that FASN is a *bonafide* oncogene in prostate cancer (Migita *et al.*, 2009), and similarly in breast cancer, fatty acid biosynthesis induces a cancer-like phenotype in noncancerous epithelial cells that is dependent on HER1/HER2 signaling (Vazquez-Martin *et al.*, 2008). A potential mechanism of FASN oncogenicity may involve cytoplasmic stabilization of  $\beta$ -catenin with palmitoylation of Wnt-1 and subsequent activation of the WNT/ $\beta$ -catenin pathway (Fiorentino *et al.*, 2008).

Recently, the crystal structure and catalytically active sites of FASN have been delineated. FASN is made up of a paired multifunctional polypeptide with seven catalytic domains. These domains (in linear order from the carboxy terminus) are: thioesterase, acyl-carrier protein,  $\beta$ -ketoacyl reductase, enoyl reductase,  $\beta$ -hydroxyacyl dehydratase, acetyl/malonyl-CoA transferase and  $\beta$ -ketoacyl synthase. There are two additional non enzymatic domains: a pseudoketoreductase; and a peripheral pseudomethyltransferase, which is probably a remnant of an ancestral methyltransferase domain maintained in some related polyketide synthases (Maier *et al.*, 2008b). Substrate shuttling is facilitated by flexible tethering of the acyl carrier protein domain and by the limited contact between the condensing and modifying portions of the multi subunit enzyme, which are mainly connected by linkers rather than direct interaction (Flavin *et al.*, 2010; Maier *et al.*, 2008). Initial work by Maier *et al.* resolved the 4.5-Å crystal structure of intact porcine FASN (Maier *et al.*, 2006); while, later, the crystal structure of mammalian FASN at 3.2-Å resolution, covering five catalytic domains, was determined (however, the flexibly tethered terminal ACP and thioesterase domains remained unresolved) (Maier *et al.*, 2008b). A significant step forward was the determination of the crystal structure of the thioesterase domain from human FASN in complex with the orlistat ligand (Pemble *et al.*, 2007). Importantly, natural product inhibitors of the ketoreductase domain and small-molecule inhibitors of the  $\beta$ -ketoacyl synthase and thioesterase domains have been described as having anti-oncogenic properties.

A conserved set of chemical reactions are employed by all organisms for fatty acid biosynthesis (Smith and Tsai, 2007; White *et al.*, 2005). Stepwise elongation of precursors is achieved by cyclic decarboxylative condensation of acyl-coenzyme A (CoA) with the elongation substrate malonyl-CoA, initiated by the starter substrate acetyl-CoA. In the priming step, the acetyl transferase loads acetyl-CoA onto the terminal thiol of the phosphopantetheine cofactor of the acyl carrier protein (ACP), which passes the acetyl moiety over to the active site cysteine of the  $\beta$ -ketoacyl synthase (KS). Malonyl transferase transfers the malonyl group of malonyl-CoA to ACP, and the KS catalyzes the

decarboxylative condensation of the acetyl and malonylmoieties to an ACP-bound  $\beta$ -ketoacyl intermediate. The  $\beta$ -carbon position is then modified by sequential action of the NADPH (the reduced form of nicotinamide adenine dinucleotide, NADP<sup>+</sup>)–dependent  $\beta$ -ketoreductase, a dehydratase, and the NADPH-dependent enoyl reductase to yield a saturated acyl product elongated by two carbon units. This acyl group functions as a starter substrate for the next round of elongation, until the growing fatty acid chain reaches a length of 16 to 18 carbon atoms and is released from ACP. In mFAS, the malonyl and acetyl transferase reactions are catalyzed by a single bifunctional protein domain, the malonylacetyl transferase, and the products are released from ACP as free fatty acids by a thioesterase (TE) domain (Smith and Tsai, 2007).

Fatty acid synthase is an attractive potential target for cancer therapy. To date, several compounds are known to inhibit FASN. These include cerulenin, C75, orlistat, C93 and naturally occurring polyphenols. Cerulenin and C75, both early small-molecule FASN inhibitors, have demonstrated significant antitumor activity. Cerulenin, isolated from *Cephalosporium caerulens*, contains an epoxy group that reacts with the ketoacyl synthase domain of FASN (Funabashi *et al.*, 1989). It was one of the first compounds to be found to inhibit FASN in breast cancer cell lines, inducing programmed cell death, and to delay disease progression in a xenograft model of ovarian cancer (Pizer *et al.*, 1996a; Pizer *et al.*, 1996b). C75 was designed after cerulenin to overcome its chemical instability (Kuhajda *et al.*, 2000). C75 is a weak, irreversible inhibitor of FASN that interacts with the  $\beta$ -ketoacyl synthase, the enoyl reductase and the thioesterase domains (Rendina and Cheng, 2005). C75 showed tumor growth inhibition in a xenograft breast cancer model (Pizer *et al.*, 2000) and chemopreventive activity for mammary cancer in transgenic mice (Alli *et al.*, 2005). More potent analogs of C75 have also been designed as FASN inhibitors (Wang *et al.*, 2009). Several natural plant-derived polyphenols have been shown to inhibit FASN, including epigallocatechin-3-gallate (EGCG) and the flavonoids luteolin, taxifolin, kaempferol, quercetin and apigenin (Brusselmans *et al.*, 2005; Li and Tian, 2004; Tian, 2006). One of the best characterized polyphenol FASN inhibitors is EGCG, a natural component of green tea. EGCG is a high micromolar time-dependent inhibitor of FASN ketoacyl reductase domain (Wang and Tian, 2001). Although EGCG is a promiscuous inhibitor targeting multiple signaling pathways (Khan *et al.*, 2006), its apoptosis-inducing effect seems to correlate with its activity at FASN (Brusselmans *et al.*, 2003). Another compound, luteolin, has the greatest effect on lipogenesis of the polyphenols and inhibits FASN directly. It has structural homology to PI3K inhibitors and has strong antioxidant activity (Brusselmans *et al.*, 2005). Recently, more potent analogs of EGCG have been developed and have been shown to inhibit tumor growth in a breast cancer xenograft model (Puig *et al.*, 2009). Orlistat is a US FDA-approved pancreatic lipase inhibitor, originally developed as an antiobesity drug, and is a potent inhibitor of FASN. Kridel *et al.* first identified orlistat in a proteomic screen for prostate cancer-specific enzymes as a potent FASN inhibitor showing antiproliferative activity against several prostate cancer cell lines *in vitro*, as well as tumor growth inhibition in a xenograft prostate cancer model (Kridel *et al.*, 2004). Orlistat is an irreversible inhibitor forming a covalent adduct with the active serine of FASN thioesterase domain as shown in a published co-crystal structure (Pemble *et al.*, 2007). In addition to the original report, orlistat

has shown modest anticancer activity in a few *in vivo* models. Inhibition of tumor FASN activity by orlistat reduces prostate tumor growth in mice xenografts and, at a high concentration, reduces proliferation and promotes apoptosis in the mouse metastatic melanoma cell line B16-F10 (helping reduce the number of mediastinal lymph node metastases) and HER2-overexpressing breast cancer cell lines. Further evidence indicates that orlistat can accelerate tumor cell apoptosis in culture at high concentrations and increase survival rates somewhat in gastric tumor-bearing mice *in vivo* (Dowling *et al.*, 2009). However, orlistat suffers from several limitations hampering its development as a systemic drug: low cell permeability, low solubility, lack of selectivity (Hoover *et al.*, 2008), poor oral bioavailability and poor metabolic stability (Zhi *et al.*, 1996). Several orlistat analogs have been developed in an attempt to improve on these limitations (Zhang *et al.*, 2008). C93 (or FAS93), a synthetic FASN inhibitor designed after the bacterial FabB inhibitor thiolactomycin, was recently developed as part of an effort to overcome C75's lack of potency and side effects (McFadden *et al.*, 2005). C93 has shown some significant tumor growth delay in non small-cell lung cancer xenograft models and ovarian cancer xenograft models, as well as some chemopreventive effects in chemically induced lung tumors (Orita *et al.*, 2007; Zhou *et al.*, 2007). Importantly, C93 did not cause anorexia and weight loss in treated animals (Orita *et al.*, 2007). Several recent reports describe new potent FASN inhibitors identified through high-throughput screening or medicinal chemistry programs. For example, a research group at Merck developed a series of 3-aryl-4-hydroxyquinolin-2(1H)-one derivatives while another research group at AstraZeneca developed a series of bisamide derivatives as FASN inhibitors (Rivkin *et al.*, 2006). FASN inhibition initiates selective apoptosis of cancer cells both *in vivo* and *in vitro*, which may involve accumulation of toxic intermediary metabolite malonyl-CoA with reduction of both membrane synthesis and phospholipid function leading to both cytostatic and cytotoxic effects (Thupari *et al.*, 2001).

Multidrug resistance is a significant problem in cancer chemotherapy and, importantly, FASN overexpression seems to be a recently identified mechanism of multidrug resistance in cancer. Liu *et al.* identified that ectopic overexpression of FASN induced drug resistance in breast cancer cell lines MCF7 and MDA-MB-468; use of orlistat sensitized these cells to anticancer therapy. The proposed mechanism is FASN overexpression may lead to a decrease in drug-induced apoptosis due to an overproduction of palmitic acid (Liu *et al.*, 2008a). This phenomenon of FASN-induced drug resistance may be exploited therapeutically through the use of FASN inhibitors solely or in combination with other chemo-therapeutic agents.

#### *Targeting PI3K signaling in cancer*

Phosphatidylinositol 3-kinases (PI3Ks) represent a family of lipid kinases that plays a key role in signal transduction, cell metabolism and survival (Engelman, 2009; Vanhaesebroeck *et al.*, 2010). The PI3K family is divided into three classes, I, II and III, based on their substrate specificity and structure. Among them, class I PI3K seems to be the most relevant in cancer. Class I PI3K has a catalytic subunit (p110) and a regulatory subunit (p85) that stabilizes p110 and inactivates its kinase activity at basal state. Physiologically,

PI3K transduces signals received from activated tyrosine kinase receptors (RTK), G protein-coupled receptors (GPCR) or from activated RAS. Upon receipt of such signals, the p85 regulatory subunit interacts with the phosphorylated tyrosine residues of activated RTKs. This engagement then causes release of the p85-mediated inhibition of p110, such that p110 can interact with the lipid membranes to phosphorylate phosphatidylinositol-4,5-bisphosphate (PIP2) to Phosphatidylinositol-3,4,5-trisphosphate (PIP3). This reaction triggers a signaling cascade through the activation of AKT and its downstream effectors. The amount of PIP3 generated and resultant PI3K pathway activation are tightly regulated by the tumor suppressor protein, phosphatase and tensin homologue deleted on chromosome 10 (PTEN). PTEN can inactivate the PI3K pathway by converting PIP3 into PIP2. The PI3K pathway can be activated not only via RTKs, but also by RAS and GPCR. RAS can activate the PI3K pathway by its direct interaction with p110 $\alpha$ , p110 $\gamma$ , and p110 $\delta$  subunits, while GPCRs can interact with p110 $\beta$  and p110 $\gamma$  subunits (Vanhaesebroeck *et al.*, 2010).

PI3K signaling is activated in human cancers via several different mechanisms (Samuels *et al.*, 2004). Increased PI3K signaling is often due to direct mutational activation or amplification of genes encoding key components of the PI3K pathway such as *PIK3CA* and *AKT1*, or loss of *PTEN* (Ikenoue *et al.*, 2005; Samuels *et al.*, 2004). PI3K also can be activated by genetic mutation and/or amplification of upstream RTKs, and possibly by mutationally activated Ras (Yuan and Cantley, 2008). The mechanism of PI3K activation in an individual cancer may suggest the most effective type of therapeutic to inhibit the pathway. More recently, somatic mutations in *PIK3CA* have been identified in a variety of human tumors, including breast, colon, and endometrial cancers and glioblastomas (Samuels and Velculescu, 2004; Shayesteh *et al.*, 1999). Most of these mutations cluster to two hot spot regions in exons 9 and 20 (Samuels and Velculescu, 2004). Exon 20 encodes the catalytic domain of p110 $\alpha$ , and mutations in this domain may constitutively activate its enzymatic activity. Exon 9 encodes the helical domain of p110 $\alpha$ , and these mutations de-repress an inhibitory interaction between the N-terminal SH2 domain of p85 and the p110 $\alpha$  catalytic subunit (Huang *et al.*, 2007). A smaller cluster of mutations is also found in the N-terminal p85 interacting domain. Interestingly, these mutations increase the lipid kinase activity of p110 $\alpha$  but do not appear to alter the interaction between p110 $\alpha$  and p85 $\alpha$  (Ikenoue *et al.*, 2005). Expression of these *PIK3CA* mutants leads to increased oncogenic potential in vitro and in vivo (Bader *et al.*, 2006). They cause constitutive signaling along the PI3K pathway in the absence of growth factors and therefore seem to prevent the usual interactions with tyrosine phosphorylated RTKs and/or adapters. Some studies have suggested that the presence of these mutations confers resistance to therapies targeting RTKs. Expressing mutated *PIK3CA* in fibroblasts and mammary epithelial cells results in transformation, growth factor-independent proliferation, and resistance to apoptosis. Additionally, transgenic mice with lung-specific induction of the kinase-domain mutant p110 $\alpha$  H1047R develop lung adenocarcinomas. Mutations in the p85 regulatory subunit *PIK3R1* have also been observed in a variety of human cancers, including glioblastomas, ovarian cancers, and colorectal cancers. Mutations in *PIK3R1* generally produce either truncations or in-frame deletions that often localize to the inter-SH2 domain of p85 $\alpha$ . Structural analyses suggest that the iSH2 domain of p85 interacts with the C2 domain of p110. Thus, it seems likely that these p85 $\alpha$

mutations also activate PI3K signaling by relieving the inhibitory effect of p85 on p110. Laboratory studies suggest that these mutations also lead to constitutive PI3K signaling (Engelman, 2009). In addition to its effects on cell growth, proliferation and survival, class IA PI3K regulates glucose metabolism through insulin signaling (Sopasakis *et al.*, 2010). It is commonly deregulated in cancer through mutations or amplifications of the PIK3CA gene or through alterations in the function of upstream tumor suppressors such as PTEN. About 80% of the mutations of the PIK3CA gene are clustered in three hotspots in the p110 $\alpha$  gene that encodes the catalytic subunit: two in the helical domain (E542K and E545K) and one in the kinase domain (H1047R). PIK3CA mutations are oncogenic, as they can induce the generation of tumors in several preclinical models without other molecular aberrations. In addition to experiments in genetically engineered mice, the first generation of PI3K $\alpha$ -specific inhibitors, while less isoform selective than the more recent compounds, have been instrumental in defining the biologic role of different PI3K isoforms in normal and cancer cells. However, these agents have provided only inconclusive data on their antitumor activity in cell lines harboring PIK3CA mutations compared to those that are PIK3CA wild-type. One of the main reasons is the limited number of cell lines in which these compounds have been evaluated. Cell lines without PIK3CA mutations often harbor alterations in oncogenic tyrosine kinase receptors, such as ERBB2 amplification, which preferentially uses the p110 $\alpha$  isoform for signal transduction. However, some of the cell lines harboring PIK3CA mutations had additional molecular aberrations, some of which are known mechanisms of resistance. The new PI3K $\alpha$ -isoform specific inhibitors have shown promising activity in cell lines harboring PIK3CA mutations. Several new generation PI3K $\alpha$ -selective inhibitors are currently being evaluated in phase I clinical trials, including BYL719 (NCT01219699), INK-1114 (NCT01449370) and GDC-0032 (NCT01296555). The clinical results of the dose escalation part of the phase I trial investigating BYL719 have recently been presented. Trial enrollment was restricted to patients with solid tumors harboring PIK3CA mutations or amplifications. This population was selected based on the higher antitumor activity observed in preclinical models with PIK3CA mutations or amplifications using the Cancer Cell Line Encyclopedia. This was the first reported study of a PI3K inhibitor in which molecular prescreening was undertaken starting from the dose escalation part. From a safety perspective, the most commonly observed adverse effects associated with BYL719 were hyperglycemia, nausea, fatigue, rash and gastrointestinal toxicities, all of which are also frequently encountered with the pan-PI3K inhibitors. A relevant question is whether an isoform-selective PI3K inhibitor is able to achieve greater target inhibition than pan-PI3K inhibitors while producing a similar degree and extent of side effects. At present, there is a paucity of published preclinical data comparing any of the PI3K $\alpha$ -selective inhibitors currently in clinical development with pan-isoform PI3K inhibitors. While early results from phase I trial of BYL719 appear encouraging, direct comparison of the preliminary efficacy results achieved with this agent against those reported with the pan-isoform PI3K inhibitors would be invalid, as none of the early phase trials involving pan-PI3K inhibitors have been specifically designed to evaluate only the PIK3CA mutant population (Brana and Siu, 2012).

### *SCF E3 ubiquitin ligases as anticancer targets*

The ubiquitin-proteasome system (UPS) regulates many biological processes through timely degradation of diverse cellular proteins. It, therefore, plays an essential role in maintaining homeostasis and in response to environmental stimuli (Hershko *et al.*, 2000). UPS-targeted protein degradation requires substrate ubiquitination, which is a multi-step enzymatic process catalyzed by a cascade of enzymes, including ubiquitin-activating enzyme E1, ubiquitin-conjugating enzyme E2, and ubiquitin ligase E3. While E1 and E2 activate and transfer ubiquitin in the reaction, E3 recognizes the substrate and catalyzes the covalent attachment of ubiquitin to the substrate (Ciechanover, 1998). Multiple runs of this reaction result in polyubiquitination of substrate. The fate of ubiquitinated proteins is determined, however, by the nature of ubiquitin attachment and the type of isopeptide linkage of the polyubiquitin chain. While the K48-linked polyubiquitination predominantly targets protein for degradation after being recognized by the proteasome, the K63-linked polyubiquitination and mono-ubiquitination normally alters protein function, cellular localization, enzyme activity, DNA repair, or interaction with other proteins (Pickart, 2000). The SCF multisubunit E3 ligase complex, consisting of Skp-1, Cullins, F-Box proteins and RBX/ROC RING finger proteins, is the largest family of ubiquitin ligases that promote the degradation of about 20% of UPS-regulated proteins, including cell cycle regulatory proteins, transcription factors, oncoproteins and tumor suppressors among others. The crystal structure of SCF-RBX complex revealed that Cul-1 acts as a scaffold that binds at its N-terminus the Skp-1 and F-box protein and at its C-terminus the RING protein RBX1. It is well established that the substrate specificity of SCF complex is determined by the F box proteins that bind to Skp1 and Cullins through its F-box domain and to substrates through its WD40 or leucine rich domains, whereas the core SCF E3 ubiquitin ligase is a complex of Cullins-RBX/ROC, in which RBX binds to E2 and facilitates ubiquitin transfer from E2 to substrates. Furthermore, the activity of SCF E3 ubiquitin ligases requires cullin neddylation, which disrupts inhibitory binding of cullin by CAND1. In the human genome, there are 69 F-box proteins, including WD40 domain containing FBXWs, leucine-rich repeats-containing FBXLs and other diverse domains-containing FBXOs, seven cullins (Cul-1, -2, 3, 4A, 4B, -5, and -7) and two RING proteins, RBX1/ROC1 and RBX2/ROC2, also known as SAG (Sensitive to Apoptosis Gene). Cullin-based assembly of SCF E3 ligase subunits can be classified into four categories: Cul1-Skp1-F-box, Cul2/5-Elongins-B/C-VHL/SOCS box, Cul3-BTB, and Cul4A/B-DDB1-DWD, making SCF/CRL the largest family of E3 ubiquitin ligases, responsible for the degradation of ~20% of all proteins subjected to proteasomal degradation (Jia and Sun, 2011).

The majority of SCF E3 ligase substrates are involved in regulation of cell cycle progression, gene transcription, signal transduction and DNA replication among others (Jia and Sun, 2009; Nakayama and Nakayama, 2006). Through targeted degradation of these substrates, SCF E3 ligases regulate many biological processes. Accumulated evidence strongly suggests that abnormal regulation of SCF E3 ubiquitin ligases contributes to uncontrolled proliferation, genomic instability, and cancer (Nakayama and Nakayama, 2006). Among the components of SCF, some are oncogenes (e.g. Skp2) that promote degradation of tumor suppressors and are amplified or overexpressed in human cancers, whereas others are

tumor-suppressors (e.g. Fbxw7) that target the degradation of oncoproteins and are mutated in human cancers (Frescas and Pagano, 2008; Nalepa *et al.*, 2006).

F-box proteins are the substrate-recognizing subunits of SCF E3 ligase which determine the substrate specificity of SCF. A single F-box protein can recognize and target multiple substrates (e.g. Skp2 targets p27, p21, p57), whereas the same substrate can be recognized and targeted by different F-box proteins (e.g. cyclin E targeted by both Skp2 and Fbxw7). More interestingly, a single F-box protein can target the degradation of several substrates with opposite biological functions (e.g. Skp2 targets p21/p27 as well as cyclin A/D1/E) (Skaar *et al.*, 2009). Thus, when or whether a particular substrate is targeted for degradation by a given F-box protein will likely be cell context dependent, leading to different biological consequences. Among ~70 F-box proteins in the human genome, only three are well studied: oncogenic Skp2, tumor suppressive Fbxw7, and  $\beta$ -TrCP, which could be tumor suppressive as well as oncogenic in a substrate dependent manner (Frescas and Pagano, 2008; Welcker and Clurman, 2008). Skp2 recognizes and promotes the degradation of several negative cell cycle regulators, including p27, p21, p130 and p57 (Deshaies and Joazeiro, 2009; Nakayama and Nakayama, 2006; Petroski and Deshaies, 2005). Skp2 is overexpressed in many human cancer types with associated p27 decrease and poor prognosis, seen in gastric cancer, colon cancer, and breast cancer (Jia and Sun, 2011). Tissue specific expression of Skp2 in mouse prostate gland caused hyperplasia, dysplasia and low-grade carcinoma (Shim *et al.*, 2003), whereas targeted expression of Skp2 in the T-lymphoid lineage co-operated with activated N-Ras to induce T cell lymphomas with a short latent period and high penetrance (Latres *et al.*, 2001). Furthermore, a knock-in mouse model showed a crucial role of Skp2 dependent degradation of p27 for the progress of colon adenomas to carcinoma (Timmerbeul *et al.*, 2006). Interestingly, in a mouse knockout model, although Skp2 disruption on its own does not induce cellular senescence, Skp2-null environment facilitates tumor-suppressive senescence response upon inactivation of tumor suppressor genes or aberrant proto-oncogenic signals. Consistently, down-regulation of Skp2 using an anti-sense oligonucleotide or siRNA silencing inhibited growth of melanoma (Katagiri *et al.*, 2006), oral cancer cells (Kudo *et al.*, 2005), glioblastoma cells and lung cancer cells (Lee and McCormick, 2005; Sumimoto *et al.*, 2005). Thus, pharmacological inhibitors of the Skp2 pathway would be of therapeutic value for cancer treatment.

One of the approach that can be used to screen for the inhibitors of SCF E3 ubiquitin ligase or its components is to disrupt interaction between SCF components, such as disruption of Cks1-Skp2 interaction (Hao *et al.*, 2005; Huang *et al.*, 2005) for p27 accumulation, or to disrupt interaction between F-box proteins and their tumor suppressive substrates (e.g.  $\beta$ -TrCP vs. I $\kappa$ B) (Chen *et al.*, 2008; Xu *et al.*, 2005). Recently, a small molecule inhibitor, CpdA, was identified from a biochemical-based screening using *in vitro* transcribed/translated and 35S-labeled p27, and an *in vitro*-reconstituted system incorporating purified cyclin E/Cdk2, Skp2, Skp1, Cul1, Roc1, and HeLa cell extract. CpdA was found to prevent incorporation of Skp2 into the SCF E3 ligase and to induce G1 arrest as well as p27-dependent cell killing *via* induction of autophagy. Furthermore, CpdA sensitized



multiple myeloma to a number of anticancer drugs, including dexamethasone, doxorubicin, melphalan and bortezomib (Chen *et al.*, 2008).

## **MATERIALS AND METHODS**

### *Protein preparation and dataset*

The crystal structure of TE domain of FASN [PDB ID: 1XKT] (Chakravarty *et al.*, 2004), PI3K $\alpha$  [PDB ID: 3HIZ] (Mandelker *et al.*, 2009) and Skp2 component of SCF E3 ubiquitin ligase [PDB ID: 2AST] (Hao *et al.*, 2005) of human origin were downloaded for Protein Data Bank. Crystal water molecules and all non-bonded heteroatoms including the docked ligand were removed from the protein structure using Accelrys Viewerlite 5.0 (Viewerlite\_5.0). The proteins were prepared using Schrödinger's protein preparation wizard (Schrödinger, 2009). Hydrogen bonds were added and optimized to the structure. Other preparation steps involved removal of bad contacts, optimization of bond lengths, creation of disulfide bonds, capping of protein terminals and conversion of selenomethionine to methionine. The missing residues were fixed manually.

A data set consisting of 1,69,109 natural compounds by 10 different suppliers was downloaded from ZINC database in SMILES format (Irwin and Shoichet, 2005). This dataset was then prepared using LigPrep's ligand preparation protocol. It generates different tautomeric, stereochemical and ionization variants of the small molecules along with energy minimization and flexible filtering. These prepared protein and small molecule dataset was then used further for virtual screening and docking studies.

### *High throughput virtual screening and docking studies*

A grid was generated surrounding the active residues of TE domain of prepared FASN protein structure using the Glide docking module of Schrödinger (Friesner *et al.*, 2004; Halgren *et al.*, 2004). Prepared data-set of natural compounds was then virtually screened against the FASN protein at desired grid coordinates using Glide model's HTVS docking protocols. The compounds above the threshold of -6.00 HTVS docking score were then selected and again subjected to docking with FASN using Glide's XP protocol for docking score refinement. The top scoring compounds above a cutoff of -8.00 XP docking score were then subject to XP docking with the skp2 component of ubiquitin ligase at the site of its interaction with cks1. The resulting top scoring compounds when then further screened against the active site of PI3K $\alpha$  protein using the same XP docking protocol. The top scoring compound was the one which showed good binding affinity for all the three target proteins at the desired sites. Thus, this compound was then inspected through MD simulations to study in detail its dynamic mode of molecular interaction with the respective protein molecules. All Glide docking studies were performed on i7 processor @ 2.8GHz with 8.00 GB RAM. Schrödinger 9 Maestro interface was compiled and run under Ubuntu 64 bits operating system.

## *Molecular dynamics simulations of ligand-bound complexes*

Desmond Molecular Dynamic System with Optimized Potentials for Liquid Simulations (OPLS) all-atom force field 2005 (Jorgensen *et al.*, 1996; Kaminski *et al.*, 2001; Xu *et al.*, 2007) was used to inspect the top scoring compounds through MD simulations. The protein-ligand complex obtained from Glide's XP docking protocol was prepared using Desmond set-up wizard. Missing residues were corrected manually. The prepared system was solvated in a triclinical periodic box of SPC water and then neutralized using an appropriate number of counter-ions. The distance between box wall and protein-ligand complex was set to more than 10Å to avoid direct interaction with its own periodic image. Energy minimization of the prepared system was done up to a maximum 10 steps using steepest descent method until a gradient threshold (25 kcal/mol/Å) is reached. Default protocol of Desmond was used to equilibrate the system. Further MD simulations were carried out on this equilibrated system for a time period of 10 ns at a constant temperature of 300K and constant pressure of 1 atm. During the simulation process, smooth particle Mesh-Ewald method was used to calculate long range electrostatic interactions. A 9 Å radius cut-off was used for coulombic short range interaction cutoff method. Frames of trajectory were captured after every 10 ps time step.

The root mean square deviation (RMSD) of the protein docked with ligand within the binding pocket was calculated for the entire simulation trajectory with reference to the first frame. The hydrophobic interactions and H-bonds were calculated using Ligplot program (Wallace *et al.*, 1995), where the H-bonds were defined as acceptor–donor atom distances of < 3.3 Å, hydrogen-acceptor atom distance of maximum 2.7Å, and acceptor-H-donor angle greater than 90°.

## **RESULTS AND DISCUSSION**

### *High Throughput virtual screening and docking studies*

After the screening of natural compound dataset against the TE domain of FASN with grid around the catalytic triad and using HTVS glide docking protocol, several hundred compounds were obtained with HTVS docking score above -6. All these ligands were then docked to the TE domain at the same grid coordinates using XP docking protocol. As a result, 5 small molecule natural compounds were obtained with XP docking score greater than -8. These selected compounds were then screened against Skp2 using the same XP docking protocol. The grid was generated around the residues which interact with the cks1, the peptide involved in recognition of p27 by Skp2 component of SCF E3 ubiquitin ligase and provide it substrate specificity. Out of those five compounds, two compounds showed considerable binding affinity for Skp2 with XP docking score above -7. These two compounds were then checked for binding affinity with the active cleft of PI3K $\alpha$ . One of the two compounds with XP docking score of -10.03 was showing very good binding affinity for PI3K $\alpha$ . Thus, (2R,3R,4S,5S,6R)-3,5-dihydroxy-2-(((Z)-4-hydroxy-3-((E)-1-hydroxy-2-((4-

hydroxybenzyl)imino)ethoxy)-1-((4-hydroxybenzyl)imino)butan-2-yl)oxy)-6-(hydroxymethyl)tetrahydro-2H-pyran-4-yl acetate (ZINC70670105, referred to as MTD) was the common compound with inhibitory nature against the TE domain of FASN (Docking score= -9.10), Skp2 (Docking score= -7.03 )and PI3K $\alpha$  (Docking score= -10.03). Figure 1 illustrates the chemical structure of MTD. Detailed analysis was done to get insights into the binding mode of interaction of MTD with each of these proteins. Since molecular docking provides only a static view of the interactions between protein and ligand, molecular dynamics simulations were performed for MTD in complex with each protein to study the dynamical behavior of the interactions.

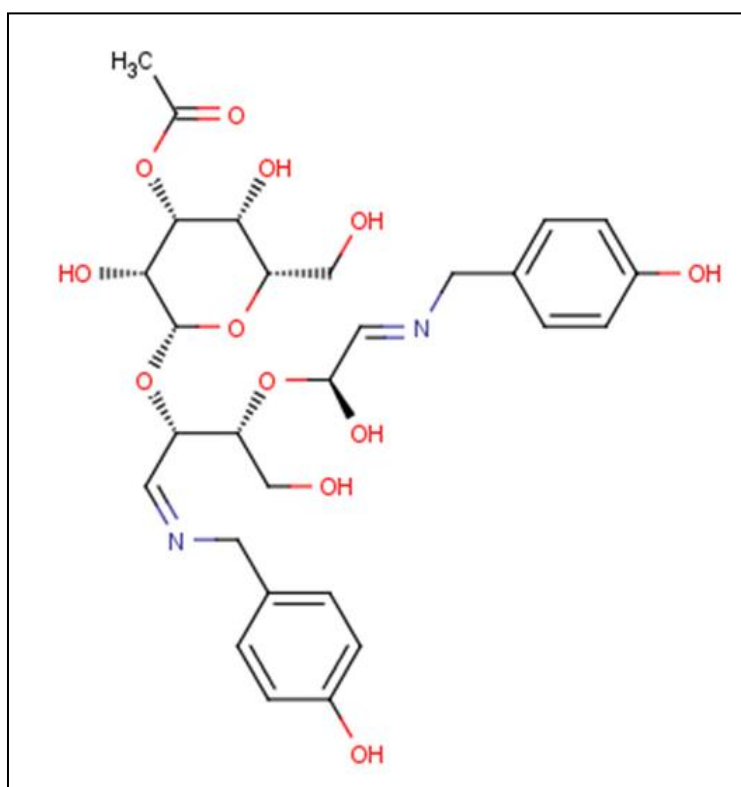


**Figure 1:** Chemical structure of MTD

#### *Interaction analysis of MTD with TE domain of FASN*

The TE carries out the chain-terminating step of fatty acid synthesis, leading to the release of palmitic acid by the hydrolysis of the acyl-S-phosphopantetheine thioester bound to the preceding acyl carrier protein (ACP) domain. However, once removed, the domain can no longer interact with the remainder of FAS to hydrolyze newly synthesized fatty acyl-S-phosphopantetheine thioester. The inhibition of FAS thioesterase (TE) was recently found to halt tumor cell proliferation and inhibit the growth of prostate tumors in mice (Kridel *et al.*, 2004).

TE is a serine active site enzyme in which the nucleophilicity of the serine residue is supported by a conserved histidine residue (Pazirandeh *et al.*, 1991). Two participants of the

catalytic triad, Ser-2308 and His-2481, were identified in the homologous chicken FAS TE by site-directed mutagenesis experiments (Pazirandeh *et al.*, 1989). The identity of third player, Asp-2338 was based on its location, where it is the only acidic residue in very close proximity to Ser-2308 and His-2481. To confirm the importance of Asp-2338, its mutation to an Ala residue was shown to eliminate TE activity (Chakravarty *et al.*, 2004).

MTD was involved in hydrophobic interaction with two of the catalytically important residues- Ser 2308 and His 2481 along with the other residues, namely Pro 2249, Tyr 2309, Phe 2370, Arg 2447 and Tyr 2462, lining the active site of TE domain (Fig. 2(A)). Strong hydrogen bonds between MTD and Ile 2250, Gln 2374, Ala 2448, Gly 2451 and Arg 2482 residues of protein were also observed (Fig. 2(B)). Hence the inhibitory activity of MTD was attributed to the blockage of active site of TE domain preventing its interaction with its natural substrate, the growing fatty acid chain. To check the dynamic stability of protein-ligand complex, TE-MTD structure was subjected to 10 ns molecular dynamics simulations. Steady RMSD graph (Fig. 3(A)) indicated the stabilization of the protein backbone during the simulation trajectory. Moreover the low RMSD values of 2.5 Å along the trajectory signified that the simulated structure did not deviated much from its initial structure during the simulations run. A shift in the position and conformation of MTD was visualized by superimposing the pre and post MD TE-MTD complexes (Fig. 3(B)). An average structure was computed for the most stable time frame, i.e., 6 to 10 ns to further analyze the changes in interaction pattern. After simulation run Asp 2338 and His 2481, two of the catalytic active residues were showing hydrophobic interactions with MTD. Other residues of TE domain involved in hydrophobic interaction included Ile 2250, Phe 2370, Ala 2448, Thr 2450, Gly 2451, Tyr 2462 and Arg 2482. Hydrogen bonds observed before MD were lost while a new hydrogen bond interaction appeared with Tyr 2343 (Fig 4(A) and 4(B)). Since MTD substantially and stably interacted with residues lining the catalytic site of TE domain including the active residues forming the catalytic triad, critical for its functioning, it can be strongly suggested that MTD can potentially inhibit FASN enzymatic activity.

Thus, the inhibition of FASN thioesterase (TE) domain would help in arresting the tumor growth as the rapidly growing cells would not be able to meet their growing energy demands for survival.

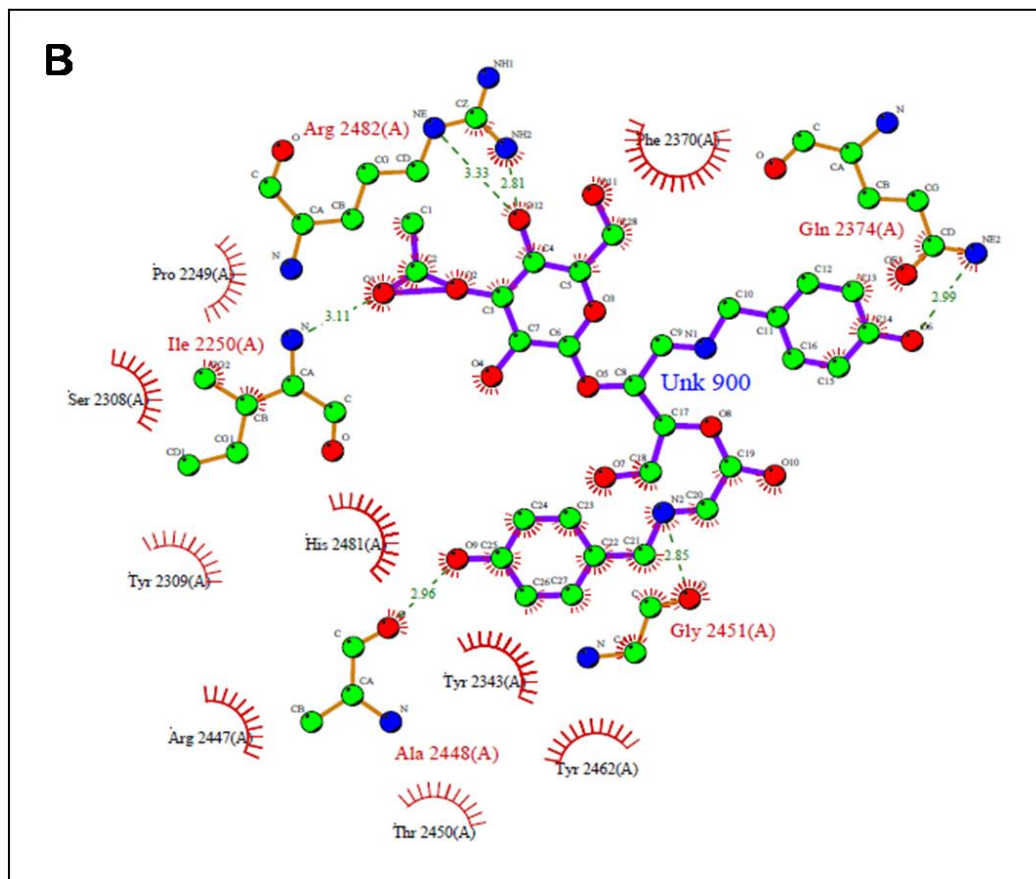
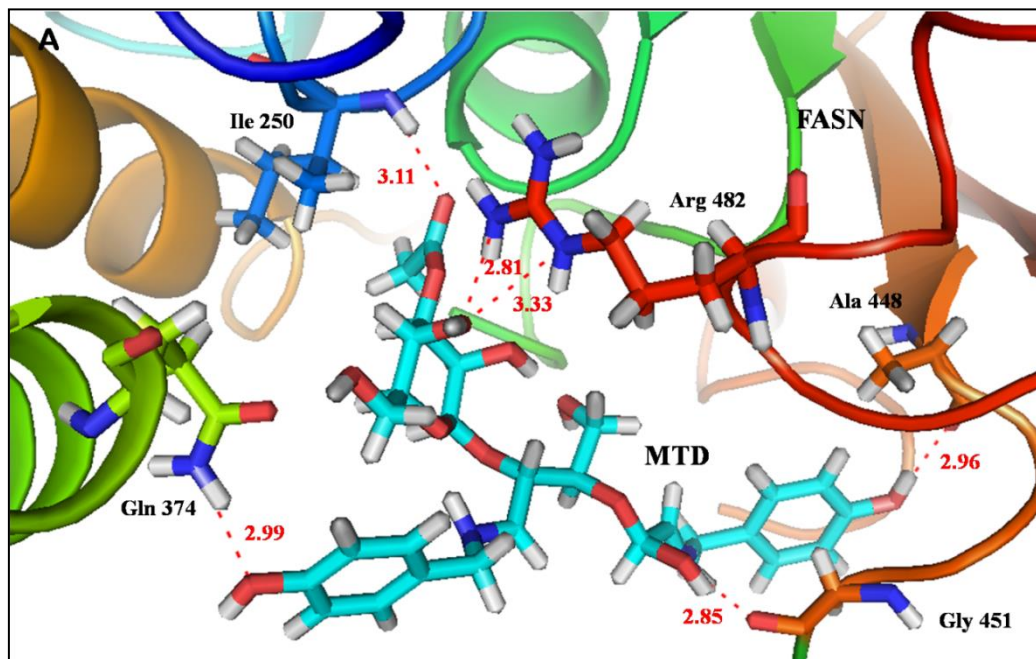


**Figure 2:** (A) Hydrogen bond interaction between MTD and TE domain of FASN (B) Ligplot showing the interactive phase between MTD and TE domain of FASN

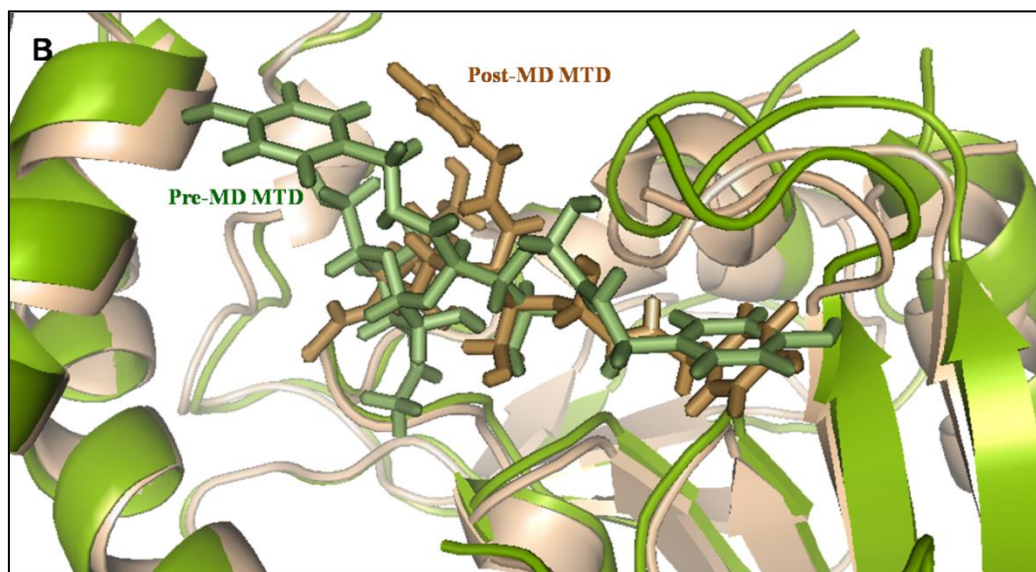
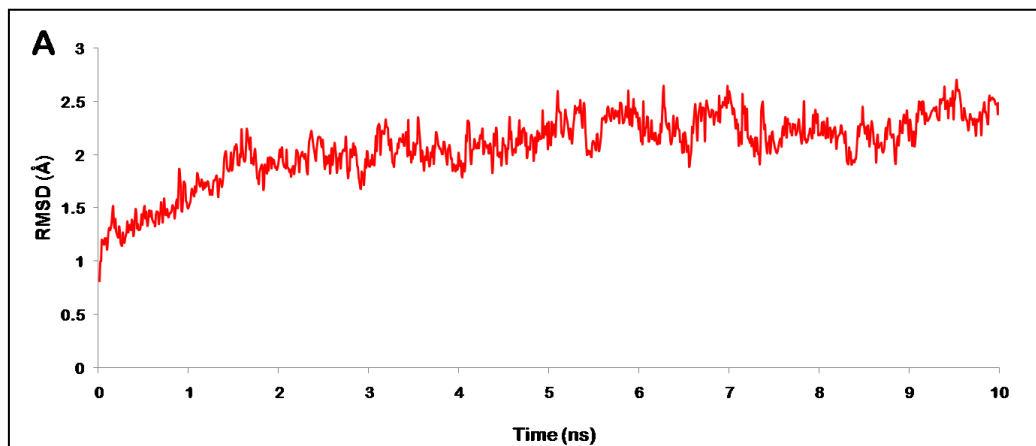


**Figure 3:** (A) RMSD trajectory of MTD bound FASN complex during the 10 ns MD simulation run (B) Superimposition of Pre-MD (green) and Post-MD (Brown) MTD-FASN complexes

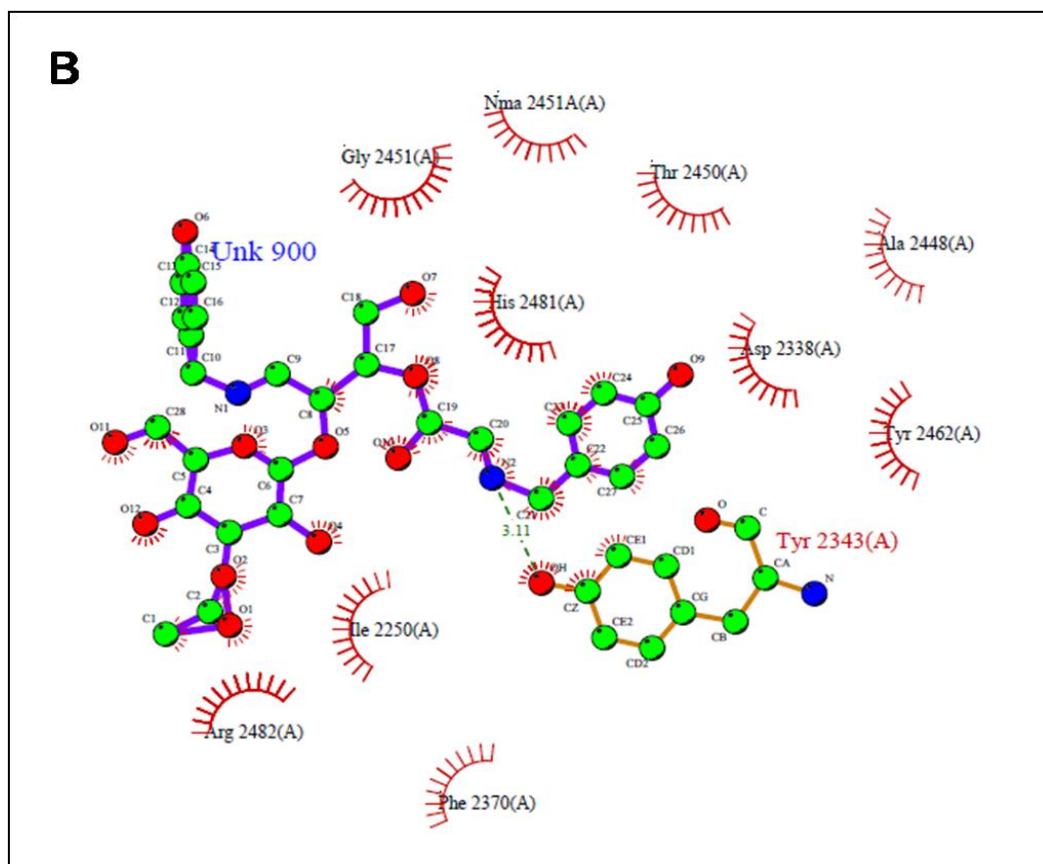
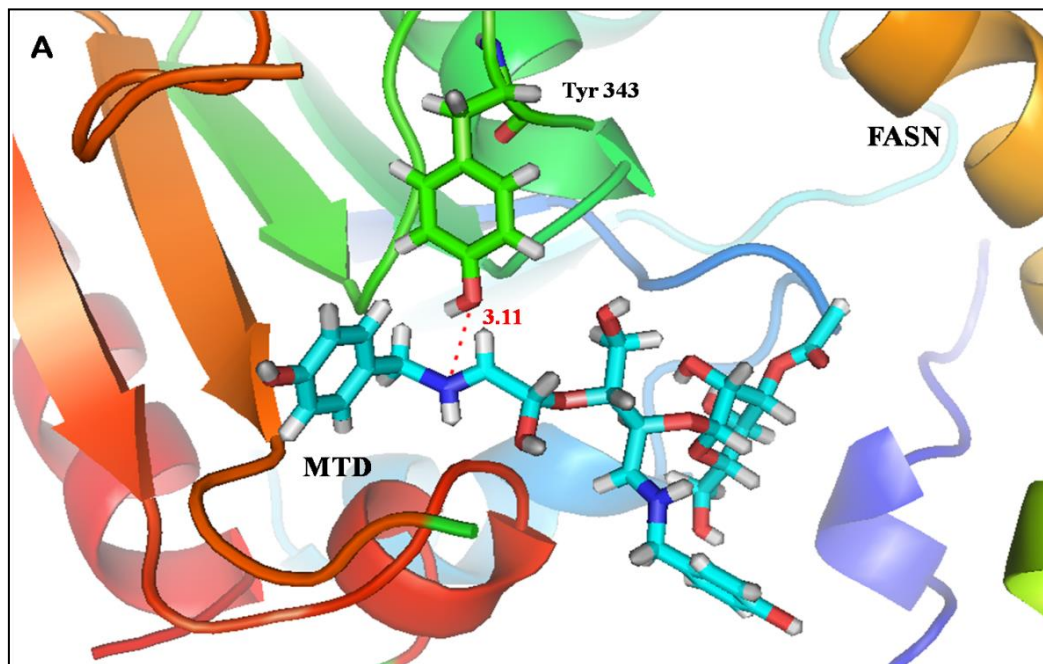


**Figure 4:** (A) Hydrogen bonding pattern in dynamically stable MTD-FASN complex (B) Ligplot of post MD MTD-FASN complex illustrating hydrogen and hydrophobic interactions

### *MTD with potential to hamper interaction between Skp2 and Cks1*

F-box proteins are members of a large family that regulates the cell cycle, the immune response, signaling cascades and developmental programmes by targeting proteins for ubiquitination. F-box proteins are the substrate-recognition components of SCF ubiquitin-protein ligases. F-box proteins not only recruit substrate, but also position it optimally for the ubiquitination reaction (Schulman *et al.*, 2000).

Hao *et al.*, 2005 deduced the crystal structure of quaternary Skp1-Skp2-Cks1-p27Kip1 complex to study the interactive phase between Skp2, Cks1 and P27<sup>Kip1</sup>. It was found that Skp2-Cks1 binding is mediated by both hydrogen bond networks and van der Waals contacts. The most extensive network of hydrogen bonds is between the Skp2 LRR domain (Trp265, Arg294, Asp319, and Arg344 side chains) and the Cks1 H2 helix (Ser41, Glu40, and Asn45 side chains and Ser41 carbonyl group). Additional hydrogen bond networks are formed by residues from the Skp2 tail (Arg398, His392, Thr400, and Thr394 side chains and backbone groups) and the Cks1 H2 helix (Glu42). Van der Waals contacts occur both at the center of the intermolecular interface and its periphery. At the center, the side chain of Phe393 from the Skp2 tail packs into a small hydrophobic pocket between the H1 and H2 helices of Cks1, making contacts to Leu31, Leu46, Pro33, Met38, and the aliphatic portion of Glu42 of Cks1. Peripheral van der Waals contacts involve Phe368 and His392 of Skp2 and Pro33 and His36 of Cks1 (Hao *et al.*, 2005).

Based on this knowledge of interaction pattern between Skp2 and Cks1, the potential of MTD to inhibit the recruitment of Cks1 by Skp2 for p27 recognition was studied. It was observed that MTD was forming hydrogen bonds with many residues of Skp2, namely Arg 167, Ser 189, Asn 190, Glu 214, Ser 238 and Arg 344. Out of these residues Arg 344 is important for binding of Cks1 to Skp2. It was hydrophobically interacting with many other essential residues like Trp 265, Asp 319, Thr 394, Arg 398 along with the neighboring amino acids, pro 166, Asp 187, Gly 215, Gly 239, Asn 262, Ser 264, Asn 289 and Ser 291 (Fig. 5(A) and 5(B)). Clearly it MTD was occupying the space required by Cks1 to interact with Skp2 thereby preventing the interaction required for ubiquitination process of p27. This complexed structure was then simulated for 10 ns to attain dynamic stability using OPLS force field in desmond MD software. The RMSD graph (Fig. 6(A)) showed that the Skp2-MTD complex initially deviated upto 4 Å and then acquired a stable trajectory and remained steady until the end. To identify the changes in the conformations before and after MD simulations, both the complexes were superimposed as shown in Fig. 6(B). An average structure computed from the most stable time frame (7-10 ns), was further analyzed for its interaction pattern and the interactions are shown in Fig. 7(A) and 7(B). In the stabilized structure post simulations, the MTD binding now involved two hydrogen bond interactions with the residues Asp 187 and Glu 214 of Skp2, in addition to hydrophobic interactions with residues Pro 166, Ser 189, Asn 190, Ser 238, Trp 265, Phe 267, Arg 398, Pro 399 and Thr 400. Many of these residues are important for the binding of Cks1 to Skp2. As ubiquitin-mediated proteolysis of the Cdk2 inhibitor p27Kip1 plays a central role in cell cycle progression, and enhanced degradation of p27Kip1 is associated with many common cancers, this analysis suggests that the binding of



MTD to Skp2 would result in substantially altered functional properties of the enzyme which would result in the inhibition of p27 degradation by SCF E3 ubiquitin ligase.

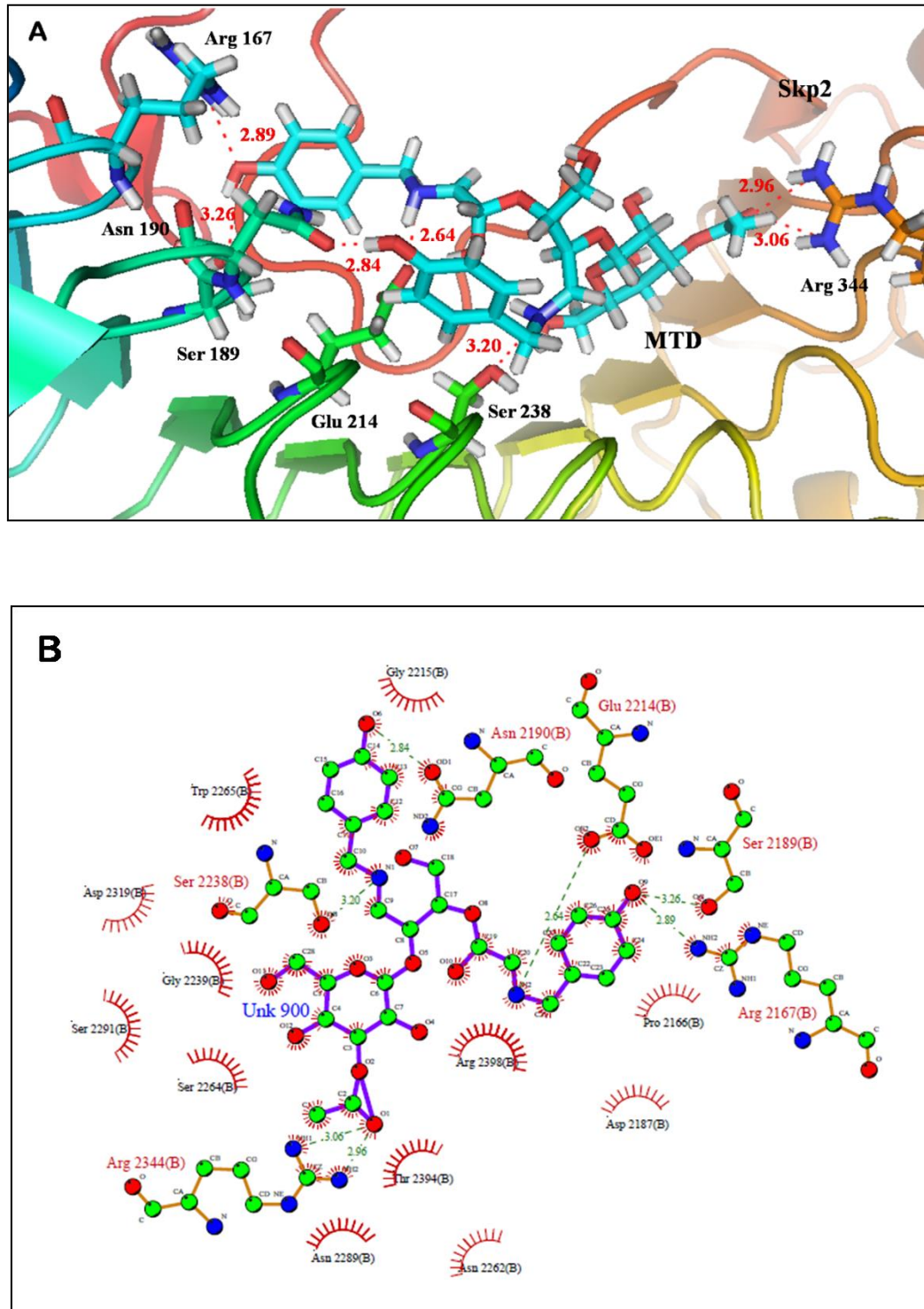


**Figure 5:** (A) Residues of Skp2 involved in hydrogen bond interaction with MTD (B) Ligplot showing  $\pi$ -bonds and hydrophobic interactions between Skp2 and MTD

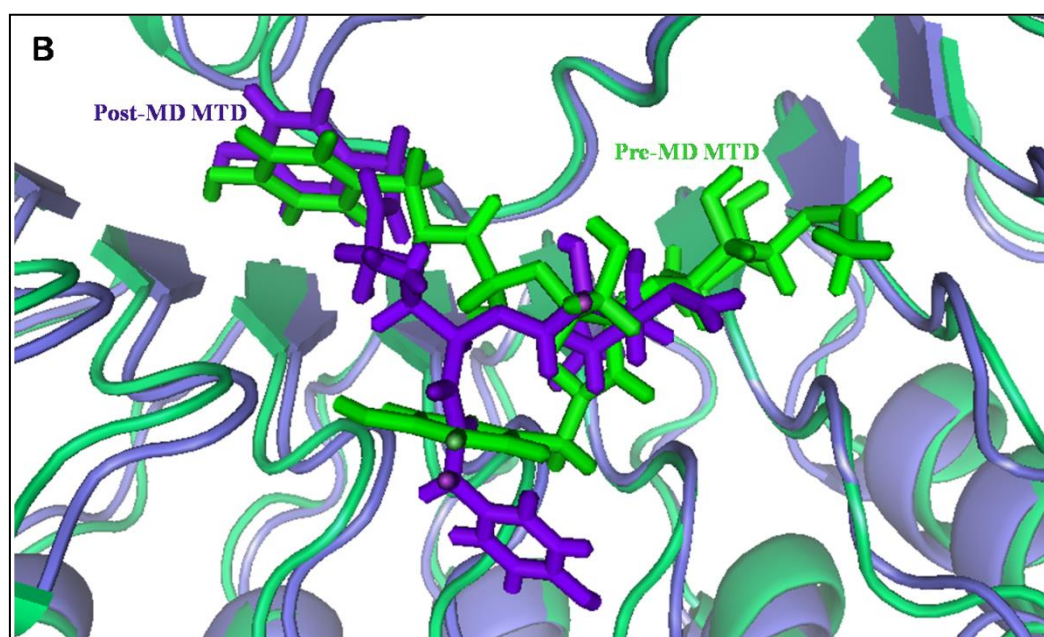
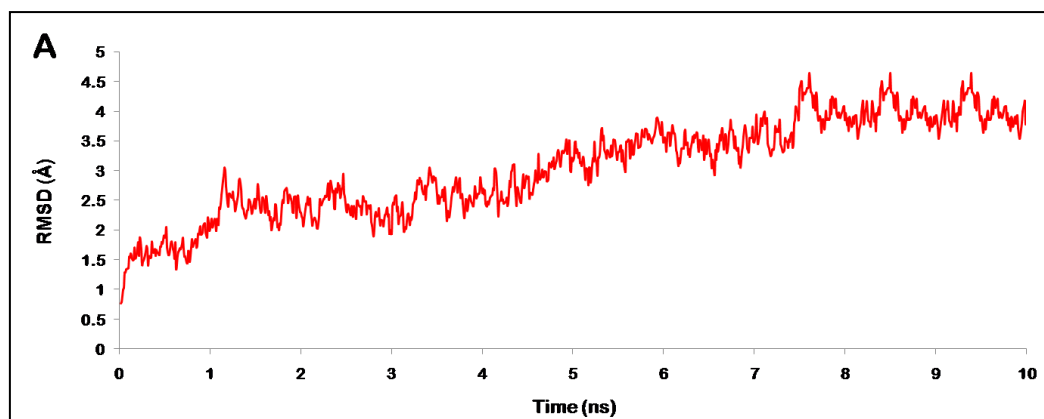


**Figure 6:** (A) RMSD trajectory of MTD-Skp2 complex during 10 ns long simulation run (B) Change in the position of MTD docked into Skp2 before (green) and after (purple) MD simulation

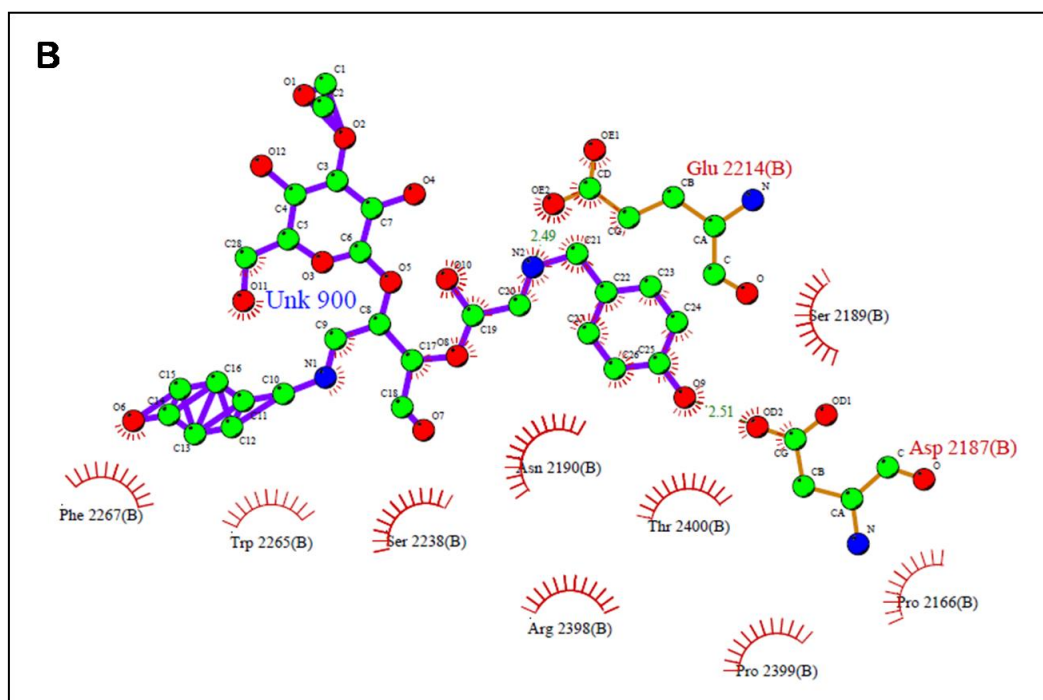
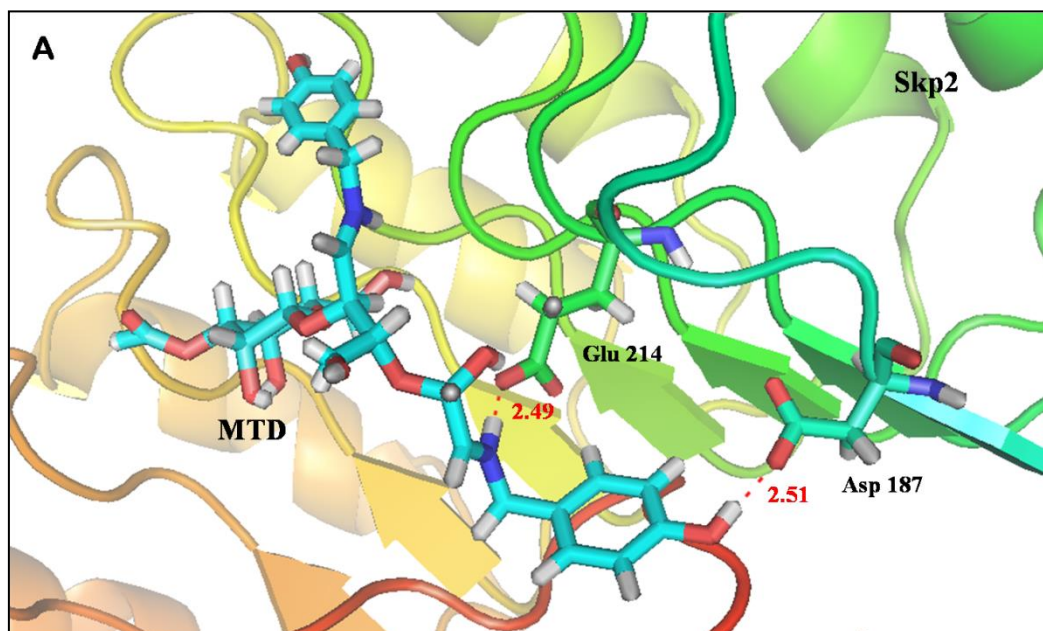


**Figure 7:** (A) Skp2 residues involved in hydrogen bonding with MTD after MD simulation (B) Ligplot showing dynamically stabilized molecular interactions between MTD and Skp2

### *MTD, a natural molecule with potential to inhibit PI3K $\alpha$*

Huang *et al.* in 2007 elucidated the structure of human p110 $\alpha$ /p85 $\alpha$  complex. The p110 $\alpha$  subunit of PI3K $\alpha$  has five domains: an N-terminal domain called ABD (adaptor binding domain) that binds to p85 $\alpha$ , a Ras binding domain (RBD), a domain called C2 that has been proposed to bind to cellular membranes, a helical domain of unknown function, and a kinase catalytic domain. (Huang *et al.*, 2007). The kinase domain harbors the catalytic site of the enzyme. In p110 $\alpha$ , the smaller N-terminal domain comprises residues 697 to 851 and the larger C-terminal domain residues 852 to 1068. On the basis of the structures of other protein kinases, the activation and catalytic loops of p110 $\alpha$  were assigned to residues 933 to 957 and 912 to 920, respectively. The substrate-binding pocket is situated between the N and C-terminal lobes of the kinase domain (Huang *et al.*, 2007).

The explicated information suggests that blocking the cleft between the N and C-terminal lobes of the kinase domain would depreciate the enzymatic activity of this enzyme. MTD was found interacting with PI3K $\alpha$  by forming hydrogen bonds with Lys 802, Val 851, Asp 915, Ser 919, Asn 920 and Asp 933. It was also forming hydrophobic contacts with many residues constituting the activation and catalytic loop, including Ser 774, Pro778, Ile 800, Asp 805, Tyr 836, Ile 848, Glu 849, Val 850, Thr 856, His 917, Ile 932 and His 936 (Fig. 8(A) and 8(B)). The molecules were found to bind substantially in the substrate binding pocket of PI3K $\alpha$ , a highly conserved domain. Thus, this provides substantial evidence for considering this screened natural compound, MTD, as a prospective drug candidate for inhibiting PI3K $\alpha$  function in cancer cases. Docking only reflects the static interactions between the protein and the ligand. To get a view about the dynamic behavior of the docked complex MD simulations were run for a time period of 10 ns. The RMSD graph (Fig. 9(A)) showed that the PI3K $\alpha$ -MTD complex initially deviated around 2 Å and then was able to acquire a stable trajectory which persisted till the end. To identify the changes in the conformations before and after MD simulations, both the complexes were superimposed as shown in Fig. 9(B). An average structure computed from the most stable time frame (4-10 ns), was further analyzed for its interaction pattern and the interactions are shown in Fig. 10(A) and 10(B). Many hydrogen bonds were lost during the MD simulation but the one with Val 851 was stable from the entire trajectory. Hydrophobic contacts were found with Met 772, Ser 774, Lys 776, Glu 849, Val 850, Thr 856, Ser 919, Asn 920, Met 922, Phe 930, Ile 932, Asn 933 and His 936. Most of the interactions remained conserved, while only the nature of interaction got changed. The ligand, MTD was still occupying the same cavity of PI3K $\alpha$ , thereby indicating a stable interaction with the protein.

Therefore inhibition of enzymatic activity of PI3K $\alpha$  by MTD can greatly effect the cancer cell growth, survival, motility, and metabolism.

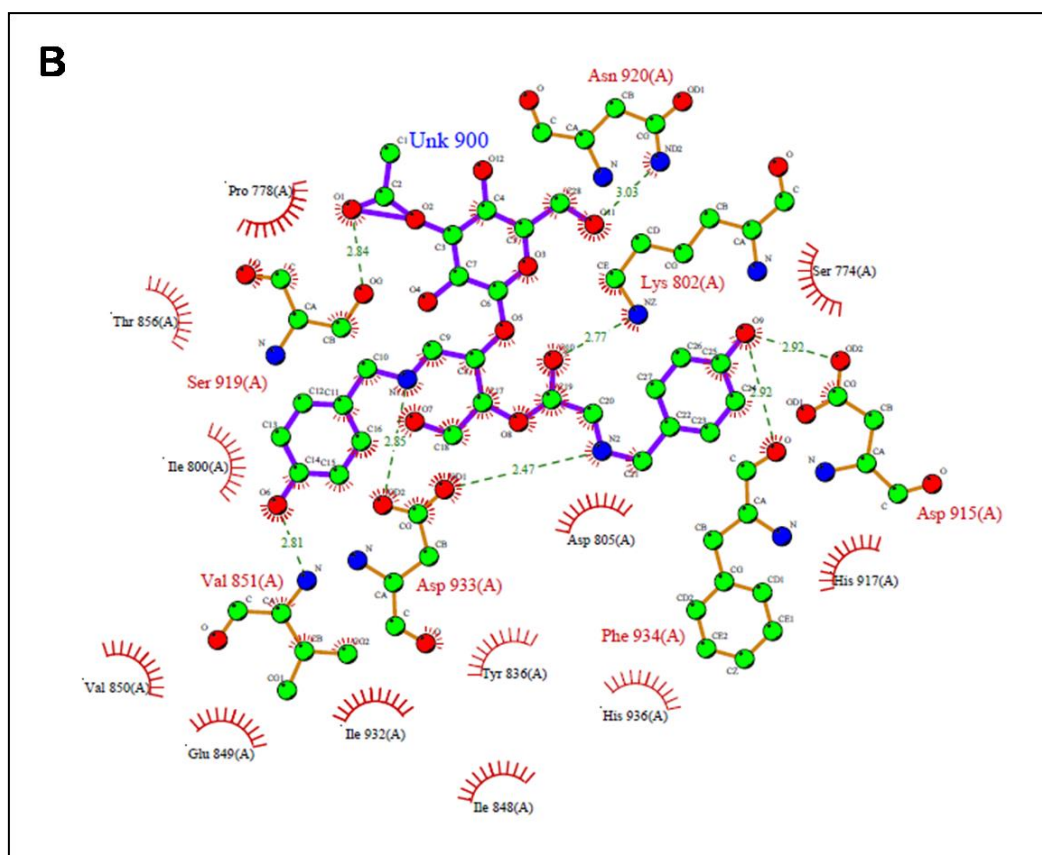
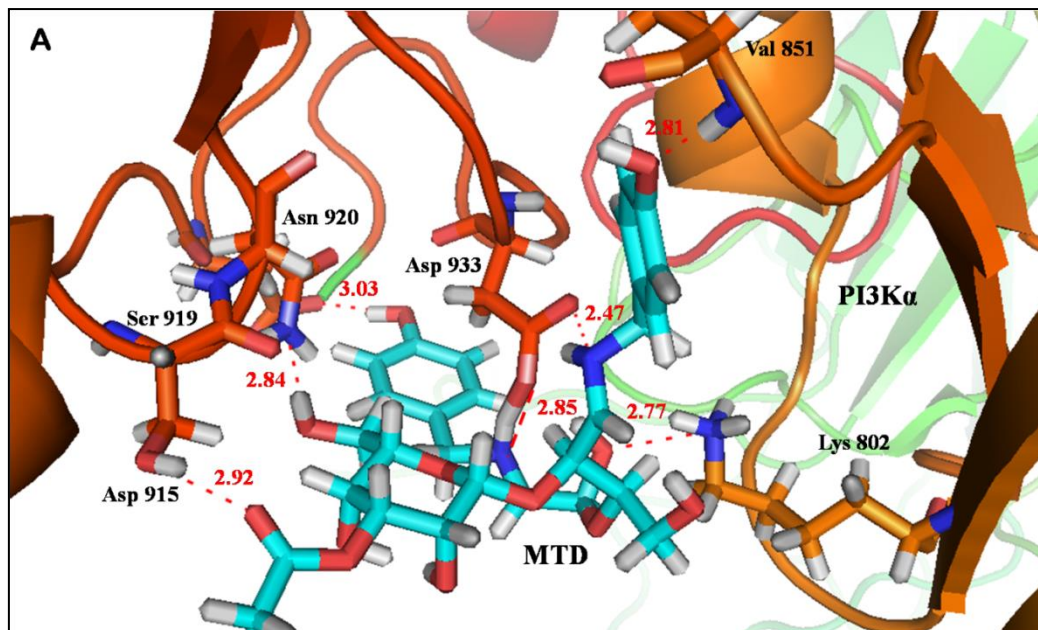


**Figure 8:** (A) Hydrogen bond interaction between MTD and residues lining the active cleft of PI3K $\alpha$  (B) Ligplot showing the hydrogen bonds and hydrophobic interactions between MTD and PI3K $\alpha$

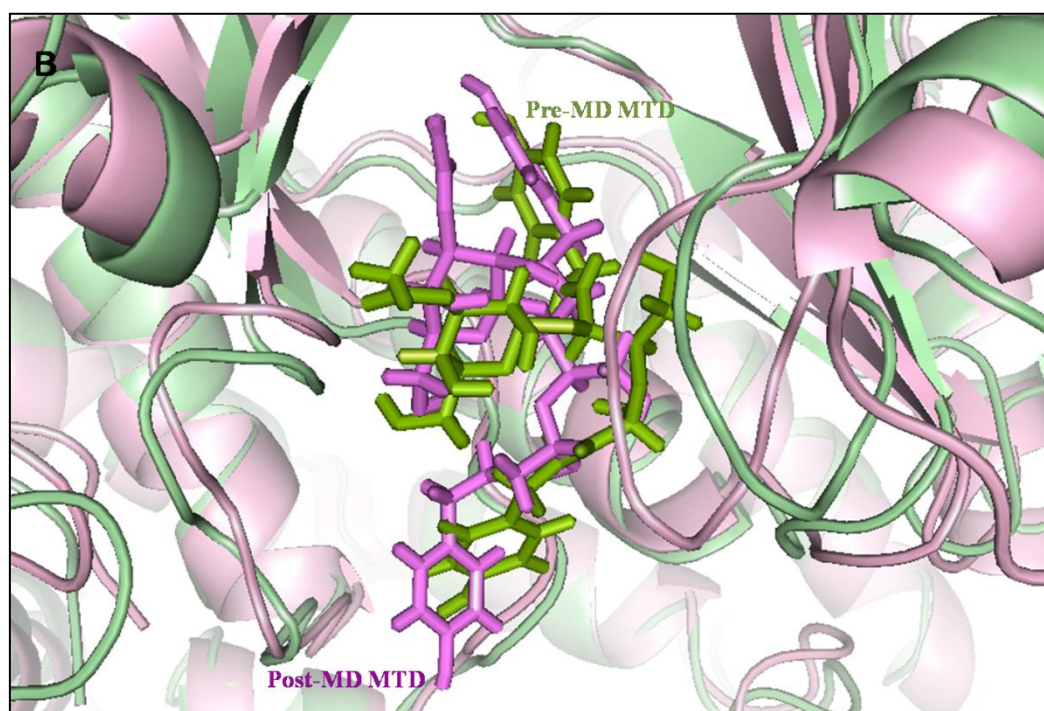
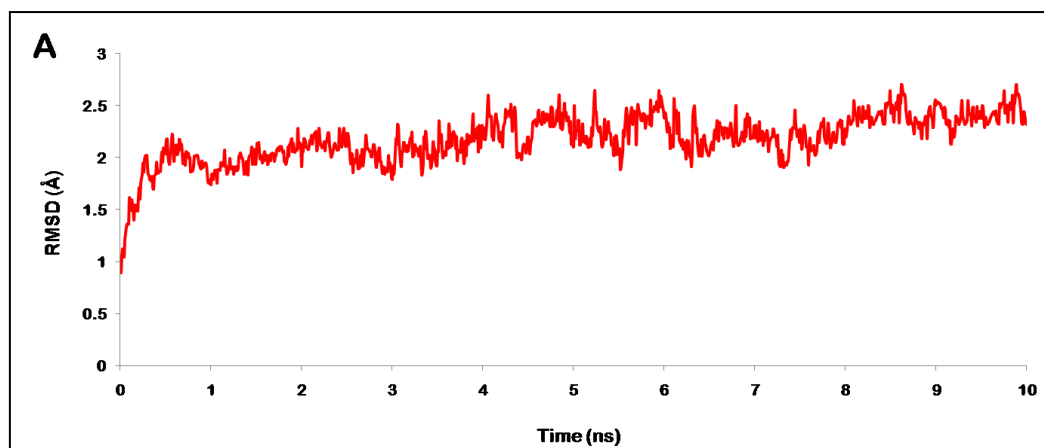


**Figure 9:** (A) RMSD trajectory of MTD-PI3K $\alpha$  complex during 10 ns long simulation run (B) Change in the position of MTD docked into PI3K $\alpha$  before (green) and after (pink) MD simulation

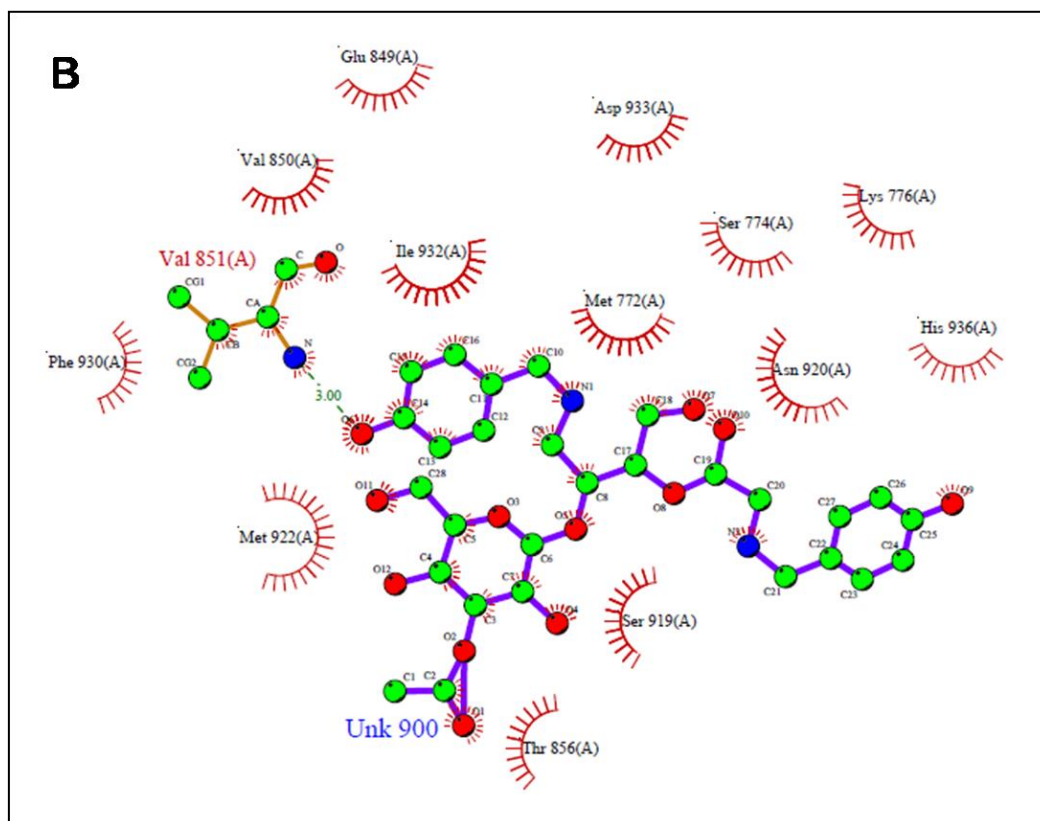
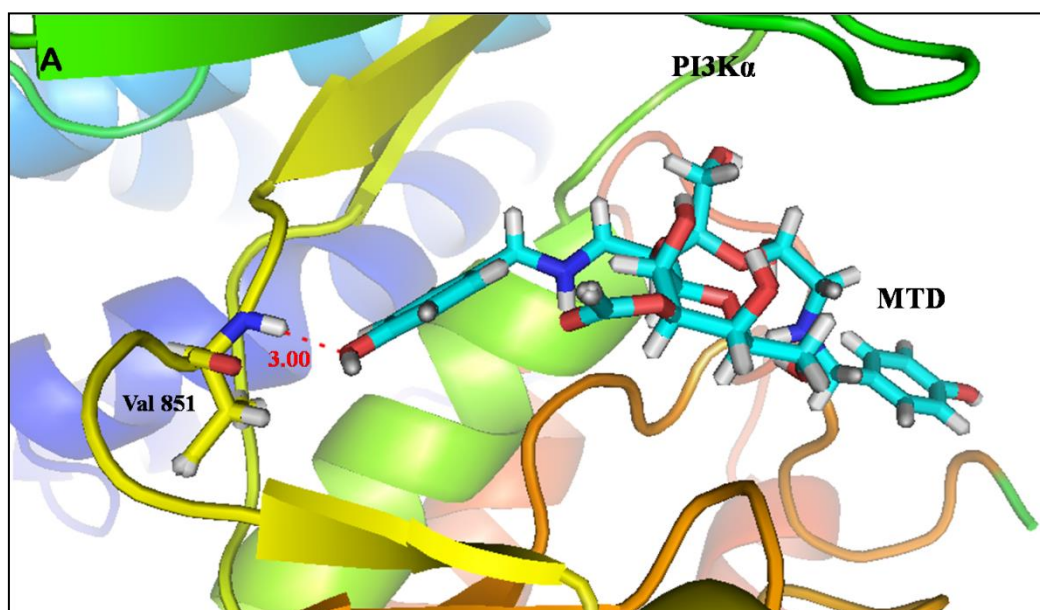


**Figure 10:** (A) PI3K $\alpha$  residues involved in hydrogen bonding with MTD after MD simulation (B) Ligplot showing dynamically stabilized molecular interactions between MTD and PI3K $\alpha$

## CONCLUSION

As discussed, drugs with multiple targets have a better chance of affecting the complex equilibrium of whole cellular networks than drugs that act on a single target. Complex diseases like cancer thus need multi-target attack. Here in we have reported a small molecule natural compound, MTD with capability to inhibit three of the important targets involved in cancer initiation, progression and survival- Fatty acid synthase, Phosphatidylinositol 3-kinase (p110 $\alpha$ ) and SCF E3 Ubiquitin Ligase. The molecule showed considerable binding affinity for all the protein molecules, interacting with their key residues essential for their enzymatic activity. The study provides evidences for consideration of these compounds as prospective small ligand molecules for the treatment of cancer. The present information could be of high value for the development of non-covalent type multi target inhibitory drugs with low toxicity to normal cells.



# CHAPTER 3

Small molecule based NK cell activation for defense against cancer

## INTRODUCTION

The response of body's immune system can be modified to fight against cancer. Attempts are being made to investigate the immunology associated with cancerous state and design more specific and effective cancer treatment. Cytotoxic T lymphocytes (CTLs) and natural killer (NK) cells are key effector cells of cellular immunity which play an important role in the antitumor defense mechanism.

Natural-killer (NK) cells, key players of the innate immune system, are white blood lymphocytes of which perform diverse biological functions like recognition and destruction of bacterial and viral infections and neoplasms. Approximately 15% of circulating lymphocytes comprise of NK cells. They are also found in peripheral tissues- the liver, peritoneal cavity and placenta. NK cells circulating in the blood are in resting state which upon activation by certain cytokines extravasate and infiltrate into pathogen-infected tissues or transformed self cells (Biron, 1997; Fogler *et al.*, 1996; Wiltout *et al.*, 1984). NK cells are a crucial part of the innate immune system as they mediate the spontaneous killing of various tumor cells. NK cells were first shown to effectively eliminate tumor cells from the circulation of mice (Riccardi *et al.*, 1980) and rats (Barlozzari *et al.*, 1983). Shortly thereafter, NK cells were shown to spontaneously kill MHC class-I-deficient tumor cells *in vitro* (Ljunggren and Kärre, 1985) and *in vivo* (Ljunggren and Kärre, 1985). More recent studies have confirmed that NK-cell-mediated cytotoxicity is important for responses against the initiation and metastasis of MHC class-I-deficient tumors *in vivo* (Smyth *et al.*, 1998; Smyth *et al.*, 1999; van den Broek *et al.*, 1995) as tumor cells are believed to alter their expression of MHC class I molecules to evade T-cell responses.

The functions of NK cells are regulated by a balance between their inhibitory and activatory receptors (Bottino *et al.*, 2004). There are several inhibitory receptors with different molecular structures and specificities for different alleles of class I molecules (Bottino *et al.*, 2004; Braud *et al.*, 1998). The lack of even a single MHC-I allele, a frequent event in cancer cells, sensitizes them to NK cell cytotoxicity. In the absence of inhibitory signals, however, NK cell cytotoxicity gets activated by a set of triggering receptors (Bottino *et al.*, 2004; Trinchieri, 1989). In general NK cells can be activated by various stimuli such as contact with dendritic cells (DC), MHC-I-negative cells, binding of IgG immunocomplexes, direct engagement of NKR by stress-induced tumor-associated molecules or pathogen-derived products, and several cytokines such as IL-1, IL-2, IL-12, IL-15, IL-18, IL-21, and type I IFNs (Brady *et al.*, 2004; Carson *et al.*, 1994; Parrish-Novak *et al.*, 2000; Trinchieri, 2003). In particular, viral and bacterial products can trigger NK cell responses directly binding to surface TLR3 and TLR9 (Moretta *et al.*, 2006; Sivori *et al.*, 2006).

Toll-like receptors (TLRs) recognize conserved molecular patterns in invading pathogens and trigger innate immune responses. TLRs are type I integral membrane glycoproteins, consisting of pathogen-binding ectodomains (ECD) and cytoplasmic signaling domains, known as Toll IL-1 receptor (TIR) domains, joined by a single transmembrane helix

(Bell *et al.*, 2003). TLR3 recognizes dsRNA, a molecular signature of most viruses via its ectodomain (ECD). TLR3 ectodomains (ECD) dimerize on oligonucleotides of at least 40–50 bp in length, the minimal length required for signal transduction. Each TLR3-ECD binds dsRNA at two sites located at opposite ends of the TLR3 “horseshoe”, and an intermolecular contact between the two TLR3-ECD C-terminal domains coordinates and stabilizes the dimer. This juxtaposition mediates downstream signaling by dimerizing the cytoplasmic Toll IL-1 Receptor (TIR) domains. The overall shape of the TLR3-ECD does not change upon binding to dsRNA (Liu *et al.*, 2008c).

In the work presented here we have reported small molecule chemical compounds of natural origin which could dimerize the TLR3 ectodomain in a manner similar to the dsRNA of viruses. These compounds also show interaction with all the residues which have been reported to be essential for signal transduction upon recognition with the dsRNA of pathogen.

## REVIEW OF LITERATURE

The high worldwide prevalence rate of cancer has led researchers to put in a hard effort to investigate the immunology associated with cancerous state and design more specific and effective cancer treatment. Cytotoxic T lymphocytes (CTLs) and natural killer (NK) cells are main effector cells of cellular immunity which play an important role in the antitumor defense mechanism. Tumor antigens (TAs) are often used as targets for therapeutic approaches against cancer. TAs can be categorized into three types; (a) TA peptides that are presented by HLA class I molecules on the tumor cell surface and are capable of evoking cellular immunity, especially cytotoxic T lymphocytes (CTLs), by being presented on HLA class II molecules of antigen-presenting cells such as macrophages and dendritic cells; (b) target molecules or ligands recognized by natural killer (NK) cell receptors; and (c) TAs that are directly expressed on the tumor cell surface and are identified by auto-antibodies or hetero-antibodies, *i.e.*, by humoral immunity (Groen, 1987; Kuroki *et al.*, 2001).

### *T cell based therapy and its limitations*

One of the effector cells that mediate the rejection of solid tumors in pre-clinical animal models is the Cytotoxic T Lymphocyte (CTL). Each CTL expresses a clonotypically unique T-cell-antigen receptor (TCR) that confers specificity for a particular target antigen. The antigens recognized by CTLs consist of peptide fragments, which are bound within the major clefts of MHC-Class-I molecules on the cell surface. Cells are exposed to immune-system scrutiny by loading peptide fragments of newly synthesized cellular proteins onto MHC-class-I molecules, which are then transported to the cell surface (Shastri *et al.*, 2002). As in normal cells, the surfaces of tumor cells contain MHC–peptide antigens that reflect their expressed ‘proteome’. T-cell lines can be generated that specifically recognize the HLA restricted antigens that are expressed by tumor cells and can be used for T cell based immunotherapy. Thus, adoptive CTL transfer (ACT) using *ex vivo* manipulated T

lymphocytes emerged as an important advancement in cancer immunotherapy, allowing for re-education and re-setting of the host immune system.

### *Limitations of T-Cell based therapy*

#### *1. Emergence of antigen-loss variants*

In a study conducted to demonstrate the ability of T-cells to provide long-term protection against tumor expressing the target antigen, in a dose-dependent manner it was observed that even in what appeared to be an idealized experimental situation, responses were incomplete and nondurable. This was attributed to the emergence of antigen-loss variants (Bathe Oliver and Nava). It has also been shown that, in general, cancer cells are typically genetically unstable. Accumulated of thousands of mutations was observed in the adenoma-colorectal cancer sequence (Boland and Ricciardiello, 1999; Cho and Vogelstein, 1992; Stoler *et al.*, 1999). Therefore antigens are expected to be heterogeneous in any given tumor.

#### *2. Down regulation of MHC-I on the surface of tumor cells*

According to the immune surveillance theory, cancer arises when the immune system is unable to recognize individual cancer cells, enabling them to escape detection. Indeed, tumor cells escape by a number of mechanisms. As tumor evolves, the immune system sequentially and consecutively eliminates cells expressing certain antigens in order of degree of immune-dominance and diminishing tumor immunogenicity. MHC down regulation is particularly detrimental to the antitumor immune response, as it results in permanent escape from immune detection (Dudley and Roopenian, 1996; Jäger *et al.*, 1996; Seung *et al.*, 1993; Urban *et al.*, 1986).

#### *3. Suppression of immune system by tumor microenvironment*

Even when tumor cells are recognized by effectors, a number of processes may interfere with their clearance. Induction of apoptosis of potentially hostile lymphocytes by tumor is one such mechanism (Hahne *et al.*, 1996; Ungefroren *et al.*, 1999; Zaks *et al.*, 1999). Thus, in addition to escape from detection by the immune system, tumor may directly influence immune effector function. For example, melanomas secrete many cytokines including IL-10 and TGF- $\beta$  which cease the CTL activity. Suppression of the immune system by TGF- $\beta$  facilitates tumor cell expansion (Liu *et al.*, 2007).

#### *4. Single antigen important for survival of tumor cell*

Targeting a single antigen is not likely to succeed unless that antigen is necessary for the function and survival of the cancer cell. This situation is rare, although one example is BCR-ABL, a constitutively activated tyrosine kinase that causes chronic myeloid leukemia (CML). Targeting such a protein has provided therapeutic success (Druker *et al.*, 2001). Unfortunately, few such targets have so far been identified and so other strategies are

required to overcome the problem of emergence of antigen loss variants. One of the potential solutions is the concomitant utilization of approaches with more bystander effect. For example, MHC non-restricted effectors such as NK or LAK cells may be helpful (Lafreniere and Rosenberg, 1985; Yasumura *et al.*, 1994), particularly in tumors where loss of MHC expression has occurred. The problem of emergence of antigen loss variants is therefore not insurmountable.

### *Role of NK cells in defense against tumors*

Natural-killer (NK) cells are white blood lymphocytes of the innate immune system that have diverse biological functions, including recognition and destruction of certain microbial infections and neoplasms. As discussed above, resting NK cells circulate in the blood, but, following activation by cytokines, they are capable of extravasation and infiltration into most tissues that contain pathogen-infected or malignant cells. NK-cell-mediated cytotoxicity is more important for responses against MHC class-I-deficient tumors *in vivo* that evade T-cell responses for their survival.

The functions of NK cells are regulated by a balance between their inhibitory and activatory receptors (Bottino *et al.*, 2004). In the absence of inhibitory signals, however, NK cell cytotoxicity must be activated by a set of triggering receptors.

### *Activation of NK cells for immunotherapeutic strategies against cancer*

#### *1. Use of IL-2 activated NK cells*

Early 1980s clinical trials started introducing IL-2-activated NK cells in the treatment of heavily tumor-burdened patients with solid primary or metastasized cancers. Subcutaneous injections of NK-stimulating doses of IL-2 or administration of pre-activated NK cells (adoptive transfer of LAK cells) showed a 15–30% positive effect in patients with advanced renal cell carcinoma (RCC) or melanoma (MEL). Unfortunately, IL-2 treatment is associated with life-threatening toxicity, essentially represented by capillary leak syndrome (Fehniger *et al.*, 2002). Another limitation of this approach is the fact that IL-2, but not IL-15, activated NK cells increase their sensitivity to apoptosis when in contact with vascular endothelium (Rodella *et al.*, 2001), likely causing a decrease in NK cell migration toward the cancer area.

#### *2. IL-15 mediated NK cell expansion*

IL-15 appears to be more efficient than IL-2 in expanding the NK cell compartment because it promotes the survival of NK cells and protects NK cells from AICD (Rodella *et al.*, 2001; Waldmann, 2002). Unfortunately, extremely high doses of IL-15 are necessary to observe meaningful antitumor effects *in vivo*; thus recently, strategies favoring IL-15 trans-presentation to NK cells have been proposed (Kobayashi *et al.*, 2005).

### 3. *IL-12 mainly enhances NK cell-mediated IFN- $\gamma$ production*

Differently from IL-2 and IL-15, IL-12 mainly enhances NK cell-mediated IFN- $\gamma$  production, and IL-1 and IL-18 potentiate the effect of IL-12 by up-regulating the IL-12Rs expression on NK cells (Ferlazzo and Münz, 2004; Hamerman *et al.*, 2005). IFN- $\gamma$  has been shown to suppress tumor angiogenesis and to induce TRAIL and FasL mediated cellular susceptibility to apoptosis in a variety of tumor cells (Smyth *et al.*, 2003) Sarkar *et al.*, 2003).

### 4. *IL-21, another promising cytokine for NK cell therapy*

IL-21, a promising cytokine able to build up NK cell antitumor activity (Nakano *et al.*, 2006), has been found to promote both the expression of genes associated with type I response and the terminal differentiation of the highly cytotoxic CD56<sup>dim</sup>/CD16<sup>+</sup>NK cell subset, which can potentially direct ADCC against tumor cells via CD16-Fc ligation (Brady *et al.*, 2004; Parrish-Novak *et al.*, 2000; Strengell *et al.*, 2002). NK cell mediated ADCC response against tumor targets can be promoted by administration of mAbs to tumor-associated Ags (Caligiuri *et al.*, 2004; Clynes *et al.*, 2000). Despite the lack of true specificity and the limited efficacy, this approach has a unique mechanism of action that does not produce cross-resistance or overlapping toxicities with conventional agents (Caligiuri *et al.*, 2004) and that can therefore be combined with cytokine-based immunotherapies.

### 5. *Early acting growth factors for NK cell differentiation*

Growth factors acting on early stages of NK cell differentiation (such as Flt3-L and SCF but also IL-7) in synergy with NK activatory cytokines have been proposed (Fehniger *et al.*, 2002). As Flt3-L induces an increase in the number of both immature and mature NK cells, treatment with Flt3-L (plus IL-7) followed by cytokines (or recombinant mAb-cytokine fusion protein) able to induce both differentiation of immature NK cells and activation of mature NK cells (like IL-21) and TLR agonists might provide a powerful strategy for NK cell-based therapies. Thus, Flt3-L, SCF, and IL-7 can be used to enhance NK cell numbers. Flt3-L induces an expansion not only of mature non-activated NK cells but also of DC (Maraskovsky *et al.*, 1996; Shaw *et al.*, 1998).

### 6. *Direct activation of NK Cells using Toll like Receptors*

NK cells can be activated by the direct engagement of surface TLR3 and TLR9, and synthetic molecules able to mimic the immunostimulatory activity of viral and bacterial products via TLRs have been developed and tested against tumor cells in combination with cytokines (Moretta *et al.*, 2006; Sivori *et al.*, 2006).

### 7. *Blocking NK inhibitory interactions with MHC-I on tumor cells*

To mimic the antitumor effect of KIR-mismatched NK cells, Abs to block NK inhibitory interactions with MHC-I on tumor cells have been tested in vivo. Mouse models of

leukemia have demonstrated efficacy of anti-KIR-blocking Abs without adverse effects on normal cells, indicating the feasibility of treatments with Ab fragments to prevent KIR/NKG2A-MHC-I interactions in cancer therapy (Koh *et al.*, 2001).

#### *Limitations of cytokine mediated activation of NK cells*

Toxicity of systemic cytokine administration and cytokine activated NK cell apoptosis are two important limitations of cytokine-mediated (and NK adoptive) immunotherapies for cancer treatment.

Hence, we have used the strategy of NK cell activation by TLR3 receptor for proposing NK cell based immunotherapy for cancer treatment.

## **MATERIALS AND METHODS**

X-ray analysis of TLR3-ECD: dsRNA has shown that each TLR3-ECD of a dimer binds dsRNA at two sites located at opposite ends of the TLR3 “horseshoe”. Intermolecular contacts between the C-terminal domains of two TLR3-ECDs stabilizes the dimer and positions the C-terminal residues within 20–25Å of each other, which is thought to be essential for transducing a signal across the plasma membrane in intact TLR3 molecules. But it has been studied that interaction between the residues at N terminal of each TLR3-ECD and dsRNA are also important as reflected by site directed mutagenesis experiments (Botos *et al.*, 2009). Hence we have identified two compounds interacting at C and N terminal respectively.

#### *Protein preparation and dataset*

Since the structure of human TLR3 in complex with dsRNA was not available, the crystal structure of TLR3 ectodomain of mouse origin was downloaded for Protein Data Bank [PDB ID: 3CIY] (Liu *et al.*, 2008b). Crystal water molecules and all non-bonded heteroatoms including the docked ligand were removed from the protein structure using Accelrys Viewerlite 5.0 (Viewerlite\_5.0). The protein was prepared using Schrödinger’s protein preparation wizard (Schrödinger, 2009). Hydrogen bonds were added and optimized to the structure. Other preparation steps involved removal of bad contacts, optimization of bond lengths, creation of disulfide bonds, capping of protein terminals and conversion of selenomethionine to methionine. The missing residues were fixed manually.

A data set consisting of 1,69,109 natural compounds by 10 different suppliers was downloaded from ZINC database in SMILES format (Irwin and Shoichet, 2005). This dataset was then prepared using LigPrep’s ligand preparation protocol. It generates different tautomeric, stereochemical and ionization variants of the small molecules along with energy minimization and flexible filtering. This prepared protein and small molecule dataset was then used further for virtual screening and docking studies.

### *High throughput virtual screening and docking studies*

A grid was generated around the important residues (as reported in the literature) of the prepared protein structure using the Glide docking module of Schrödinger. Prepared dataset of natural compounds was then virtually screened against the prepared protein at desired grid coordinates using Glide model's HTVS docking protocols. The compounds above the threshold of 6.00 HTVS docking score were then selected and again subjected to docking using Glide's XP protocol for docking score refinement. The top scoring compounds were then inspected through MD simulations. All Glide docking studies were performed on Intel® Xeon (R) CPU X3450 @ 2.67GHz of hp origin with 6.00 GB RAM. Schrödinger 9 Maestro interface was compiled and run under Ubuntu 64 bits operating system.

### *Molecular Dynamics Simulations of ligand-bound complex*

Desmond Molecular Dynamic System with Optimized Potentials for Liquid Simulations (OPLS) all-atom force field 2005 was used to inspect the top scoring compounds through MD simulations. The protein-ligand complex obtained from Glide's XP docking protocol was prepared using Desmond set-up wizard. Missing residues were corrected manually. The prepared system was solvated in a triclinical periodic box of SPC water and then neutralized using an appropriate number of counter-ions. The distance between box wall and protein-ligand complex was set to more than 10Å to avoid direct interaction with its own periodic image. Energy minimization of the prepared system was done up to a maximum 10 steps using steepest descent method until a gradient threshold (25 kcal/mol/Å) is reached. Default protocol of Desmond was used to equilibrate the system. Further MD simulations were carried out on this equilibrated system for a time period of 10 ns at a constant temperature of 300K and constant pressure of 1 atm with a time step of 2 fs. During the simulations process, smooth particle Mesh-Ewald method was used to calculate long range electrostatic interactions. A 9 Å radius cut-off was used for coulombic short range interaction cutoff method. Frames of trajectory were captured after every 10 ps time step.

The root mean square deviation (RMSD) of the protein docked with ligand within the binding pocket was calculated for the entire simulations trajectory with reference to the first frame. The hydrophobic interactions and H-bonds were calculated using Ligplot program (Wallace *et al.*, 1995), where the H-bonds were defined as acceptor-donor atom distances of < 3.3 Å, hydrogen-acceptor atom distance of maximum 2.7Å, and acceptor-H-donor angle greater than 90°.

## **RESULTS AND DISCUSSION**

### *Virtual screening of 1,69,109 natural compounds downloaded from ZINC database*

The library of natural compounds prepared using Schrödinger's protein preparation wizard was screened against the crystal structure of TLR3 at both C and N terminals



respectively using high throughput virtual screening protocol of Glide. Many compounds were found having a glide docking score of more than -6.00, indicating a considerable binding affinity for the specific sites within the protein molecule. These several hundred compounds were further analyzed for their binding affinity with more precision using the XP docking protocol of glide. In one of the screenings, the top scoring natural compound, [(2S,3R,5R,10R,12S,13S,14R,17R)-17-[(1R,4S)-4,5-dihydroxy-1-(hydroxymethyl)-5-methyl-hexyl]-2,12-dih (Fig. 1(A), referred to as DHM) was having XP docking score of -11.43 which indicated a very strong binding affinity for the C terminal residues of TLR3 and it was also able to hold two molecules of TLR3 together forming a dimer, an essential requirement for initiating the cascade of intracellular signaling. The hunt for molecule that could interact with important residues at N-terminal ended with the compound, N-(2-(1H-imidazol-4-yl)ethyl)-2-((5-hydroxy-4-oxo-2-phenyl-4H-chromen-7-yl)oxy)acetamide (referred to as IEH) having an XP docking score of -6.05. Fig. 1(B) illustrates the chemical structure of this compound.

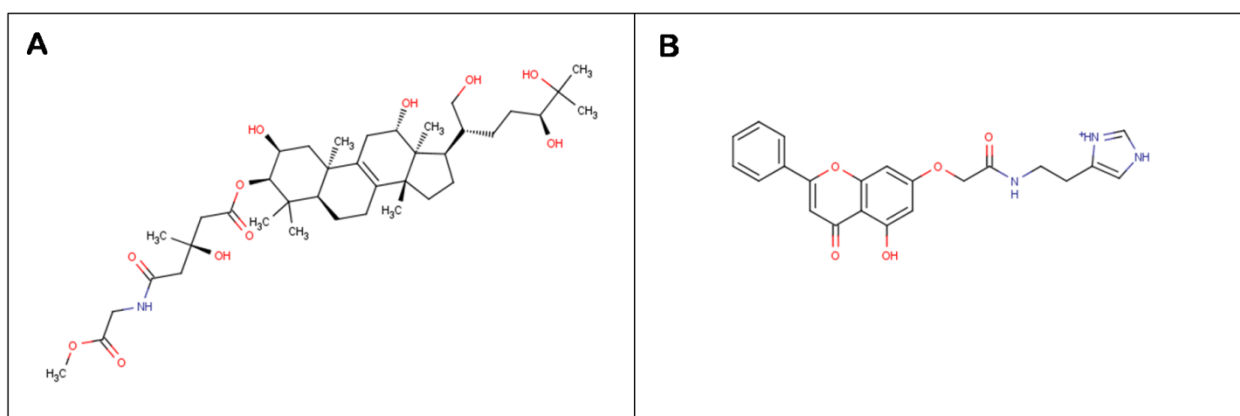


**Figure 1:** Chemical structure of (A) DHM and (B) IEH

#### *Interaction analysis of DHM at C-terminal of TLR3 dimer*

hTLR3-ECD structure bound to dsRNA was not available, hence we have used the mTLR3-ECD dimer for our study. mTLR3-ECD had 78% sequence identity with hTLR3-ECD and as expected the structures of the two ECDs were also highly homologous (Liu *et al.*, 2008b). The structure of the TLR3 signaling complex, consisting of two mTLR3-ECD molecules bound to one 46 bp dsRNA oligonucleotide was used to identify multiple intermolecular contacts that stabilize this active complex. It was found that dsRNA interacts with both an N-terminal and a C-terminal site on the glycan-free surface of each mTLR3-ECD, which are on opposite sides of the dsRNA with the C-termini (Fig. 2(A)) in contact and the N-termini (Fig. 3(A)) outstretched at opposing ends of the linear dsRNA molecule. Another important fact was that the overall structure of mTLR3-ECD does not change upon binding to dsRNA, supporting a signaling mechanism in which ligand-induced receptor dimerization brings the two cytoplasmic TIR domains into contact, thus triggering a downstream signaling cascade (Liu *et al.*, 2008b). The dsRNA in the complex retains a typical A-DNA-like structure, in which the ribose-phosphate backbone and the position of the

grooves are the major determinants of binding. The mTLR3-ECD interacts with the sugar phosphate backbones, but not with individual bases. This explains why TLR3 lacks specificity for any particular nucleotide sequence (Alexopoulou *et al.*, 2001; Liu *et al.*, 2008b).

The first site of dsRNA:TLR3 interaction is located close to the C-terminus of TLR3. In the complex, these binding sites from two mTLR3-ECD monomers face each other across the dsRNA. It was elucidated that the residues within contact distance of the RNA include Asn515, Asn517, His539, Asn541 and Arg544, which all are found well-conserved in vertebrates (Liu *et al.*, 2008b). The screened ligand, DHM was interacting strongly at C terminal stabilizing the dimer (Fig. 2(B)). It was found forming hydrogen bonds with Asn 541, Ser 571, Leu 595 and Asn 597 of chain A and Asn 541, Ser 571, Gly 573 and Asn 597 of chain B. Hydrophobic contacts included Asn 517, His 539, Asn 540, Asn 572, Gly 573 and Asn 596 of chain A along with residues Asn 540, Asn 572, Leu 595 and Asn 596 of chain B ((Fig. 2(C) and 2(D)). Mutational analysis previously showed that His539 and Asn541 are two crucial residues, which upon substitution make the receptor incapable of binding to dsRNA, whereas site directed mutations at Asn517 and Arg544 do not alter the activity of the receptor, indicating that these latter residues are not that essential for binding (Bell *et al.*, 2006). The selected natural compound, DHM was interacting with both His539 and Asn541 thus substantiating our hypothesis. Thus, we can propose DHM as a small molecule of natural origin that has the potential for stabilizing the dimerized TLR3 complex bringing the intracellular domains closer for the functional activity.

#### *IEH interacting with functionally important residues at N terminal of TLR3*

The second dsRNA:TLR3 interaction site is located on the N-terminal end (of the glycan-free surface of TLR3 and is formed by residues His39, His60, Arg64, Phe84, Ser86, His108, and Glu110. A striking feature of this site is the presence of three conserved residues: His39, His60, and His108. These residues appear to interact with consecutive phosphate groups on one dsRNA chain. In addition, less well-conserved residues Arg64, Phe84, Ser86 and Glu110 also interact with the ligand. To test the functional importance of the three His residues, these residues were mutated to Ala or Glu and the function ability of the mutant proteins examined. It was found that His39Ala and His60Ala were inactive, indicating their importance for dsRNA binding. In contrast, His108Ala retained the activity, but mutation to glutamate resulted in loss of function. These findings implied that His108 is not essential for ligand-binding, but due to its close proximity to the negatively-charged phosphate groups in the dsRNA, mutation to a negatively-charged glutamate disrupted ligand binding via electrostatic repulsion. Hence it was concluded that except for these C and N terminal interactions discussed above, no other interactions exist to cause the two ECDs to dimerize on the dsRNA (Liu *et al.*, 2008b).

Interaction of IEH with N terminal of TLR3 (Fig. 3(B)) was studied in detail to check whether all the important residues were involved in interaction or not. Ser 86, Glu 110 and Ser 134 of receptor molecule were forming Hydrogen bonds with the ligand. Other residues-

His 39, His 60, Asn 61, Gln 62, Phe 84, Asn 85, His 108, Asn 109, Ser 132 and Asn 133 of TLR3 were involved in hydrophobic contacts with IEH. These interactions were including all the important residues required for dsRNA binding (Fig 3(C)).

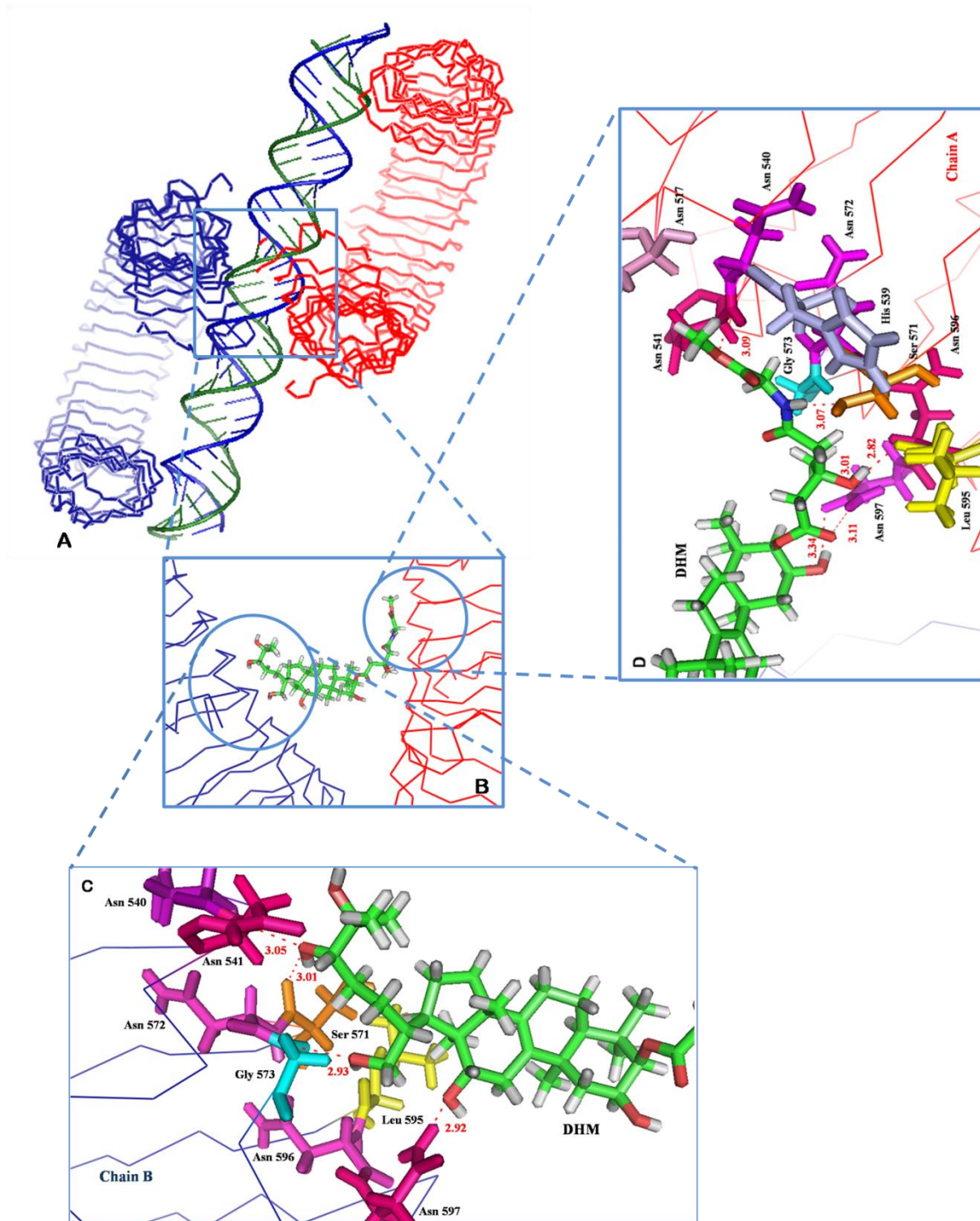


**Figure 2:** (A) Interaction between TLR3 and the dsRNA at C terminal thereby stabilizing the functional receptor dimer (B) DHM, natural compound interacting at the C terminal site of TLR3 molecules (C) Hydrogen and hydrophobic interactions of DHM with chain A of dimerized TLR3 receptor (D) Molecular interaction pattern shown by DHM with chain B of functionally active TLR3 dimer

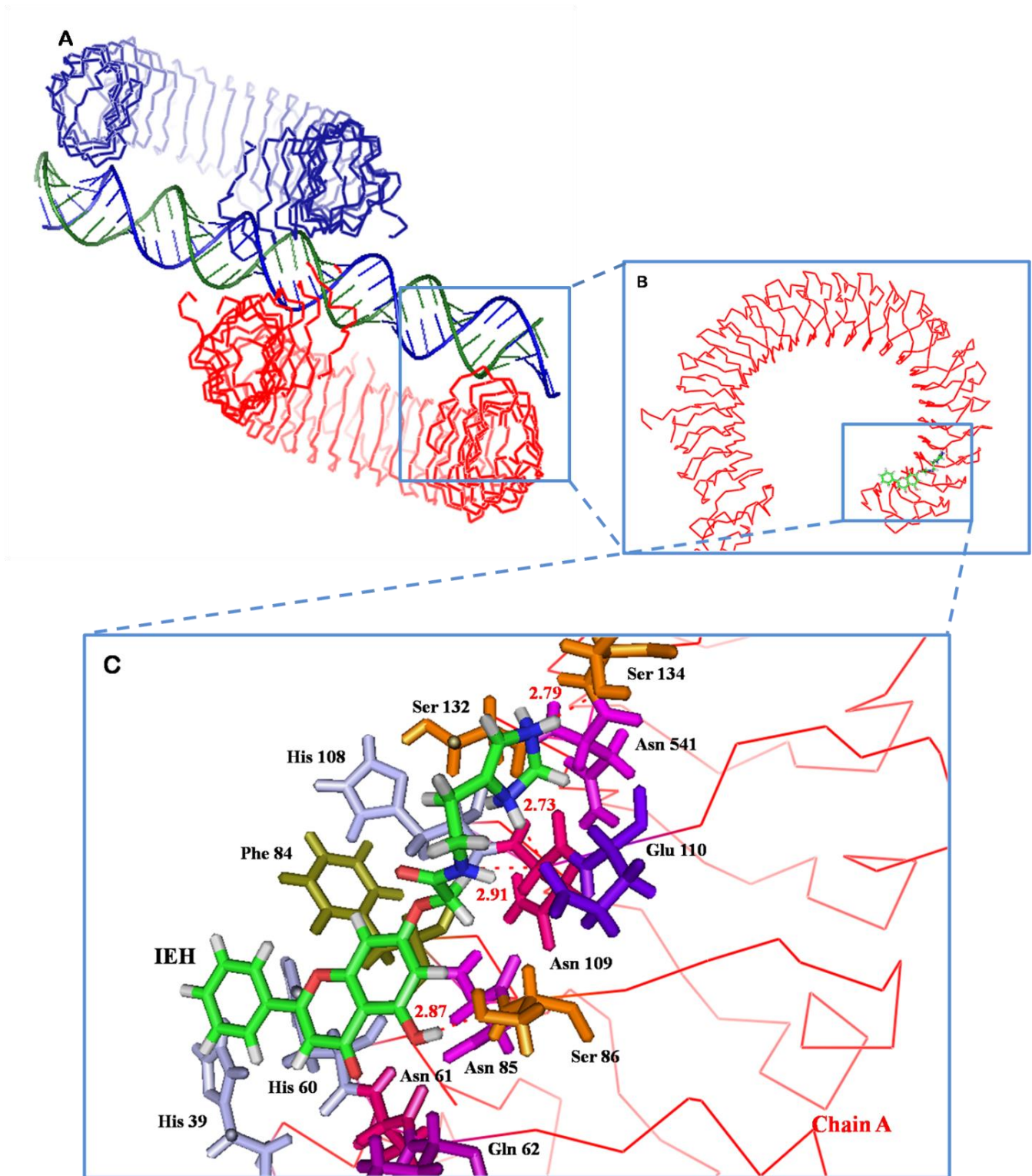


**Figure 3:** (A) Binding of dsRNA at the N terminal of TLR3 (B) IEH, the screened natural compound bound at the N terminal region of TLR3 (C) IEH mimicking the interactions between dsRNA and TLR3 N terminal

## CONCLUSION

The signaling complex structures of the TLRs with their respective ligands illustrate the tremendous diversity displayed in recognizing these different pathogen-associated molecular patterns. Using this knowledge in relation to TLR3, we studied the conditions required for the formation of a functionally active TLR3 complex. The dsRNA comes in contact with the C and N terminal residues of two TLR3 molecules, thereby holding them together in such a way that their intracellular domains come in close proximity. In this study we have reported two small molecules of natural origin that act in a manner similar to dsRNA by interacting with C and N terminal residing important residues of TLR3. Thus, these compounds have the potential to stimulating the innate immune system by activating NK cells *in vivo* to eliminate cancerous cells.

## **FUTURE PROSPECTS**

Cancer being a major global health problem has become an important and highly active area of research. Even though the paradigm for cancer treatment has evolved from relatively nonspecific cytotoxic agents to selective, mechanism-based therapeutics, not all the therapeutic approaches being used so far, are efficacious enough. Thus, it is becoming imperative to uncover new paradigms for cancer therapy. Because of the overlapping molecular mechanisms there is an urgent need for more work to untangle the signaling networks and shed light on their tightly controlled regulation and the process by which they influence each other, especially in terms of cellular growth and proliferation. This knowledge would further facilitate the development of new approach of target therapies for the treatment of cancer. These would have a high specificity towards tumors or cancerous cells, thus providing a broader therapeutic window with less toxicity to healthy and rapidly dividing cells. More recently, an improved understanding of cancer pathogenesis has given rise to new treatment options, including targeted agents and cancer immunotherapy. Targeted approaches aim to inhibit molecular pathways that are crucial for tumor growth and maintenance; whereas, immunotherapy endeavours to stimulate a host immune response that effectuates long-lived tumor destruction. Targeted therapies and cytotoxic agents also modulate immune responses, which raises the possibility that these treatment strategies can be effectively combined with immunotherapy to improve clinical outcomes. Thus, the drug candidates proposed in this study can be used in combination for better clinical results.

## REFERENCES

Acharya, C., Coop, A., Polli, J.E., and Mackerell, A.D., Jr. (2011). Recent advances in ligand-based drug design: relevance and utility of the conformationally sampled pharmacophore approach. *Current computer-aided drug design* 7, 10-22.

Agoston, V., Csermely, P., and Pongor, S. (2005). Multiple weak hits confuse complex systems: a transcriptional regulatory network as an example. *Physical review. E, Statistical, nonlinear, and soft matter physics* 71, 051909.

Akamatsu, M. (2002). Current state and perspectives of 3D-QSAR. *Current topics in medicinal chemistry* 2, 1381-1394.

Alexopoulou, L., Holt, A.C., Medzhitov, R., and Flavell, R.A. (2001). Recognition of double-stranded RNA and activation of NF-kappaB by Toll-like receptor 3. *Nature* 413, 732-738.

Alli, P.M., Pinn, M.L., Jaffee, E.M., McFadden, J.M., and Kuhajda, F.P. (2005). Fatty acid synthase inhibitors are chemopreventive for mammary cancer in neu-N transgenic mice. *Oncogene* 24, 39-46.

Alo, P.L., Galati, G.M., Sebastiani, V., Ricci, F., Visca, P., Mariani, L., Romagnoli, F., Lombardi, G., and Tondo, U.D. (2005). Fatty acid synthase expression in Paget's disease of the vulva. *International journal of gynecological pathology : official journal of the International Society of Gynecological Pathologists* 24, 404-408.

American\_Cancer\_Society (2011). *Chemotherapy Principles: An Indepth Discussion of the Techniques and Its Role in Cancer Treatment*. (American Cancer Society).

Bader, A.G., Kang, S., and Vogt, P.K. (2006). Cancer-specific mutations in PIK3CA are oncogenic in vivo. *Proceedings of the National Academy of Sciences of the United States of America* 103, 1475-1479.

Bader, A.G., Kang, S., Zhao, L., and Vogt, P.K. (2005). Oncogenic PI3K deregulates transcription and translation. *Nature reviews. Cancer* 5, 921-929.

Barlozzari, T., Reynolds, C., and Herberman, R. (1983). In vivo role of natural killer cells: involvement of large granular lymphocytes in the clearance of tumor cells in anti-asialo GM1-treated rats. *The Journal of Immunology* 131, 1024-1027.

Bathe Oliver, F., and Nava, D.-H. (2003). Therapeutic limitations in tumor-specific CD8+ memory T cell engraftment. *BMC cancer* 3:21.

Bell, J.K., Askins, J., Hall, P.R., Davies, D.R., and Segal, D.M. (2006). The dsRNA binding site of human Toll-like receptor 3. *Proceedings of the National Academy of Sciences of the United States of America* *103*, 8792-8797.

Bell, J.K., Mullen, G.E., Leifer, C.A., Mazzoni, A., Davies, D.R., and Segal, D.M. (2003). Leucine-rich repeats and pathogen recognition in Toll-like receptors. *Trends in immunology* *24*, 528-533.

Biron, C.A. (1997). Activation and function of natural killer cell responses during viral infections. *Current opinion in immunology* *9*, 24-34.

Bohl, C.E., Chang, C., Mohler, M.L., Chen, J., Miller, D.D., Swaan, P.W., and Dalton, J.T. (2004). A ligand-based approach to identify quantitative structure-activity relationships for the androgen receptor. *J Med Chem* *47*, 3765-3776.

Boland, C.R., and Ricciardiello, L. (1999). How many mutations does it take to make a tumor? *Proceedings of the National Academy of Sciences* *96*, 14675-14677.

Borisy, A.A., Elliott, P.J., Hurst, N.W., Lee, M.S., Lehar, J., Price, E.R., Serbedzija, G., Zimmermann, G.R., Foley, M.A., Stockwell, B.R., *et al.* (2003). Systematic discovery of multicomponent therapeutics. *Proceedings of the National Academy of Sciences of the United States of America* *100*, 7977-7982.

Botos, I., Liu, L., Wang, Y., Segal, D.M., and Davies, D.R. (2009). The toll-like receptor 3:dsRNA signaling complex. *Biochimica et biophysica acta* *1789*, 667-674.

Bottino, C., Moretta, L., Pende, D., Vitale, M., and Moretta, A. (2004). Learning how to discriminate between friends and enemies, a lesson from natural killer cells. *Molecular immunology* *41*, 569-575.

Brady, J., Hayakawa, Y., Smyth, M.J., and Nutt, S.L. (2004). IL-21 induces the functional maturation of murine NK cells. *Journal of immunology* *172*, 2048-2058.

Brana, I., and Siu, L.L. (2012). Clinical development of phosphatidylinositol 3-kinase inhibitors for cancer treatment. *BMC medicine* *10*, 161.

Braud, V.M., Allan, D.S., O'Callaghan, C.A., Söderström, K., D'Andrea, A., Ogg, G.S., Lazetic, S., Young, N.T., Bell, J.I., and Phillips, J.H. (1998). HLA-E binds to natural killer cell receptors CD94/NKG2A, B and C. *Nature* *391*, 795-799.

Brusselmans, K., De Schrijver, E., Heyns, W., Verhoeven, G., and Swinnen, J.V. (2003). Epigallocatechin-3-gallate is a potent natural inhibitor of fatty acid synthase in intact cells and selectively induces apoptosis in prostate cancer cells. *International journal of cancer. Journal international du cancer* *106*, 856-862.



Brusselmans, K., Vrolix, R., Verhoeven, G., and Swinnen, J.V. (2005). Induction of cancer cell apoptosis by flavonoids is associated with their ability to inhibit fatty acid synthase activity. *The Journal of biological chemistry* 280, 5636-5645.

Cain, R.J., and Ridley, A.J. (2009). Phosphoinositide 3-kinases in cell migration. *Biology of the cell / under the auspices of the European Cell Biology Organization* 101, 13-29.

Caligiuri, M.A., Velardi, A., Scheinberg, D.A., and Borrello, I.M. (2004). Immunotherapeutic approaches for hematologic malignancies. *ASH Education Program Book 2004*, 337-353.

Cantley, L.C. (2002). The phosphoinositide 3-kinase pathway. *Science* 296, 1655-1657.

Carpenter, C.L., Auger, K.R., Chanudhuri, M., Yoakim, M., Schaffhausen, B., Shoelson, S., and Cantley, L.C. (1993). Phosphoinositide 3-kinase is activated by phosphopeptides that bind to the SH2 domains of the 85-kDa subunit. *The Journal of biological chemistry* 268, 9478-9483.

Carson, J., Van Aller, G., Lehr, R., Sinnamon, R., Kirkpatrick, R., Auger, K., Dhanak, D., Copeland, R., Gontarek, R., and Tummino, P. (2008). Effects of oncogenic p110alpha subunit mutations on the lipid kinase activity of phosphoinositide 3-kinase. *Biochem. J* 409, 519-524.

Carson, W.E., Giri, J.G., Lindemann, M., Linett, M.L., Ahdieh, M., Paxton, R., Anderson, D., Eisenmann, J., Grabstein, K., and Caligiuri, M.A. (1994). Interleukin (IL) 15 is a novel cytokine that activates human natural killer cells via components of the IL-2 receptor. *The Journal of experimental medicine* 180, 1395-1403.

Chakravarty, B., Gu, Z., Chirala, S.S., Wakil, S.J., and Quioco, F.A. (2004). Human fatty acid synthase: structure and substrate selectivity of the thioesterase domain. *Proceedings of the National Academy of Sciences of the United States of America* 101, 15567-15572.

Chen, Q., Xie, W., Kuhn, D.J., Voorhees, P.M., Lopez-Girona, A., Mendy, D., Corral, L.G., Krenitsky, V.P., Xu, W., Moutouh-de Parseval, L., *et al.* (2008). Targeting the p27 E3 ligase SCF(Skp2) results in p27- and Skp2-mediated cell-cycle arrest and activation of autophagy. *Blood* 111, 4690-4699.

Cheng, H., Bagrodia, S., Bailey, S., Edwards, M., Hoffman, J., Hu, Q., Kania, R., Knighton, D.R., Marx, M.A., and Ninkovic, S. (2010). Discovery of the highly potent PI3K/mTOR dual inhibitor PF-04691502 through structure based drug design. *MedChemComm* 1, 139-144.

Cheng, H., Hoffman, J.E., Le, P.T., Pairish, M., Kania, R., Farrell, W., Bagrodia, S., Yuan, J., Sun, S., Zhang, E., *et al.* (2013). Structure-based design, SAR analysis and antitumor activity of PI3K/mTOR dual inhibitors from 4-methylpyridopyrimidinone series. *Bioorganic & medicinal chemistry letters* 23, 2787-2792.

Cho, K.R., and Vogelstein, B. (1992). Genetic alterations in the adenoma–carcinoma sequence. *Cancer* 70, 1727-1731.

Ciechanover, A. (1998). The ubiquitin-proteasome pathway: on protein death and cell life. *The EMBO journal* 17, 7151-7160.

Clynes, R.A., Towers, T.L., Presta, L.G., and Ravetch, J.V. (2000). Inhibitory Fc receptors modulate in vivo cytotoxicity against tumor targets. *Nature medicine* 6, 443-446.

Courtney, K.D., Corcoran, R.B., and Engelman, J.A. (2010). The PI3K pathway as drug target in human cancer. *Journal of clinical oncology : official journal of the American Society of Clinical Oncology* 28, 1075-1083.

Csermely, P. (2004). Strong links are important, but weak links stabilize them. *Trends in biochemical sciences* 29, 331-334.

Csermely, P., Agoston, V., and Pongor, S. (2005). The efficiency of multi-target drugs: the network approach might help drug design. *Trends in pharmacological sciences* 26, 178-182.

De Schrijver, E., Brusselmans, K., Heyns, W., Verhoeven, G., and Swinnen, J.V. (2003). RNA interference-mediated silencing of the fatty acid synthase gene attenuates growth and induces morphological changes and apoptosis of LNCaP prostate cancer cells. *Cancer research* 63, 3799-3804.

Deshaies, R.J., and Joazeiro, C.A. (2009). RING domain E3 ubiquitin ligases. *Annual review of biochemistry* 78, 399-434.

Dikshit, R., Gupta, P.C., Ramasundarahettige, C., Gajalakshmi, V., Aleksandrowicz, L., Badwe, R., Kumar, R., Roy, S., Suraweera, W., Bray, F., *et al.* (2012). Cancer mortality in India: a nationally representative survey. *Lancet* 379, 1807-1816.

Dowling, S., Cox, J., and Cenedella, R.J. (2009). Inhibition of fatty acid synthase by Orlistat accelerates gastric tumor cell apoptosis in culture and increases survival rates in gastric tumor bearing mice in vivo. *Lipids* 44, 489-498.

Druker, B.J., Talpaz, M., Resta, D.J., Peng, B., Buchdunger, E., Ford, J.M., Lydon, N.B., Kantarjian, H., Capdeville, R., and Ohno-Jones, S. (2001). Efficacy and safety of a specific inhibitor of the BCR-ABL tyrosine kinase in chronic myeloid leukemia. *New England Journal of Medicine* 344, 1031-1037.

Dudley, M.E., and Roopenian, D.C. (1996). Loss of a unique tumor antigen by cytotoxic T lymphocyte immunoselection from a 3-methylcholanthrene-induced mouse sarcoma reveals secondary unique and shared antigens. *The Journal of experimental medicine* 184, 441-447.

Dunlap, J., Le, C., Shukla, A., Patterson, J., Presnell, A., Heinrich, M.C., Corless, C.L., and Troxell, M.L. (2010). Phosphatidylinositol-3-kinase and AKT1 mutations occur early in breast carcinoma. *Breast cancer research and treatment* 120, 409-418.

Engelman, J.A. (2009). Targeting PI3K signalling in cancer: opportunities, challenges and limitations. *Nature Reviews Cancer* 9, 550-562.

Engelman, J.A., Chen, L., Tan, X., Crosby, K., Guimaraes, A.R., Upadhyay, R., Maira, M., McNamara, K., Perera, S.A., Song, Y., *et al.* (2008). Effective use of PI3K and MEK inhibitors to treat mutant Kras G12D and PIK3CA H1047R murine lung cancers. *Nature medicine* 14, 1351-1356.

Engelman, J.A., Luo, J., and Cantley, L.C. (2006). The evolution of phosphatidylinositol 3-kinases as regulators of growth and metabolism. *Nature reviews. Genetics* 7, 606-619.

Feher, M., and Schmidt, J.M. (2003). Property distributions: differences between drugs, natural products, and molecules from combinatorial chemistry. *J Chem Inf Comput Sci* 43, 218-227.

Fehniger, T.A., Cooper, M.A., and Caligiuri, M.A. (2002). Interleukin-2 and interleukin-15: immunotherapy for cancer. *Cytokine & growth factor reviews* 13, 169-183.

Ferlazzo, G., and Münz, C. (2004). NK cell compartments and their activation by dendritic cells. *The Journal of Immunology* 172, 1333-1339.

Fiorentino, M., Zadra, G., Palescandolo, E., Fedele, G., Bailey, D., Fiore, C., Nguyen, P.L., Migita, T., Zamponi, R., Di Vizio, D., *et al.* (2008). Overexpression of fatty acid synthase is associated with palmitoylation of Wnt1 and cytoplasmic stabilization of beta-catenin in prostate cancer. *Laboratory investigation; a journal of technical methods and pathology* 88, 1340-1348.

Flavin, R., Peluso, S., Nguyen, P.L., and Loda, M. (2010). Fatty acid synthase as a potential therapeutic target in cancer. *Future Oncol* 6, 551-562.

Fogler, W.E., Volker, K., McCormick, K.L., Watanabe, M., Ortaldo, J.R., and Wilttrout, R.H. (1996). NK cell infiltration into lung, liver, and subcutaneous B16 melanoma is mediated by VCAM-1/VLA-4 interaction. *The Journal of Immunology* 156, 4707-4714.

Foldes, J., Shih, M.S., and Parfitt, A.M. (1990). Frequency distributions of tetracycline-based measurements: implications for the interpretation of bone formation indices in the absence of double-labeled surfaces. *Journal of bone and mineral research : the official journal of the American Society for Bone and Mineral Research* 5, 1063-1067.

Frescas, D., and Pagano, M. (2008). Deregulated proteolysis by the F-box proteins SKP2 and beta-TrCP: tipping the scales of cancer. *Nature reviews. Cancer* 8, 438-449.

Friesner, R.A., Banks, J.L., Murphy, R.B., Halgren, T.A., Klicic, J.J., Mainz, D.T., Repasky, M.P., Knoll, E.H., Shelley, M., Perry, J.K., *et al.* (2004). Glide: a new approach for rapid, accurate docking and scoring. 1. Method and assessment of docking accuracy. *J Med Chem* 47, 1739-1749.

Funabashi, H., Kawaguchi, A., Tomoda, H., Omura, S., Okuda, S., and Iwasaki, S. (1989). Binding site of cerulenin in fatty acid synthetase. *Journal of biochemistry* 105, 751-755.

Graner, E., Tang, D., Rossi, S., Baron, A., Migita, T., Weinstein, L.J., Lechpammer, M., Huesken, D., Zimmermann, J., Signoretti, S., *et al.* (2004). The isopeptidase USP2a regulates the stability of fatty acid synthase in prostate cancer. *Cancer cell* 5, 253-261.

Graupera, M., Guillermet-Guibert, J., Foukas, L.C., Phng, L.K., Cain, R.J., Salpekar, A., Pearce, W., Meek, S., Millan, J., Cutillas, P.R., *et al.* (2008). Angiogenesis selectively requires the p110alpha isoform of PI3K to control endothelial cell migration. *Nature* 453, 662-666.

Groen, T. (1987). Tumor-associated antigens. *Tumor Immunology; Mechanisms, Diagnosis, Therapy*. Elsevier, Amsterdam, 13-27.

Guerreiro, A.S., Fattet, S., Fischer, B., Shalaby, T., Jackson, S.P., Schoenwaelder, S.M., Grotzer, M.A., Delattre, O., and Arcaro, A. (2008). Targeting the PI3K p110 $\alpha$  isoform inhibits medulloblastoma proliferation, chemoresistance, and migration. *Clinical Cancer Research* 14, 6761-6769.

Hahne, M., Rimoldi, D., Schröter, M., Romero, P., Schreier, M., French, L., Schneider, P., Bornand, T., Fontana, A., and Lienard, D. (1996). Melanoma cell expression of Fas (Apo-1/CD95) ligand: implications for tumor immune escape. *Science* 274, 1363-1366.

Halgren, T.A., Murphy, R.B., Friesner, R.A., Beard, H.S., Frye, L.L., Pollard, W.T., and Banks, J.L. (2004). Glide: a new approach for rapid, accurate docking and scoring. 2. Enrichment factors in database screening. *J Med Chem* 47, 1750-1759.

Hamerman, J.A., Ogasawara, K., and Lanier, L.L. (2005). NK cells in innate immunity. *Current opinion in immunology* 17, 29-35.

Hao, B., Zheng, N., Schulman, B.A., Wu, G., Miller, J.J., Pagano, M., and Pavletich, N.P. (2005). Structural basis of the Cks1-dependent recognition of p27(Kip1) by the SCF(Skp2) ubiquitin ligase. *Molecular cell* 20, 9-19.

Hershko, A., Ciechanover, A., and Varshavsky, A. (2000). Basic Medical Research Award. The ubiquitin system. *Nature medicine* 6, 1073-1081.

Holloway, M.K. (1998). A priori prediction of ligand affinity by energy minimization. *Perspectives in drug discovery and design* 9, 63-84.

Hoover, H.S., Blankman, J.L., Niessen, S., and Cravatt, B.F. (2008). Selectivity of inhibitors of endocannabinoid biosynthesis evaluated by activity-based protein profiling. *Bioorganic & medicinal chemistry letters* 18, 5838-5841.

Huang, C.-H., Mandelker, D., Schmidt-Kittler, O., Samuels, Y., Velculescu, V.E., Kinzler, K.W., Vogelstein, B., Gabbelli, S.B., and Amzel, L.M. (2007). The structure of a human p110 $\alpha$ /p85 $\alpha$  complex elucidates the effects of oncogenic PI3K $\alpha$  mutations. *Science* 318, 1744-1748.

Huang, J., Sheung, J., Dong, G., Coquilla, C., Daniel-Issakani, S., and Payan, D.G. (2005). High-throughput screening for inhibitors of the e3 ubiquitin ligase APC. *Methods in enzymology* 399, 740-754.

Huang, S. (2002). Rational drug discovery: what can we learn from regulatory networks? *Drug discovery today* 7, S163-169.

Ikenoue, T., Kanai, F., Hikiba, Y., Obata, T., Tanaka, Y., Imamura, J., Ohta, M., Jazag, A., Guleng, B., Tateishi, K., *et al.* (2005). Functional analysis of PIK3CA gene mutations in human colorectal cancer. *Cancer research* 65, 4562-4567.

Innocenzi, D., Alo, P.L., Balzani, A., Sebastiani, V., Silipo, V., La Torre, G., Ricciardi, G., Bosman, C., and Calvieri, S. (2003). Fatty acid synthase expression in melanoma. *Journal of cutaneous pathology* 30, 23-28.

Irwin, J.J., and Shoichet, B.K. (2005). ZINC--a free database of commercially available compounds for virtual screening. *Journal of chemical information and modeling* 45, 177-182.

Isakoff, S.J., Engelman, J.A., Irie, H.Y., Luo, J., Brachmann, S.M., Pearlman, R.V., Cantley, L.C., and Brugge, J.S. (2005). Breast cancer-associated PIK3CA mutations are oncogenic in mammary epithelial cells. *Cancer research* 65, 10992-11000.

Jäger, E., Ringhoffer, M., Karbach, J., Arand, M., Oesch, F., and Knuth, A. (1996). Inverse relationship of melanocyte differentiation antigen expression in melanoma tissues and CD8+ cytotoxic-T-cell responses: Evidence for immunoselection of antigen-loss variants in vivo. *International Journal of Cancer* 66, 470-476.

Jia, L., and Sun, Y. (2009). RBX1/ROC1-SCF E3 ubiquitin ligase is required for mouse embryogenesis and cancer cell survival. *Cell division* 4, 16.

Jia, L., and Sun, Y. (2011). SCF E3 ubiquitin ligases as anticancer targets. *Current cancer drug targets* *11*, 347-356.

Jorgensen, W.L., Maxwell, D.S., and Tirado-Rives, J. (1996). Development and testing of the OPLS all-atom force field on conformational energetics and properties of organic liquids. *Journal of the American Chemical Society* *118*, 11225-11236.

Kaelin, W.G., Jr. (2004). Gleevec: prototype or outlier? *Science's STKE : signal transduction knowledge environment* *2004*, pe12.

Kaminski, G.A., Friesner, R.A., Tirado-Rives, J., and Jorgensen, W.L. (2001). Evaluation and reparametrization of the OPLS-AA force field for proteins via comparison with accurate quantum chemical calculations on peptides. *The Journal of Physical Chemistry B* *105*, 6474-6487.

Kang, S., Denley, A., Vanhaesebroeck, B., and Vogt, P.K. (2006). Oncogenic transformation induced by the p110beta, -gamma, and -delta isoforms of class I phosphoinositide 3-kinase. *Proceedings of the National Academy of Sciences of the United States of America* *103*, 1289-1294.

Katagiri, Y., Hozumi, Y., and Kondo, S. (2006). Knockdown of Skp2 by siRNA inhibits melanoma cell growth in vitro and in vivo. *Journal of dermatological science* *42*, 215-224.

Katso, R., Okkenhaug, K., Ahmadi, K., White, S., Timms, J., and Waterfield, M.D. (2001). Cellular function of phosphoinositide 3-kinases: implications for development, homeostasis, and cancer. *Annual review of cell and developmental biology* *17*, 615-675.

Khan, N., Afaq, F., Saleem, M., Ahmad, N., and Mukhtar, H. (2006). Targeting multiple signaling pathways by green tea polyphenol (-)-epigallocatechin-3-gallate. *Cancer research* *66*, 2500-2505.

Kobayashi, H., Dubois, S., Sato, N., Sabzevari, H., Sakai, Y., Waldmann, T.A., and Tagaya, Y. (2005). Role of trans-cellular IL-15 presentation in the activation of NK cell-mediated killing, which leads to enhanced tumor immunosurveillance. *Blood* *105*, 721-727.

Koh, C.Y., Blazar, B.R., George, T., Welniak, L.A., Capitini, C.M., Raziuddin, A., Murphy, W.J., and Bennett, M. (2001). Augmentation of antitumor effects by NK cell inhibitory receptor blockade in vitro and in vivo. *Blood* *97*, 3132-3137.

Kridel, S.J., Axelrod, F., Rozenkrantz, N., and Smith, J.W. (2004). Orlistat is a novel inhibitor of fatty acid synthase with antitumor activity. *Cancer research* *64*, 2070-2075.

Kudo, Y., Kitajima, S., Ogawa, I., Kitagawa, M., Miyauchi, M., and Takata, T. (2005). Small interfering RNA targeting of S phase kinase-interacting protein 2 inhibits cell growth of oral cancer cells by inhibiting p27 degradation. *Mol Cancer Ther* 4, 471-476.

Kuhajda, F.P. (2000). Fatty-acid synthase and human cancer: new perspectives on its role in tumor biology. *Nutrition* 16, 202-208.

Kuhajda, F.P. (2006). Fatty acid synthase and cancer: new application of an old pathway. *Cancer research* 66, 5977-5980.

Kuhajda, F.P., Pizer, E.S., Li, J.N., Mani, N.S., Frehywot, G.L., and Townsend, C.A. (2000). Synthesis and antitumor activity of an inhibitor of fatty acid synthase. *Proceedings of the National Academy of Sciences of the United States of America* 97, 3450-3454.

Kuroki, M., Ueno, A., Matsumoto, H., Abe, H., Li, T., Imakiire, T., Yamauchi, Y., Uno, K., Shirota, K., and Shibaguchi, H. (2001). Significance of tumor-associated antigens in the diagnosis and therapy of cancer: an overview. *Anticancer research* 22, 4255-4264.

Kurosu, H., Maehama, T., Okada, T., Yamamoto, T., Hoshino, S.-i., Fukui, Y., Ui, M., Hazeki, O., and Katada, T. (1997). Heterodimeric phosphoinositide 3-kinase consisting of p85 and p110 $\beta$  is synergistically activated by the  $\beta\gamma$  subunits of G proteins and phosphotyrosyl peptide. *Journal of Biological Chemistry* 272, 24252-24256.

Kusakabe, T., Nashimoto, A., Honma, K., and Suzuki, T. (2002). Fatty acid synthase is highly expressed in carcinoma, adenoma and in regenerative epithelium and intestinal metaplasia of the stomach. *Histopathology* 40, 71-79.

Lafreniere, R., and Rosenberg, S. (1985). Adoptive immunotherapy of murine hepatic metastases with lymphokine activated killer (LAK) cells and recombinant interleukin 2 (IL 2) can mediate the regression of both immunogenic and nonimmunogenic sarcomas and an adenocarcinoma. *The Journal of Immunology* 135, 4273-4280.

Latres, E., Chiarle, R., Schulman, B.A., Pavletich, N.P., Pellicer, A., Inghirami, G., and Pagano, M. (2001). Role of the F-box protein Skp2 in lymphomagenesis. *Proceedings of the National Academy of Sciences of the United States of America* 98, 2515-2520.

Lee, M.L., and Schneider, G. (2001). Scaffold architecture and pharmacophoric properties of natural products and trade drugs: application in the design of natural product-based combinatorial libraries. *J Comb Chem* 3, 284-289.

Lee, S.H., and McCormick, F. (2005). Downregulation of Skp2 and p27/Kip1 synergistically induces apoptosis in T98G glioblastoma cells. *Journal of molecular medicine* 83, 296-307.

Li, B.H., and Tian, W.X. (2004). Inhibitory effects of flavonoids on animal fatty acid synthase. *Journal of biochemistry* 135, 85-91.

Lipton, S.A. (2004). Turning down, but not off. *Nature* 428, 473-473.

Liu, H., Liu, Y., and Zhang, J.T. (2008a). A new mechanism of drug resistance in breast cancer cells: fatty acid synthase overexpression-mediated palmitate overproduction. *Mol Cancer Ther* 7, 263-270.

Liu, L., Botos, I., Wang, Y., Leonard, J.N., Shiloach, J., Segal, D.M., and Davies, D.R. (2008b). Structural basis of toll-like receptor 3 signaling with double-stranded RNA. *Science* 320, 379-381.

Liu, V.C., Wong, L.Y., Jang, T., Shah, A.H., Park, I., Yang, X., Zhang, Q., Lonning, S., Teicher, B.A., and Lee, C. (2007). Tumor evasion of the immune system by converting CD4+ CD25- T cells into CD4+ CD25+ T regulatory cells: role of tumor-derived TGF- $\beta$ . *The Journal of Immunology* 178, 2883-2892.

Ljunggren, H.-G., and Kärre, K. (1985). Host resistance directed selectively against H-2-deficient lymphoma variants. Analysis of the mechanism. *The Journal of experimental medicine* 162, 1745-1759.

Maier, T., Jenni, S., and Ban, N. (2006). Architecture of mammalian fatty acid synthase at 4.5 Å resolution. *Science* 311, 1258-1262.

Maier, T., Leibundgut, M., and Ban, N. (2008). The crystal structure of a mammalian fatty acid synthase. *Science* 321, 1315-1322.

Mandelker, D., Gabelli, S.B., Schmidt-Kittler, O., Zhu, J., Cheong, I., Huang, C.H., Kinzler, K.W., Vogelstein, B., and Amzel, L.M. (2009). A frequent kinase domain mutation that changes the interaction between PI3K $\alpha$  and the membrane. *Proceedings of the National Academy of Sciences of the United States of America* 106, 16996-17001.

Maraskovsky, E., Brasel, K., Teepe, M., Roux, E.R., Lyman, S.D., Shortman, K., and McKenna, H.J. (1996). Dramatic increase in the numbers of functionally mature dendritic cells in Flt3 ligand-treated mice: multiple dendritic cell subpopulations identified. *The Journal of experimental medicine* 184, 1953-1962.

McFadden, J.M., Medghalchi, S.M., Thupari, J.N., Pinn, M.L., Vadlamudi, A., Miller, K.I., Kuhajda, F.P., and Townsend, C.A. (2005). Application of a flexible synthesis of (5R)-thiolactomycin to develop new inhibitors of type I fatty acid synthase. *J Med Chem* 48, 946-961.

Menendez, J.A., and Lupu, R. (2004). Fatty acid synthase-catalyzed de novo fatty acid biosynthesis: from anabolic-energy-storage pathway in normal tissues to jack-of-all-trades in cancer cells. *Archivum immunologiae et therapiae experimentalis* 52, 414-426.



Menendez, J.A., and Lupu, R. (2006). Oncogenic properties of the endogenous fatty acid metabolism: molecular pathology of fatty acid synthase in cancer cells. *Current opinion in clinical nutrition and metabolic care* 9, 346-357.

Menendez, J.A., and Lupu, R. (2007). Fatty acid synthase and the lipogenic phenotype in cancer pathogenesis. *Nature reviews. Cancer* 7, 763-777.

Menendez, J.A., Lupu, R., and Colomer, R. (2005). Targeting fatty acid synthase: potential for therapeutic intervention in her-2/neu-overexpressing breast cancer. *Drug news & perspectives* 18, 375-385.

Migita, T., Ruiz, S., Fornari, A., Fiorentino, M., Priolo, C., Zadra, G., Inazuka, F., Grisanzio, C., Palescandolo, E., Shin, E., *et al.* (2009). Fatty acid synthase: a metabolic enzyme and candidate oncogene in prostate cancer. *Journal of the National Cancer Institute* 101, 519-532.

Miled, N., Yan, Y., Hon, W.C., Perisic, O., Zvelebil, M., Inbar, Y., Schneidman-Duhovny, D., Wolfson, H.J., Backer, J.M., and Williams, R.L. (2007). Mechanism of two classes of cancer mutations in the phosphoinositide 3-kinase catalytic subunit. *Science* 317, 239-242.

Milgram, L.Z., Witters, L.A., Pasternack, G.R., and Kuhajda, F.P. (1997). Enzymes of the fatty acid synthesis pathway are highly expressed in in situ breast carcinoma. *Clinical cancer research : an official journal of the American Association for Cancer Research* 3, 2115-2120.

Mizoguchi, M., Nutt, C.L., Mohapatra, G., and Louis, D.N. (2004). Genetic alterations of phosphoinositide 3-kinase subunit genes in human glioblastomas. *Brain pathology* 14, 372-377.

Moretta, L., Ferlazzo, G., Bottino, C., Vitale, M., Pende, D., Mingari, M.C., and Moretta, A. (2006). Effector and regulatory events during natural killer–dendritic cell interactions. *Immunological reviews* 214, 219-228.

Nakano, H., Kishida, T., Asada, H., Shin-Ya, M., Shinomiya, T., Imanishi, J., Shimada, T., Nakai, S., Takeuchi, M., and Hisa, Y. (2006). Interleukin-21 triggers both cellular and humoral immune responses leading to therapeutic antitumor effects against head and neck squamous cell carcinoma. *The journal of gene medicine* 8, 90-99.

Nakayama, K.I., and Nakayama, K. (2006). Ubiquitin ligases: cell-cycle control and cancer. *Nature reviews. Cancer* 6, 369-381.

Nalepa, G., Rolfe, M., and Harper, J.W. (2006). Drug discovery in the ubiquitin-proteasome system. *Nature reviews. Drug discovery* 5, 596-613.

Ocampo, M.T., Chaung, W., Marenstein, D.R., Chan, M.K., Altamirano, A., Basu, A.K., Boorstein, R.J., Cunningham, R.P., and Teebor, G.W. (2002). Targeted deletion of mNth1 reveals a novel DNA repair enzyme activity. *Molecular and cellular biology* 22, 6111-6121.

Ogino, S., Nosho, K., Meyerhardt, J.A., Kirkner, G.J., Chan, A.T., Kawasaki, T., Giovannucci, E.L., Loda, M., and Fuchs, C.S. (2008). Cohort study of fatty acid synthase expression and patient survival in colon cancer. *Journal of clinical oncology : official journal of the American Society of Clinical Oncology* 26, 5713-5720.

Orita, H., Coulter, J., Lemmon, C., Tully, E., Vadlamudi, A., Medghalchi, S.M., Kuhajda, F.P., and Gabrielson, E. (2007). Selective inhibition of fatty acid synthase for lung cancer treatment. *Clinical cancer research : an official journal of the American Association for Cancer Research* 13, 7139-7145.

Papp, B., Pal, C., and Hurst, L.D. (2004). Metabolic network analysis of the causes and evolution of enzyme dispensability in yeast. *Nature* 429, 661-664.

Parrish-Novak, J., Dillon, S.R., Nelson, A., Hammond, A., Sprecher, C., Gross, J.A., Johnston, J., Madden, K., Xu, W., and West, J. (2000). Interleukin 21 and its receptor are involved in NK cell expansion and regulation of lymphocyte function. *Nature* 408, 57-63.

Pazirandeh, M., Chirala, S., Huang, W., and Wakil, S. (1989). Characterization of recombinant thioesterase and acyl carrier protein domains of chicken fatty acid synthase expressed in *Escherichia coli*. *Journal of Biological Chemistry* 264, 18195-18201.

Pazirandeh, M., Chirala, S., and Wakil, S. (1991). Site-directed mutagenesis studies on the recombinant thioesterase domain of chicken fatty acid synthase expressed in *Escherichia coli*. *Journal of Biological Chemistry* 266, 20946-20952.

Pemble, C.W.t., Johnson, L.C., Kridel, S.J., and Lowther, W.T. (2007). Crystal structure of the thioesterase domain of human fatty acid synthase inhibited by Orlistat. *Nature structural & molecular biology* 14, 704-709.

Petrelli, A., and Giordano, S. (2008). From single- to multi-target drugs in cancer therapy: when aspecificity becomes an advantage. *Current medicinal chemistry* 15, 422-432.

Petroski, M.D., and Deshaies, R.J. (2005). Function and regulation of cullin-RING ubiquitin ligases. *Nature reviews. Molecular cell biology* 6, 9-20.

Philp, A.J., Campbell, I.G., Leet, C., Vincan, E., Rockman, S.P., Whitehead, R.H., Thomas, R.J., and Phillips, W.A. (2001). The phosphatidylinositol 3'-kinase p85alpha gene is an oncogene in human ovarian and colon tumors. *Cancer research* 61, 7426-7429.

Pickart, C.M. (2000). Ubiquitin in chains. *Trends in biochemical sciences* 25, 544-548.

Piyathilake, C.J., Frost, A.R., Manne, U., Bell, W.C., Weiss, H., Heimbürger, D.C., and Grizzle, W.E. (2000). The expression of fatty acid synthase (FASE) is an early event in the development and progression of squamous cell carcinoma of the lung. *Human pathology* 31, 1068-1073.

Pizer, E.S., Jackisch, C., Wood, F.D., Pasternack, G.R., Davidson, N.E., and Kuhajda, F.P. (1996a). Inhibition of fatty acid synthesis induces programmed cell death in human breast cancer cells. *Cancer research* 56, 2745-2747.

Pizer, E.S., Thupari, J., Han, W.F., Pinn, M.L., Chrest, F.J., Frehywot, G.L., Townsend, C.A., and Kuhajda, F.P. (2000). Malonyl-coenzyme-A is a potential mediator of cytotoxicity induced by fatty-acid synthase inhibition in human breast cancer cells and xenografts. *Cancer research* 60, 213-218.

Pizer, E.S., Wood, F.D., Heine, H.S., Romantsev, F.E., Pasternack, G.R., and Kuhajda, F.P. (1996b). Inhibition of fatty acid synthesis delays disease progression in a xenograft model of ovarian cancer. *Cancer research* 56, 1189-1193.

Puig, T., Turrado, C., Benhamu, B., Aguilar, H., Relat, J., Ortega-Gutierrez, S., Casals, G., Marrero, P.F., Urruticoechea, A., Haro, D., *et al.* (2009). Novel Inhibitors of Fatty Acid Synthase with Anticancer Activity. *Clinical cancer research : an official journal of the American Association for Cancer Research* 15, 7608-7615.

Qiu, Y., and Kung, H.J. (2000). Signaling network of the Btk family kinases. *Oncogene* 19, 5651-5661.

Rendina, A.R., and Cheng, D. (2005). Characterization of the inactivation of rat fatty acid synthase by C75: inhibition of partial reactions and protection by substrates. *The Biochemical journal* 388, 895-903.

Riccardi, C., Santoni, A., Barlozzari, T., Puccetti, P., and Herberman, R. (1980). In vivo natural reactivity of mice against tumor cells. *International Journal of Cancer* 25, 475-486.

Rivkin, A., Kim, Y.R., Goulet, M.T., Bays, N., Hill, A.D., Kariv, I., Krauss, S., Ginanni, N., Strack, P.R., Kohl, N.E., *et al.* (2006). 3-Aryl-4-hydroxyquinolin-2(1H)-one derivatives as type I fatty acid synthase inhibitors. *Bioorganic & medicinal chemistry letters* 16, 4620-4623.

Roche, S., Downward, J., Raynal, P., and Courtneidge, S.A. (1998). A function for phosphatidylinositol 3-kinase beta (p85alpha-p110beta) in fibroblasts during mitogenesis: requirement for insulin- and lysophosphatidic acid-mediated signal transduction. *Molecular and cellular biology* 18, 7119-7129.

Rodella, L., Zamai, L., Rezzani, R., Artico, M., Peri, G., Falconi, M., Facchini, A., Pelusi, G., and Vitale, M. (2001). Interleukin 2 and interleukin 15 differentially predispose natural killer cells to apoptosis mediated by endothelial and tumour cells. *British journal of haematology* *115*, 442-450.

Rogawski, M.A. (2000). Low affinity channel blocking (uncompetitive) NMDA receptor antagonists as therapeutic agents--toward an understanding of their favorable tolerability. *Amino acids* *19*, 133-149.

Rossi, S., Graner, E., Febbo, P., Weinstein, L., Bhattacharya, N., Onody, T., Buble, G., Balk, S., and Loda, M. (2003). Fatty acid synthase expression defines distinct molecular signatures in prostate cancer. *Molecular cancer research : MCR* *1*, 707-715.

Rossi, S., Ou, W., Tang, D., Bhattacharya, N., Dei Tos, A.P., Fletcher, J.A., and Loda, M. (2006). Gastrointestinal stromal tumours overexpress fatty acid synthase. *The Journal of pathology* *209*, 369-375.

Samuels, Y., and Velculescu, V.E. (2004). Oncogenic mutations of PIK3CA in human cancers. *Cell cycle* *3*, 1221-1224.

Samuels, Y., Wang, Z., Bardelli, A., Silliman, N., Ptak, J., Szabo, S., Yan, H., Gazdar, A., Powell, S.M., Riggins, G.J., *et al.* (2004). High frequency of mutations of the PIK3CA gene in human cancers. *Science* *304*, 554.

Sarbassov, D.D., Guertin, D.A., Ali, S.M., and Sabatini, D.M. (2005). Phosphorylation and regulation of Akt/PKB by the rictor-mTOR complex. *Science* *307*, 1098-1101.

Schrödinger (2009). Schrödinger Suite 2009: Protein Preparation Wizard; Epik version 2.0, Schrödinger, LLC, New York, NY, 2009; Impact version 5.5, Schrödinger, LLC, New York, NY, 2009; Prime version 2.1, Schrödinger, LLC, New York, NY, 2009.

Schulman, B.A., Carrano, A.C., Jeffrey, P.D., Bowen, Z., Kinnucan, E.R., Finnin, M.S., Elledge, S.J., Harper, J.W., Pagano, M., and Pavletich, N.P. (2000). Insights into SCF ubiquitin ligases from the structure of the Skp1-Skp2 complex. *Nature* *408*, 381-386.

Sebolt-Leopold, J.S., and English, J.M. (2006). Mechanisms of drug inhibition of signalling molecules. *Nature* *441*, 457-462.

Seung, S., Urban, J.L., and Schreiber, H. (1993). A tumor escape variant that has lost one major histocompatibility complex class I restriction element induces specific CD8+ T cells to an antigen that no longer serves as a target. *The Journal of experimental medicine* *178*, 933-940.

Shastri, N., Schwab, S., and Serwold, T. (2002). Producing nature's gene-chips: the generation of peptides for display by MHC class I molecules. *Annual review of immunology* 20, 463-493.

Shaw, R.J., and Cantley, L.C. (2006). Ras, PI (3) K and mTOR signalling controls tumour cell growth. *Nature* 441, 424-430.

Shaw, S.G., Maung, A.A., Steptoe, R.J., Thomson, A.W., and Vujanovic, N.L. (1998). Expansion of functional NK cells in multiple tissue compartments of mice treated with Flt3-ligand: implications for anti-cancer and anti-viral therapy. *The Journal of Immunology* 161, 2817-2824.

Shayesteh, L., Lu, Y., Kuo, W.L., Baldocchi, R., Godfrey, T., Collins, C., Pinkel, D., Powell, B., Mills, G.B., and Gray, J.W. (1999). PIK3CA is implicated as an oncogene in ovarian cancer. *Nature genetics* 21, 99-102.

Shim, E.H., Johnson, L., Noh, H.L., Kim, Y.J., Sun, H., Zeiss, C., and Zhang, H. (2003). Expression of the F-box protein SKP2 induces hyperplasia, dysplasia, and low-grade carcinoma in the mouse prostate. *Cancer research* 63, 1583-1588.

Shurbaji, M.S., Kalbfleisch, J.H., and Thurmond, T.S. (1996). Immunohistochemical detection of a fatty acid synthase (OA-519) as a predictor of progression of prostate cancer. *Human pathology* 27, 917-921.

Siegel, R., Naishadham, D., and Jemal, A. (2012). Cancer statistics, 2012. *CA Cancer J Clin* 62, 10-29.

Sivori, S., Carlomagno, S., Moretta, L., and Moretta, A. (2006). Comparison of different CpG oligodeoxynucleotide classes for their capability to stimulate human NK cells. *European journal of immunology* 36, 961-967.

Skaar, J.R., D'Angiolella, V., Pagan, J.K., and Pagano, M. (2009). SnapShot: F Box Proteins II. *Cell* 137, 1358, 1358 e1351.

Skolnik, E.Y., Margolis, B., Mohammadi, M., Lowenstein, E., Fischer, R., Drepps, A., Ullrich, A., and Schlessinger, J. (1991). Cloning of PI3 kinase-associated p85 utilizing a novel method for expression/cloning of target proteins for receptor tyrosine kinases. *Cell* 65, 83-90.

Smith, S., and Tsai, S.C. (2007). The type I fatty acid and polyketide synthases: a tale of two megasynthases. *Natural product reports* 24, 1041-1072.

Smyth, M.J., Kelly, J.M., Baxter, A.G., Körner, H., and Sedgwick, J.D. (1998). An essential role for tumor necrosis factor in natural killer cell-mediated tumor rejection in the peritoneum. *The Journal of experimental medicine* *188*, 1611-1619.

Smyth, M.J., Takeda, K., Hayakawa, Y., Peschon, J.J., van den Brink, M.R., and Yagita, H. (2003). Nature's TRAIL—on a path to cancer immunotherapy. *Immunity* *18*, 1-6.

Smyth, M.J., Thia, K.Y., Cretney, E., Kelly, J.M., Snook, M.B., Forbes, C.A., and Scalzo, A.A. (1999). Perforin is a major contributor to NK cell control of tumor metastasis. *The Journal of Immunology* *162*, 6658-6662.

Sopasakis, V.R., Liu, P., Suzuki, R., Kondo, T., Winnay, J., Tran, T.T., Asano, T., Smyth, G., Sajan, M.P., Farese, R.V., *et al.* (2010). Specific roles of the p110alpha isoform of phosphatidylinositol 3-kinase in hepatic insulin signaling and metabolic regulation. *Cell metabolism* *11*, 220-230.

Stoler, D.L., Chen, N., Basik, M., Kahlenberg, M.S., Rodriguez-Bigas, M.A., Petrelli, N.J., and Anderson, G.R. (1999). The onset and extent of genomic instability in sporadic colorectal tumor progression. *Proceedings of the National Academy of Sciences* *96*, 15121-15126.

Strengell, M., Sareneva, T., Foster, D., Julkunen, I., and Matikainen, S. (2002). IL-21 up-regulates the expression of genes associated with innate immunity and Th1 response. *The Journal of Immunology* *169*, 3600-3605.

Sumimoto, H., Yamagata, S., Shimizu, A., Miyoshi, H., Mizuguchi, H., Hayakawa, T., Miyagishi, M., Taira, K., and Kawakami, Y. (2005). Gene therapy for human small-cell lung carcinoma by inactivation of Skp-2 with virally mediated RNA interference. *Gene therapy* *12*, 95-100.

Sun, H. (2008). Pharmacophore-based virtual screening. *Curr Med Chem* *15*, 1018-1024.

Swinnen, J.V., Brusselmans, K., and Verhoeven, G. (2006). Increased lipogenesis in cancer cells: new players, novel targets. *Current opinion in clinical nutrition and metabolic care* *9*, 358-365.

Szuromi, P., Vinson, V., and Marshall, E. (2004). Rethinking drug discovery. *Science* *303*, 1795-1795.

Takahiro, T., Shinichi, K., and Toshimitsu, S. (2003). Expression of fatty acid synthase as a prognostic indicator in soft tissue sarcomas. *Clinical cancer research : an official journal of the American Association for Cancer Research* *9*, 2204-2212.

Thupari, J.N., Pinn, M.L., and Kuhajda, F.P. (2001). Fatty acid synthase inhibition in human breast cancer cells leads to malonyl-CoA-induced inhibition of fatty acid oxidation and cytotoxicity. *Biochemical and biophysical research communications* 285, 217-223.

Tian, W.X. (2006). Inhibition of fatty acid synthase by polyphenols. *Current medicinal chemistry* 13, 967-977.

Timmerbeul, I., Garrett-Engele, C.M., Kossatz, U., Chen, X., Firpo, E., Grunwald, V., Kamino, K., Wilkens, L., Lehmann, U., Buer, J., *et al.* (2006). Testing the importance of p27 degradation by the SCFskp2 pathway in murine models of lung and colon cancer. *Proceedings of the National Academy of Sciences of the United States of America* 103, 14009-14014.

Torbett, N.E., Luna-Moran, A., Knight, Z.A., Houk, A., Moasser, M., Weiss, W., Shokat, K.M., and Stokoe, D. (2008). A chemical screen in diverse breast cancer cell lines reveals genetic enhancers and suppressors of sensitivity to PI3K isoform-selective inhibition. *The Biochemical journal* 415, 97-110.

Trinchieri, G. (1989). Biology of natural killer cells. *Adv immunol* 47, 376.

Trinchieri, G. (2003). Interleukin-12 and the regulation of innate resistance and adaptive immunity. *Nature Reviews Immunology* 3, 133-146.

Ungefroren, H., Voss, M., Bernstorff, W.V., Schmid, A., Kremer, B., and Kalthoff, H. (1999). Immunological escape mechanisms in pancreatic carcinoma. *Annals of the New York Academy of Sciences* 880, 243-251.

Urban, J., Kripke, M., and Schreiber, H. (1986). Stepwise immunologic selection of antigenic variants during tumor growth. *The Journal of Immunology* 137, 3036-3041.

van den Broek, M.F., Kägi, D., Zinkernagel, R.M., and Hengartner, H. (1995). Perforin dependence of natural killer cell-mediated tumor control in vivo. *European journal of immunology* 25, 3514-3516.

Vanhaesebroeck, B., Guillermet-Guibert, J., Graupera, M., and Bilanges, B. (2010). The emerging mechanisms of isoform-specific PI3K signalling. *Nature reviews. Molecular cell biology* 11, 329-341.

Vazquez-Martin, A., Colomer, R., Brunet, J., Lupu, R., and Menendez, J.A. (2008). Overexpression of fatty acid synthase gene activates HER1/HER2 tyrosine kinase receptors in human breast epithelial cells. *Cell proliferation* 41, 59-85.

Verma, J., Khedkar, V.M., and Coutinho, E.C. (2010). 3D-QSAR in drug design--a review. *Current topics in medicinal chemistry* 10, 95-115.

Verma, R.P., and Hansch, C. (2008). Camptothecins: a SAR/QSAR study. *Chemical reviews* 109, 213-235.

Viewerlite\_5.0 Viewerlite 5.0: Discovery Studio Visualizer. pp. Accelrys Inc., San Diego, USA.

Visca, P., Sebastiani, V., Botti, C., Diodoro, M.G., Lasagni, R.P., Romagnoli, F., Brenna, A., De Joannon, B.C., Donnorso, R.P., Lombardi, G., *et al.* (2004). Fatty acid synthase (FAS) is a marker of increased risk of recurrence in lung carcinoma. *Anticancer research* 24, 4169-4173.

VlifeMDS (2004). VLifeMDS 3.0, Molecular Design Suite. (Vlife Sciences Technologies Pvt. Ltd. Pune, India).

Wade, R.C., Henrich, S., and Wang, T. (2004). Using 3D protein structures to derive 3D-QSARs. *Drug Discovery Today: Technologies* 1, 241-246.

Waldmann, T. (2002). The contrasting roles of IL-2 and IL-15 in the life and death of lymphocytes: implications for the immunotherapy of rheumatological diseases. *Arthritis Res* 4, S161-S167.

Wallace, A.C., Laskowski, R.A., and Thornton, J.M. (1995). LIGPLOT: a program to generate schematic diagrams of protein-ligand interactions. *Protein engineering* 8, 127-134.

Wang, W.Q., Zhao, X.Y., Wang, H.Y., and Liang, Y. (2008). Increased fatty acid synthase as a potential therapeutic target in multiple myeloma. *Journal of Zhejiang University. Science. B* 9, 441-447.

Wang, X., Lin, J., Chen, Y., Zhong, W., Zhao, G., Liu, H., Li, S., Wang, L., and Li, S. (2009). Novel fatty acid synthase (FAS) inhibitors: design, synthesis, biological evaluation, and molecular docking studies. *Bioorganic & medicinal chemistry* 17, 1898-1904.

Wang, X., and Tian, W. (2001). Green tea epigallocatechin gallate: a natural inhibitor of fatty-acid synthase. *Biochemical and biophysical research communications* 288, 1200-1206.

Welcker, M., and Clurman, B.E. (2008). FBW7 ubiquitin ligase: a tumour suppressor at the crossroads of cell division, growth and differentiation. *Nature reviews. Cancer* 8, 83-93.

White, S.W., Zheng, J., Zhang, Y.M., and Rock (2005). The structural biology of type II fatty acid biosynthesis. *Annual review of biochemistry* 74, 791-831.

Wiltrout, R.H., Mathieson, B.J., Talmadge, J.E., Reynolds, C.W., Zhang, S., Herberman, R.B., and Ortaldo, J.R. (1984). Augmentation of organ-associated natural killer activity by biological response modifiers. Isolation and characterization of large granular lymphocytes from the liver. *The Journal of experimental medicine* 160, 1431-1449.



Xu, S., Patel, P., Abbasian, M., Giegel, D., Xie, W., Mercurio, F., and Cox, S. (2005). In vitro SCFbeta-Trcp1-mediated I kappa Balpha ubiquitination assay for high-throughput screen. *Methods in enzymology* 399, 729-740.

Xu, Z., Luo, H.H., and Tieleman, D.P. (2007). Modifying the OPLS-AA force field to improve hydration free energies for several amino acid side chains using new atomic charges and an off-plane charge model for aromatic residues. *Journal of computational chemistry* 28, 689-697.

Yasumura, S., Lin, W.-c., Hirabayashi, H., Vujanovic, N.L., Herberman, R.B., and Whiteside, T.L. (1994). Immunotherapy of liver metastases of human gastric carcinoma with interleukin 2-activated natural killer cells. *Cancer research* 54, 3808-3816.

Yu, J., Wjasow, C., and Backer, J.M. (1998). Regulation of the p85/p110 $\alpha$  Phosphatidylinositol 3'-Kinase DISTINCT ROLES FOR THE N-TERMINAL AND C-TERMINAL SH2 DOMAINS. *Journal of Biological Chemistry* 273, 30199-30203.

Yuan, J., Mehta, P.P., Yin, M.-J., Sun, S., Zou, A., Chen, J., Rafidi, K., Feng, Z., Nickel, J., and Engebretsen, J. (2011). PF-04691502, a potent and selective oral inhibitor of PI3K and mTOR kinases with antitumor activity. *Molecular cancer therapeutics* 10, 2189-2199.

Yuan, T.L., and Cantley, L.C. (2008). PI3K pathway alterations in cancer: variations on a theme. *Oncogene* 27, 5497-5510.

Zaks, T.Z., Chappell, D.B., Rosenberg, S.A., and Restifo, N.P. (1999). Fas-mediated suicide of tumor-reactive T cells following activation by specific tumor: selective rescue by caspase inhibition. *The Journal of Immunology* 162, 3273-3279.

Zhang, W., Richardson, R.D., Chamni, S., Smith, J.W., and Romo, D. (2008). Beta-lactam congeners of orlistat as inhibitors of fatty acid synthase. *Bioorganic & medicinal chemistry letters* 18, 2491-2494.

Zhao, J.J., Liu, Z., Wang, L., Shin, E., Loda, M.F., and Roberts, T.M. (2005). The oncogenic properties of mutant p110alpha and p110beta phosphatidylinositol 3-kinases in human mammary epithelial cells. *Proceedings of the National Academy of Sciences of the United States of America* 102, 18443-18448.

Zhao, L., and Vogt, P.K. (2008). Class I PI3K in oncogenic cellular transformation. *Oncogene* 27, 5486-5496.

Zhi, J., Melia, A.T., Funk, C., Viger-Chougnet, A., Hopfgartner, G., Lausecker, B., Wang, K., Fulton, J.S., Gabriel, L., and Mulligan, T.E. (1996). Metabolic profiles of minimally absorbed orlistat in obese/overweight volunteers. *Journal of clinical pharmacology* 36, 1006-1011.

Zhou, W., Han, W.F., Landree, L.E., Thupari, J.N., Pinn, M.L., Bililign, T., Kim, E.K., Vadlamudi, A., Medghalchi, S.M., El Meskini, R., *et al.* (2007). Fatty acid synthase inhibition activates AMP-activated protein kinase in SKOV3 human ovarian cancer cells. *Cancer research* 67, 2964-2971.